Summer 2024

Mining Contamination of Legacy Deposits on Floodplains Along Turkey Creek, Western Border of the Ozark Highlands

Hannah Riley Eades
Missouri State University, Eades97@live.missouristate.edu

MINING CONTAMINATION OF LEGACY DEPOSITS ON FLOODPLAINS ALONG TURKEY CREEK, WESTERN BORDER OF THE OZARK HIGHLANDS

A Master's Thesis

Presented to

The Graduate College of

Missouri State University

In Partial Fulfillment

Of the Requirements for the Degree

Master of Science, Geography and Geology

By

Hannah Eades

August 2024

MINING CONTAMINATION OF LEGACY DEPOSITS ON FLOODPLAINS ALONG TURKEY CREEK, WESTERN BORDER OF THE OZARK HIGHLANDS

Earth, Environment, and Sustainability

Missouri State University, August 2024

Master of Science

Hannah Eades

ABSTRACT

Historical mining activities in the Tri State mining district in Southwest Missouri from 1850 to 1950 resulted in widespread metal contamination of stream sediments. Beginning in the 1840s, land disturbances associated with Euro-American settlement and agricultural expansion increased runoff and soil erosion rates resulting in the deposition of contaminated alluvium or legacy sediment on floodplains. This study assesses zinc (Zn) and lead (Pb) contaminated legacy deposits in cut-bank exposures along floodplains in Turkey Creek Watershed (119 km²) which drained mining areas in Missouri. Ore production histories were used date metal contamination profiles and calculate floodplain deposition rates in legacy deposits. Twelve sample reaches and 23 floodplain cores were collected from three mining sub-districts, in downstream order: Oronogo-Duenweg, Joplin; and Zincite. The average depth of Zn and Pb contamination was 1.8 m ranging from 0.3 to 2.8 m. Floodplain surfaces (<0.3 m) were contaminated in more than half of the cores. Average concentrations in contaminated floodplain deposits decreased by sub district as follows: Joplin, 10,387 ppm Zn and 1,354 ppm Pb; Zincite, 9,169 ppm Zn and 1,167 ppm Pb; and Oronogo, 4,938 ppm Zn and 426 ppm Pb. Legacy sediment depths averaged 1.3 m ranging from 0.6 to 2.3 m. The depth of legacy sediment generally increased with drainage area as did floodplain sedimentation rates. Sedimentation rates were greatest during the mining and agriculture growth period averaging 1.6 cm/yr from 1870-to 1930 and lowest in the post-mining period averaging 0.2 cm/yr from 1930 to 2021.

KEYWORDS: floodplain deposition, mining pollution, Tri-State Mining District, Ozark Highlands, Lead, Zinc

MINING CONTAMINATION OF LEGACY DEPOSITS ON FLOODPLAINS ALONG TURKEY CREEK, WESTERN BORDER OF THE OZARK HIGHLANDS

By

Hannah Eades

A Master's Thesis
Submitted to the Graduate College
Of Missouri State University
In Partial Fulfillment of the Requirements
For the Degree of Master of Science, Geography and Geology

August 2024

Approved:

Robert Pavlowsky, Ph.D., Thesis Committee Chair

Marc Owen, M.S., Committee Member

Tasnuba Jerrin, Ph.D., Committee Member

Julie Masterson, Ph.D., Dean of the Graduate College

ACKNOWLEDGEMENTS

I would like to thank my advisor and committee chair Dr. Robert Pavlowsky for his guidance and support throughout my time at Missouri State University. I am grateful for all that I have learned working on this project as well as the many others I was a part of with the Ozarks Environmental Water Resource Institute (OEWRI). I would also like to thank my committee member, Dr. Tasnuba Jerrin for her feedback and help on my thesis draft. A special thank you to my third committee member, Marc Owen; this thesis would not have been possible without your steadfast support and advice. I also want to thank Joss Hess for his patience and troubleshooting abilities in all things GIS. Thank you to all the OEWRI graduate assistants: Teri Arceneaux, Katie Grong, Hannah Bieser, Partick Saulys, Elandé Engelbrecht, and Michael Ferguson for all their help in the field and for making my time in this program so enjoyable. A special shoutout to the women of OWERI (Katie, Teri, Hannah B., and Elandé), I cherished all the laughs, venting sessions, field work, coffee runs, campfires, and nights out on the town. I feel so lucky to have had the friendships and support of such incredibly talented and intelligent women. Funding for my research assistantship was provided through external grants from the Natural Resource Conservation Service and the Missouri Department of Natural Resources. Support for my thesis research and travel was provided by OEWRI and the Graduate College. Finally, I would like to extend my gratitude and love to my parents, my friends (Hunter, Brooke, Sawyer, and Heather) and my dog Lou for each of the very special roles they played in the completion of this thesis.

TABLE OF CONTENTS

LIST OF TABLES

LIST OF FIGURES

INTRODUCTION

Floodplain deposits contain a sediment record of the past hydrological and depositional processes responsible for channel development and its present-day form (Thayer and Ashmore 2016). Therefore, stratigraphic studies of floodplains are essential for understanding the environmental history of a river systems as well as the watershed it drains (Meade, 1982; Knox, 1987; Pizzuto et al., 2016; Owen et al., 2011). Euro-American settlement during the middle and late 1800's in the Midwest USA cleared natural vegetation for logging and agriculture, decreased soil infiltration rates, increased runoff volumes and flood peaks, resulting in increased sediment yields and changes in channel form (Knox, 1977; 2006; Trimble, 1983; Magilligan, 1985; Lecce and Pavlowsky, 2001; Belby et al., 2019). Upstream channels responded to larger floods by lateral channel migration and widening thus increasing bank erosion rates and sediment loads and accelerating flood routing to downstream channels (Lecce and Pavlowsky, 2001). Soil erosion rates generally increased by a factor of ten during the settlement period (Meade, 1982). As a result, deposition rates of fine-grained sediment increased on floodplains along lowland valleys of most streams in watersheds affected by crop, livestock, and timber agriculture (James, 2013; Belby et al., 2019).

Legacy Sediment

Historical overbank floodplain deposits mainly formed as the result of watershed disturbances during the initial period of agricultural expansion and resource exploitation have been described as post-settlement or legacy deposits (Knox, 1977, 1987; James, 2013; Donovan et al., 2015). Legacy sedimentation is episodic and heterogeneous across a landscape and

depends upon the sediment source, capacity of the channel, valley constraints, connectivity, and other geomorphic and hydrological factors (James, 2013). The main mode of deposition of legacy sediment is by vertical accretion, otherwise referred to as overbank sedimentation where historical floods reached the top of the channel and deposited suspended sediments (Knox, 1987) (Figure 1).

Pre-settlement floodplains tend to have more developed soil profiles formed at lower elevations on the valley floor compared to modern floodplains (Figure 2). As runoff and erosion rates continued to increase with land use intensity, fine-grained sediment was deposited on top of older floodplains forming higher banks resulting in deeper and incising channels that were eventually cut off from the active floodplain since flood waters were directed downstream rather than spreading out across the floodplain (Figure 2). Not until the 1920's did soil conservation practices get introduced to reduce excessive erosion rates, but the damage had already been done. Streams began to adjust to increased flood frequency, higher sediment loads, and bank erosion resulting in channel widening, higher sediment transport rates, and the transfer of legacy sediment further downstream (Figure 2). Although conservation practices advanced rapidly since the 1920's, present-day sedimentation rates on floodplains are typically still higher compared to pre-colonial times in Midwest watersheds (Belby et al., 2019). Floodplain deposits containing legacy sediment often overlie Holocene surfaces and have features that represent anthropogenic origins including pollution from mining and industrial runoff, mixed textures, and mineralogy relative to older deposits, and anthropogenic artifacts (Pavlowsky et al., 2017).

The assumption of steady state equilibrium is not appropriate for geomorphic analysis of stream channels affected by historical land use changes over periods from 10 to 100 years. Channel form is adjusting to both increased flood magnitude and frequency and lack of balance

between upland sediment delivery, sediment pulses, and storage rates of sediment in the channel or on the floodplain (Trimble, 1983). Watersheds effected by land disturbances associated with early agricultural practices were affected by an increase in sediment deposition and longer-term storage on floodplains to counter the excess channel loads from slope and upland erosion (Knox, 1977; Trimble 1983). Legacy deposits are now of environmental concern since they can be remobilized by channel erosion to add to contemporary sediment loads and, in some regions, may contain toxic metals released by large-scale mining during the post-settlement period (Pavlowsky et al., 2017). In general, increased erosion and sediment transport in rivers cause negative impacts to human health, the economy, and the environment (Walling and He, 1998). Further, sediment and sedimentation are a major water quality concern and the non-point source pollutant of primary concern in the United States (Neary and Riekerk, 1988).

Mining Contamination

Metal pollutants have been used as geochemical indicators to evaluate watershed changes and to quantify sedimentation rates by comparing fluctuations of metal concentrations with mining history in their study area (Macklin, 1985; Knox, 1987; James, 1989; Lecce and Pavlowsky, 2001; Dennis et al., 2008; Pizzuto et al. 2016). For example, greater than 40 percent of tailings released into a watershed from mining activities can be deposited in floodplain deposits (Jeffery et al., 1988; Pavlowsky et al., 2017). Some studies have found increasing floodplain sedimentation rates during and right after the periods of extensive mining (Gilbert, 1917; Macklin, 1985; Knox, 1987; Lecce and Pavlowsky, 2001). However, mining pollutants can enter streams at the same time, but independently of more widespread watershed disturbances, and have relatively low impact on sedimentation processes (Pavlowsky et al.,

2017). Two endmembers of channel response to mining inputs have been described (Lewin and Macklin, 1987). Passive dispersal occurs when mining wastes are transported with the natural sediment load without disturbing channel and floodplain processes. In contrast, active transformation involves the complete disruption of the pre-mining channel form and sediment characteristics due to the excessive inputs of tailings, sediment, and flood water (Lewin and Macklin, 1987; Macklin et al., 2006).

Heavy metals associated with mining activities are a concern due to their prolonged residence times in sediment and soils and tendency for bioaccumulation in plants and animals (Macklin and Klimek, 1992; Macklin et al., 2006). Although floodplains can deposit and store mining wastes thus reducing downstream dispersal rates, over the long-term stored metals can be released back into the stream long after initial contamination as floodplain deposits erode and weather (Bradley, 1989). Understanding how floodplain sedimentation and associated heavy metal contamination varies spatially, temporally, and vertically throughout a fluvial system is crucial to effective environmental planning and remediation efforts and can be useful for determining the sedimentation history of a watershed (USEPA, 2004; USFW, 2013).

Mining contaminants that enter streams in association with tailings particles or sorbed strongly to natural sediments can be used as stratigraphic markers to indentify the age and origin of floodplain strata and link deposits specifically to human impacts (Macklin, 1985; Macklin et al., 1994; Knox, 1987; Lecce, 1997; Lecce and Pavlowsky 2001, 2014; Owen et al., 2011). Channel segments that have been less susceptible to lateral migration and received constant overbank deposition throughout the mining period are ideal for evaluating rates of vertical accretion using mining metal profiles (Macklin, 1985; Knox, 1989). Importantly, fluctuations in mining-metal concentrations in floodplain cores profiles can be linked to the calendar year of

operation and level of productivity of the upstream mine source so that relatively accurate and precise interpretations of sediment age or time of deposition can be made in many cases (Macklin, 1985; Knox, 1987; Lecce and Pavlowsky, 2001). Evaluating overbank profiles in this way requires considerations of basin size and land use history (Macklin et al., 1994). Systematic sampling of different ages and geomorphic features below mining locations as well as a detailed history of mining in the study area are necessary for dependable results (Macklin et al., 1994).

Both channel and floodplain deposits can be contaminated with heavy metals for several hundred kilometers downstream of the mining source (Horowitz, 1991). Coarser materials in the fine gravel fraction will be transported at slower rates and remain nearer to its source in bed and bar deposits, while finer sediments in the silt and clay fractions will be transported further downstream and deposited in overbank floodplains (Pavlowsky et al., 2017). In confined valleys with higher slopes, such as in headwater streams, the transport capacity of the channel will be greater and therefore contaminated sediment, especially that of smaller particle size will be carried further downstream (Pavlowsky et al., 2017). However, where floodplains are unconfined and slope decreases the sediment storage capacity of the channel and floodplain will increase with overbank deposition and lateral accretion (i.e., point bar deposition) is more likely to occur (Pavlowsky et al., 2017). In general, metal concentrations tend to decrease downstream due to mixing and dilution with cleaner sediment and deposition of contaminated sediment (Lecce and Pavlowsky, 1997; Dennis et al., 2008). However, sediment metal concentrations do not always decrease downstream with increasing distance below source due to effects of pulsed transport, mixing with tributary inputs, and locally high or low sedimentation areas (Graf, 1985, 1996; Dennis et al., 2008).

The reworking of contaminated floodplain deposits or continued erosion of tailings piles can lead complex patterns of ongoing contamination and concerns about a lasting source of metal contamination long after mining has stopped (Rowan et al., 1995; Miller, 1997; Macklin et al., 2006). Stored mining sediment can reenter the stream through bank erosion, weathering, and human disturbances only to be stored again downstream by overbank sedimentation or in point bar deposits by lateral accretion (Macklin et al., 1997; Dennis et al., 2008). Reaches with both high concentrations or total storage of metals and high stream power (i.e., relatively high slope and flow depth) are those most susceptible to bank erosion and most likely to release metals downstream (Lecce and Pavlowsky, 1997). Another factor that can increase bank erosion and stream power is the expansion of meander belts in the upstream reaches of a watershed due to increased stream power (Lecce and Pavlowsky, 1997). Channel erosion and metal reworking may also result in ongoing contamination of downstream channels since incised channels tend to contain flood waters, increase flow velocities, limit flooding and deposition on adjacent floodplains, and rapidly flush contaminated sediment downstream (Lecce and Pavlowsky, 1997).

Background

This study investigates the occurrence, sedimentology/geomorphology, and mining contamination, including metal profile dating, of historical floodplain deposits in Turkey Creek watershed (119 km²) which drains Joplin, Missouri along the western boundary of the Ozark Highlands. The watershed is located within Tri-State Mining District (TSMD) of southwest Missouri, eastern Kansas and northeast Oklahoma which was a leading producer of lead (Pb), zinc (Zn) ore from 1850 to 1970 producing 23 million tons of Zn concentrate and four million tons of Pb (Barks, 1977; McCauly et al., 1983; Johnson et al., 2016). Large quantities of fine

tailings from dry gravity, wet shaking, or froth floatation milling methods were discharged or eroded into Turkey Creek from active and abandoned mine sites (Taggart, 1945). Channel and floodplain sediments in Turkey Creek are contaminated with Zn, Pb, and other metals (Juracek, 2013; Gutierrez et al., 2019, 2020; Hillerman, 2022). Tailings piles and base remnants are still found in some areas of the watershed and tailings deposits are noticeable in some cutbank exposures along Turkey Creek. By 1990 the US Environmental Protection Agency included Turkey Creek within the Oronogo-Duenweg Mining Belt Superfund site and remediation efforts are still ongoing (Gutierrez et al., 2020).

Studies in other locations with similar environmental histories have used contaminated over-bank deposits to evaluate the sedimentation history of floodplains in watersheds (Macklin, 1985; Macklin et al., 1994; 1997; Knox, 1987; Lecce and Pavlowsky, 2001; Pavlowsky et al., 2017). In this study, metal contamination profiles in floodplain deposits along Turkey Creek are used to identify and date legacy floodplain deposits giving insight into the sedimentation history of the watershed and how it has been impacted by land use change, channel disturbances, and extensive mining activities. Previous studies of floodplains in the Ozark Highlands have found legacy deposits in southwest (Carlson, 1999; Owen et al., 2011) and southeast Missouri (Pavlowsky et al., 2017). Legacy floodplain deposits in this region ranged from 0.5-3.5 m in depth and are a result of increased run-off and sediment yields from land use disturbances such as land clearing and extensive mining activities (Carlson, 1999; Owen et al., 2011, Pavlowsky et al., 2017). Fully understanding the extent of floodplain contamination along Turkey Creek and identifying the patterns of heavy metal distribution in a historically mined basin is crucial for determining long term environmental risks and for future restoration and planning purposes.

It is generally known that Pb, Zn, and Cadmium (Cd) concentrations in channel and floodplain sediments exceed background concentrations and sediment quality criteria in TSMD streams (Juracek, 2013; Smith, 2016; Klager and Juracek, 2017; Pope, 2005; Gutierrez et al., 2020). Most studies of TSMD stream have focused mainly on contaminated channel sediment (Pope, 2005; Juracek 2013; Smith, 2016; Klager and Juracek 2017; Garvin et al., 2017; Gutierrez et al., 2015, 2019, 2020). Only a few studies have evaluated metal concentrations in floodplain deposits in the TSMD (Juracek, 2013; Smith, 2016; Garvin et al., 2017), two of which included limited sampling of floodplains of Turkey Creek (Juracek, 2013; Smith, 2016). However, there have been no studies of the downstream and vertical trends of metal contamination in floodplain deposits along streams draining the TSMD. Further, this study will be the first to use contamination stratigraphy to determine sedimentation history and nature of legacy floodplain deposits in in TSMD.

Purpose and Objectives

The objectives of this study are (1) assess forms, stratigraphy, and contamination of floodplain deposits by sampling at cutbank exposures and surveying channel cross-sections; (2) evaluate the different contamination trends among different alluvial features including terrace, floodplain, and bench deposits; (3) develop an ore production chronology to use mining-metal profiles and other stratigraphic markers to date legacy deposits; and (4) use the dated stratigraphy to determine historical trends in floodplain deposition rates and evaluate trends in comparison to land use changes in the watershed. Understanding the interaction of historical floodplain development with the delivery of active channel sediment and tailings offers more insight into the extent of contamination still present in Turkey Creek even after remediation efforts in the

area. The results from this study shed light on the potential for remobilization of contamination sediment that could continue to pollute downstream reaches. The degree and spatial distribution of Zn and Pb in floodplains found in this study could be used as a preface for further research in the storage and potential transport of contaminated sediment in the future and raises concerns for the state of other watersheds in the TSMD.

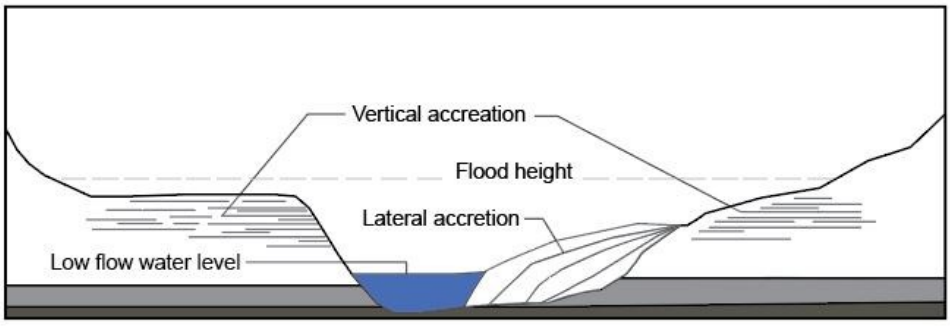

Figure 1. Types of deposition: lateral and vertical accretion.

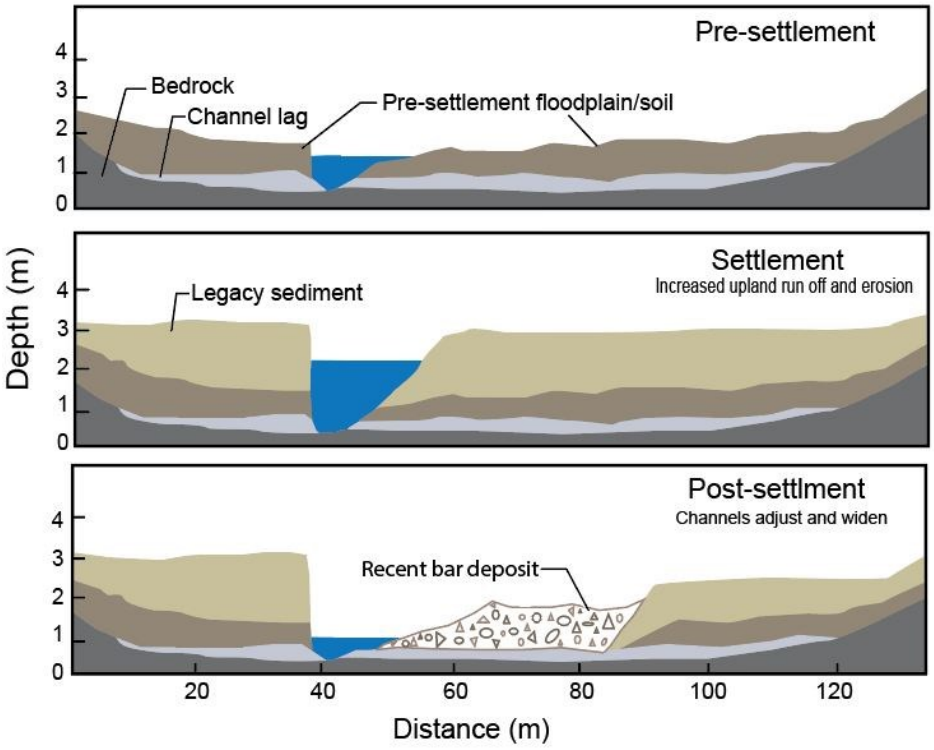

Figure 2. The change in channel morphology from pre-settlement to the present. Adapted from Donovan et al. (2015).

STUDY AREA

Turkey Creek Watershed is 30 km long and drains 120 km² of the western edge of the Springfield Plain, a subsection of the Ozark Highlands (Nigh and Schroeder, 2002). The Springfield Plain has gentle topography and is underlain mainly by cherty Mississippian limestone (Brosius and Sawin, 2001). Turkey Creek's headwaters are in Newton County, flowing north into Jasper County through Joplin where it flows west continuing across Jasper County until it drains into the Spring River in Kansas about a half mile west of the state line. The Spring River Basin drains about 6,475 km^2 at this point (Juracek, 2013).

Regional Physiography, Geology, and Soils

The bedrock geology of the Turkey Creek watershed consists mainly of limestone and dolomite of the Mississippian Warsaw Formation which outcrops on most uplands and along tributary streams (Figure 3). The Burlington-Keokuk limestone underlies the Warsaw Formation and outcrops at lower elevations of the watershed as well as along the main channel of Turkey Creek (Figure 3). The Pennsylvanian Cherokee group consists of mainly shale with interbedded sandstones and limestone and is present in dispersed outcrops throughout the watershed (Figure 3). Mineralization generally occurs in limestone host rocks with calcite vugs or replacements by sulfide minerals, jasperoid, and dolomite (Hagni and Saadallah, 1965). The main ore minerals in this area are sphalerite (Zn) and galena (Pb) and are most common near areas rich in either dolomite (carbonate) or jasperoid (silicate) (Hagni and Saadallah, 1965).

The main soil orders present in the Turkey Creek Watershed are Mollisols (44%), Alfisols (42%), and Ultisols (9%) with the remaining five percent consisting of Entisols,

Vertisols, and mine dumps and quarries (NRCS, 2020) (Figure 4). Mollisols typically indicate areas that were once dominated by prairieand Schroeder, 2002). Floodplain soils in the Turkey Creek watershed are generally classified into four series: Cedargap gravelly silt loam, Bearthicket silt loam, Pomme silt loam, and Pomme-Rueter Complex (Figure 5). The Cedargap series is the most common floodplain soil along Turkey Creek with all but one sampling site for this study located on it (Figure 5). Cedargap is a mollisol with a cumulic A horizon (indicating relatively recent deposition) formed in fine or cherty alluvium parent material. It is typically well drained and found along channels, forming in the younger active floodplain (NRCS, 2020). Bearthicket is the second most prominent floodplain soil series in the watershed and the remaining sampling site is located within this series (Figure 5). Bearthicket is found all along the main channel in pockets along the edges of the Cedargap series, this series is occasionally flooded and forms on floodplains and low terraces. This series is an alfisol with silty alluvium parent material and well-defined argillic (Bt) horizons, however, none of the cut-bank exposures evaluated for this study had Bt horizons (NRCS, 2020) (Figure 5).

Legacy sediment overlying buried soils (Ab horizons) frequently occurred throughout the watershed on floodplains along tributaries and the main channel. These historical sediments are typically fine grained, light tan in color, and may overlie a darker A horizon formed in Holocene overbank or channel deposits. Along Turkey Creek, mining contaminated soils occur above Ab horizons when present indicating the historical timing of legacy floodplain deposition. However, as will be described, high concentration of Zn and other metals can be found stratigraphically below buried soils due to natural mineralization or the vertical or lateral transport of mining metals by ground water.

Hydrology and Climate

The Spring River basin is part of the Springfield plain physiographic subsection which has rolling hills and meandering streams with a subhumid continental climate (Nigh and Schroeder, 2002; Juracek, 2013). Streams in this region typically transport bed load consisting of sand and chert gravel (Nigh and Schroder, 2002). The mean annual precipitation in Joplin Missouri from 1948-2020 was 110 cm (HPRCC, 2022). There are no discharge gaging sites in Turkey Creek but there is a long running gage on Shoal Creek (1,106 km²) (USGS #07187000) (USGS, 2021a) which also drains to Spring River located just south of Turkey Creek. Over a 79-year period this gage has an average annual discharge of 19 m^3/s and a median discharge of 12 m^3/s. Assuming a drainage area correction for discharge is valid for watersheds in similar geology, the estimated mean annual discharge would be 2.1 m^3/s and median discharge 1.3 m^3/s for Turkey Creek at its confluences with Spring River (USGS, 2021a).

Streams in the Springfield plains region typically experience their highest discharges in the late winter and early spring and lowest in summer and fall (Nigh and Schroeder, 2002). Flash flooding is very common in this region, and it is during these times of increased run-off and flooding that suspended sediment concentrations increase dramatically in these streams (Nigh and Schroeder, 2002). The gage record on Shoal Creek indicated that exceptionally large floods occurred during World War II (1941 and 1943) and again in 2016 and 2017. Several discharge gages on the Spring River indicate an increase in flood stages and frequency of large floods since 1980. In general, the frequency of floods and magnitude of peak discharge has been increasing since 1990 in the Ozark Highlands (Heimann et al., 2018).

Landcover and County History

The Springfield plains region of the Ozark Highlands once formed the transition zone between prairie in the west and forest to the east (Nigh and Schroeder, 2002). Turkey Creek lies in the western most portion of this region in the Spring River prairie/Savanna dissected plain land-type association (Figure 6) (Nigh and Schroeder, 2002). In the past this area consisted of prairies on the flatlands and hardwood savannas on hillslopes with interspersed glades at sandstone and limestone outcrops (Nigh and Schroeder, 2002). Prior to Euro-American settlement, Turkey Creek watershed was mainly covered by prairie, proof of which can be observed in the large areas mollisol soils within the watershed (Nigh and Schroeder, 2002). The landscape has dramatically changed since settlement as original savannah and riparian forests were removed, cropland and pastures replaced most of the prairies, and invasive vegetation spread throughout the watershed (Nigh and Schroeder, 2002).

County Agriculture and Population. Jasper county was established in 1841, before this it was the northern part of Newton County formed in 1838 (MCDS, 2020). Agriculture in this region was dominated by livestock, corn, and wheat (Nigh and Schroeder, 2002). The population of Jasper County began to grow as ores were discovered and mining camps were established near present-day Joplin in the 1840-50s (Winslow et al., 1894; Martin, 1945). The population of Jasper County remained less than 20,000 until after the Civil War and the onset of the mining boom around 1870 when the population more than doubled between 1870 to 1880 (Figure 7). New ore bodies and mining sites were discovered quickly in and around the city limits and by 1874 the population of Joplin surged to 5,000 with as many as 1,000 people employed at the mines (Martin, 1945).

While farmland conversion increased during the period before the mining boom, farmland area in Jasper County increased by 60% between 1870 and 1880 (USDA, 2021) (Figure

7). The population in Jasper County continued to increase with the growing mining industry and by 1890 the population of Joplin reached 10,000 with the cities of Webb City and Carterville to the north reaching 8,000 (Martin, 1945). Farmland improvements also continued to increase but at a slower rate (Figure 7). Population declined between 1910 and 1920 while farmland area actually increased during this time period (Figure 7). Mining production crashed in 1918 (Martin, 1945) and between 1910-1920 the population of Jasper County decreased by more than 10,000 people (MCDS, 2020) (Figure 7). As mining slowed down after 1920, there was a subtle spike in farmland area in Jasper County as mining areas and miners transitioned to agriculture, but population still decreased further by 3% (Figure 7). Mining completely stopped in 1947 and between 1940-1970 the population remained steady at around 79,000 (Figure 7). After 1970, the population increased and farmland decreased. Between 1970 and 2000 the population of Jasper County increased by over 20,000 people (Figure 7). In the 2020 census, the population of Jasper County was listed as 122,761 (MCDS, 2020).

Mining History. Mining areas in Turkey Creek are considered to be part of the much larger Tri-State mining district which covers an area of approximately 6,500 km² in parts of southwest Missouri, northeast Oklahoma, and southeast Kansas (Pope, 2005). For about 100 years (1850-1950) this area was a leading producer of zinc and lead ore in the United States with a total ore production greater than half a billion tons (Hinrichs, 1996). Of the total ores mined, approximately 5 percent were usable, leaving 95 percent as on-site wastes as indicated by extensive tailing piles left behind on abandoned mine lands (Hinrichs, 1996). In 1848 lead was discovered along Joplin Creek in an area called Leadville with more discoveries being made during the next few years in the area of present-day Joplin (Martin, 1945). By 1850 there were small Pb mines on Center and Turkey Creeks in Jasper County (Winslow et al., 1894; Hagni et

al., 1986; Martin, 1945). By 1854 mines on Center and Turkey Creeks were estimated to be producing a couple hundred tons of galena annually (Martin, 1945).

The first Pb smelter was constructed in Newton County in 1852 with another smelter built in Jasper County on Center Creek in 1853 (Martin, 1945) (Table 1). An estimated 776 tons of Pb ore was smelted at these two hearths between 1850 and 1854 (Martin, 1945). Between 1850 and 1861 mining gradually increased with new discoveries and the construction of more Pb smelters but remained small scale until coming to a halt in 1861 because of the Civil War (Hagni et al., 1986; Martin, 1945) (Table 1). After the Civil War, mining resumed and began to expand in 1865 with more surface prospecting and new camps being established (Hagni et al., 1986). Mining within the boundary of present-day Joplin remained minimal until 1870 when large Pb ore deposits were discovered and the Moon diggings on the Joplin Branch were opened with furnaces running 24 hours a day and 7 days a week (Winslow et al., 1894; Martin, 1945).

After 1870, shallow rich Zn ores were discovered on Joplin Creek (Hagni et al., 1986). In 1872 the first Zn ore was shipped out of Joplin (Martin, 1945) (Table 1). Around 1880 railroads from Kansas City and St. Louis extended into Jasper County and Zn smelters were erected in the area including one in Joplin (Hagni et al., 1986, Martin, 1945). Between 1880 and 1889 the production of Pb and Zn increased by more than eight-times compared to the previous decade coming in at around an average of 114,000 tons annually (Hagni et al., 1986). The Missouri golden years for Zn production occurred between 1890-1910 with the opening of large tonnage sheet-ground mines which again doubled the average annual production from the last decade (Hagni et al., 1986; Martin, 1945) (Table 1). The average annual production continued to increase but once major Zn ores were discovered in Pitcher Oklahoma mining companies began to move out of Missouri by 1920 (Hagni et al., 1986). Small mining operations were present in

Missouri after 1920 but production slowed drastically during the great depression (1930-1939) and almost all production in Missouri ceased by 1947 (Hagni et al., 1986).

There were many mining companies and property changed hands so often it is difficult to assign sections of the Turkey Creek watershed to one mining operation and timeline. For this study, the watershed is broken into three sub districts, Zincite in the western most portion, Joplin in the central portion, including all of Joplin Branch, and Webb City in the northeast and eastern portion of the watershed (Figure 8). Small scale Pb mining began in 1850 in these sub-districts but was not extensive until the start of the Zn mining boom in 1870 (Martin, 1945).

Mining Contamination Studies

One of the first published assessments of the spatial distribution of sediment contamination in the TSMD was completed in 2005 for the Spring River and it's Kansas and Missouri tributary streams (Pope, 2005). The highest concentrations of Pb and Zn in stream bed sediment occurred in tributaries with the most extensive mining history and in the reaches of these tributaries that were within or just downstream of a mining source (Pope, 2005). Since this first study, more work has been done to assess contamination levels and variability in stream sediments in Kansas (Klager and Juracek, 2017; Garvin et al., 2017) and Missouri (Smith, 2016; Garvin et al., 2017; Gutierrez et al., 2015; 2019; 2020). Fewer studies have evaluated floodplain contamination variability in the TSMD and those that have refer mostly to streams in Kansas (Juracek 2013; Garvin et al., 2017).

Turkey Creek was one of the two Missouri floodplains included in the 2013 study by Juracek, his study on the Turkey Creek floodplain was just upstream of the Spring River in the same location as site 4 in this study. Juracek (2013) collected three cores with three samples in

each core at six-inch intervals. Most of the surficial floodplain Pb and Zn concentrations exceeded TSMD-specific probable effects concentrations (PECs) and three of the bulk samples exceeded the action levels of 800 ppm Pb and 6,400 ppm Zn for Zn and five for Pb (i.e., USEPA 2010). Overall, the tributaries in the Spring River basin with a history of extensive mining had Zn and Pb concentrations typically exceeding TSMD-PECs (Juracek, 2013).

There was one other floodplain study on Turkey Creek with one transect (200 m) containing six floodplain cores (Smith, 2016). This transect was located about 0.43 km downstream of site 5 of the present study. Samples furthest from Turkey Creek (200 m away) contained Zn concentrations greater than the CPEC (2,083 ppm) throughout the entire core (5 m) (Smith, 2016). The highest concentrations measured in the Turkey Creek floodplain by Smith (2016) were found in the upper 30 cm with 6,620 ppm Zn and 789 ppm Pb. However, the study did not attempt to link landform age or sedimentology to the degree or depth of contamination.

Sediment Quality Guidelines. Environmental effect thresholds and levels of concern are useful for determining potential risk areas as well as for using as markers for contamination variability stratigraphically. The U.S. EPA began using non-enforceable sediment quality guidelines (SQGs) for various trace element concentrations in 1997. These level-of-concern concentrations were calculated based on the concentrations of trace elements in sediment related to incidences of adverse biological effects in aquatic organisms (USEPA, 1997). One such guideline that will be referenced in this study is the probable-effects concentration (PEC) which is the level at which toxic effects usually occur (USEPA, 1997). This guideline is not used as a regulatory tool but is assumed to provide accurate predictions for sediment toxicity (USEPA, 1997; MacDonald et al., 2000; Juracek, 2013). Rather than using nationwide PECs, TSMD-

specific guidelines are referenced because they more accurately represent background metals levels and geochemical processes in the Turkey Creek watershed.

In general, published sediment toxicity indicators and clean-up targets vary throughout the TSMD. Ingersoll et al. (2009) reported PECs for sediment toxicity in Grand Lake, OK sediments as 2,083 ppm Zn and 150 ppm Pb. These values are widely used in studies evaluating sediment contamination in the TSMD (Juracek, 2013). However, two record-of-decision reports released by the U.S. EPA for Orenogo-Duenweg Mining Belt (2004) and Newton County Mine Tailings Superfund Site (2010) reported soil action levels that put human health and terrestrial vertebrates at unacceptable risk at 6,400 ppm Zn and 400 ppm Pb (Table 2). Further, the record of decision amendment plan for the Oronogo-Duenweg Mining Belt Superfund Site in Jasper County reported tributary sediment cleanup levels as 2,949 ppm Zn and 219 ppm Pb (USEPA, 2013).

Background Concentrations. Determination of the background concentrations for metals is one of the first steps required for evaluating the degree of contamination in an area. Previous studies in the TSMD (Juracek 2013; Smith 2016) refer to a study by Pope (2005) who reported background concentrations of Zn and Pb to be 100 ppm and 20 ppm, respectively (Table 3). When referencing results to a national average, many studies (Juracek, 2013) use Horowitz et al. 1991, which found average background concentrations of Zn and Pb to be 88 ppm and 23 ppm (Table 3). The most site-specific study occurred in the Oronogo-Duenweg Mining Belt which reported background levels concentrations of 91 ppm Pb and 433 ppm Zn (USEPA, 2004) (Table 3).

Efforts were made to account for potential natural enrichment due to proximity to shallow ores or ground water containing high concentrations of dissolved metals. Some studies

have found that vertical profiles of Zn and Pb in floodplain deposits can be affected both by the primary deposition of contaminated sediment and the chemical remobilization of metals from ore bodies or other contaminated deposits (Hudson-Edwards et al., 1998). A possible sign of remobilization due to ground water fluctuations is the accumulation of Iron (Fe) and Manganese (Mn) oxyhydroxides or increased decomposition of organic matter within alluvial deposits (Hudson-Edwards et al., 1998). Turkey Creek's channels contain placer or float lead ores (i.e., galena) to such high concentrations that they were directly mined for Pb in the early 1800's. To account for natural enrichment and chemical remobilization we evaluate both upland and main channel background values.

Table 1. Mining history timeline.

Year	Event	Source
1850	Pb mining starts in Turkey Creek Watershed	Winslow et al., 1894
1853	Pb smelting begins in Jasper County	Winslow et al., 1894
1861-1865	Civil War	Martin, 1945
1869	Pre-mining boom, Pb peak	Winslow et al., 1894
1872	First Zn ore shipped out of Joplin - Mining "boom" starts	Winslow et al., 1894
1880	Rail roads extended into Joplin and Zn smelter build in Joplin	Martin, 1945
1903	Zn-Pb production peak Joplin sub-district	Martin, 1945
1900-1910	Population of Jasper County peaks	MCDC, 2022
1915-1917	Overall total production peak (Duenweg, Joplin and Zincite)	Martin, 1945
1918	Production crash	Martin, 1945
1926	Zincite sub-district late peak	Martin, 1945
1942	Late Oronogo peak (WWII)	Martin, 1945
1947	The last operations in Missouri stopped	Martin, 1945

Table 2. U.S. EPA contamination thresholds for Pb and Zn (Ingersoll et al., 2009)[1], (MacDonald et al., 2000)[2], (USEPA, 2004, 2010)[3].

Trace Element	TSMD- Probable effect threshold[1]	General Probable effect threshold for channel sediment[2]	EPA Remedial action levels (MO)[3]
	Guideline Value (mg/kg)	Guideline Value (mg/kg)	Guideline Value (mg/kg)
Pb	150	128	400
Zn	2,083	459	6,400

Table 3. Background concentrations referenced by other studies in the TSMD region.

Trace Element	Mean background concentrations in TSMD (ppm)		Background Nationally (ppm)
	Pope (2005)	USEPA (2004)	Horowitz et al. (1991)
Pb	20	91	23
Zn	100	433	88

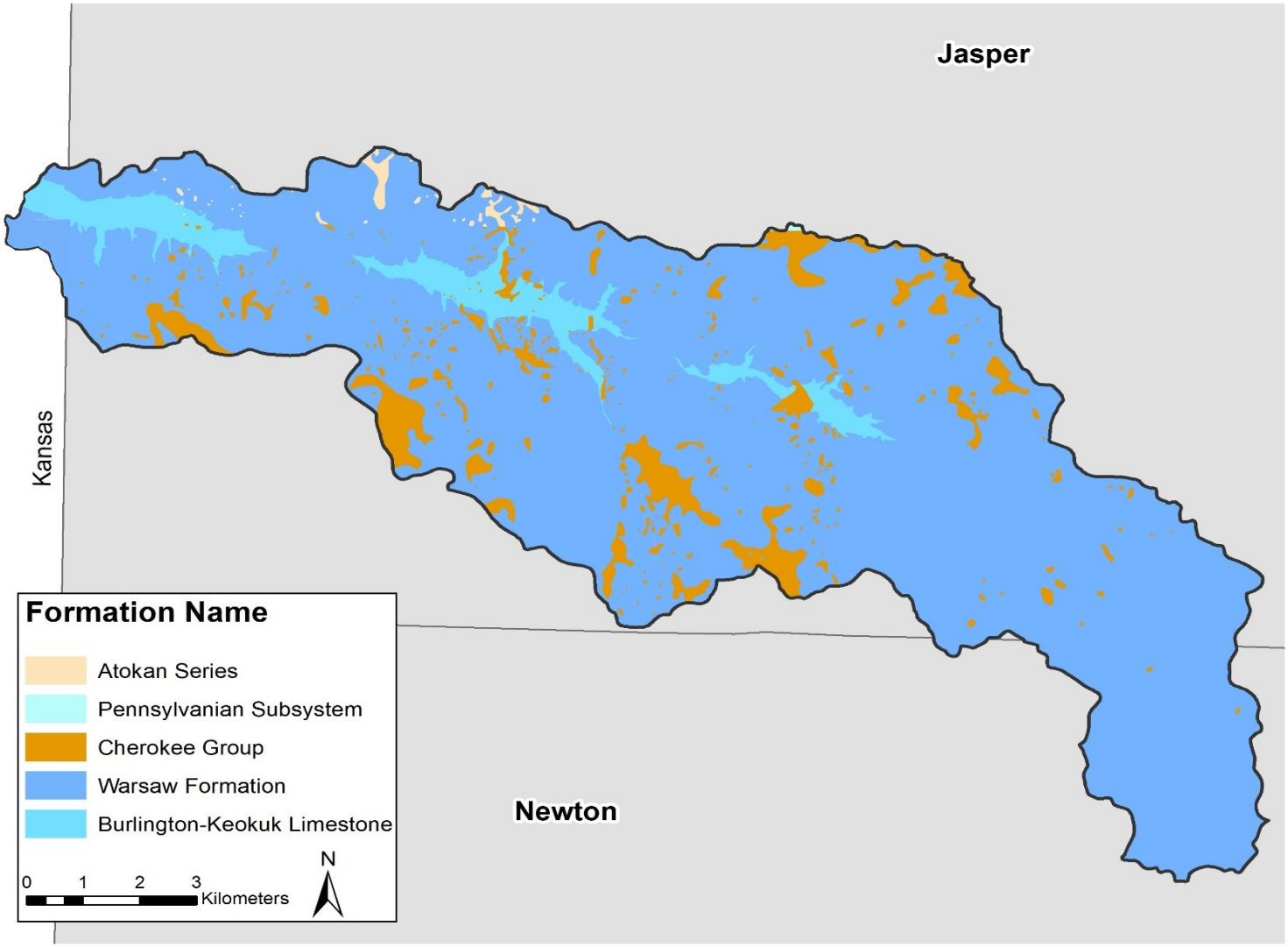

Figure 3. Bedrock geology (MDNR, 2022).

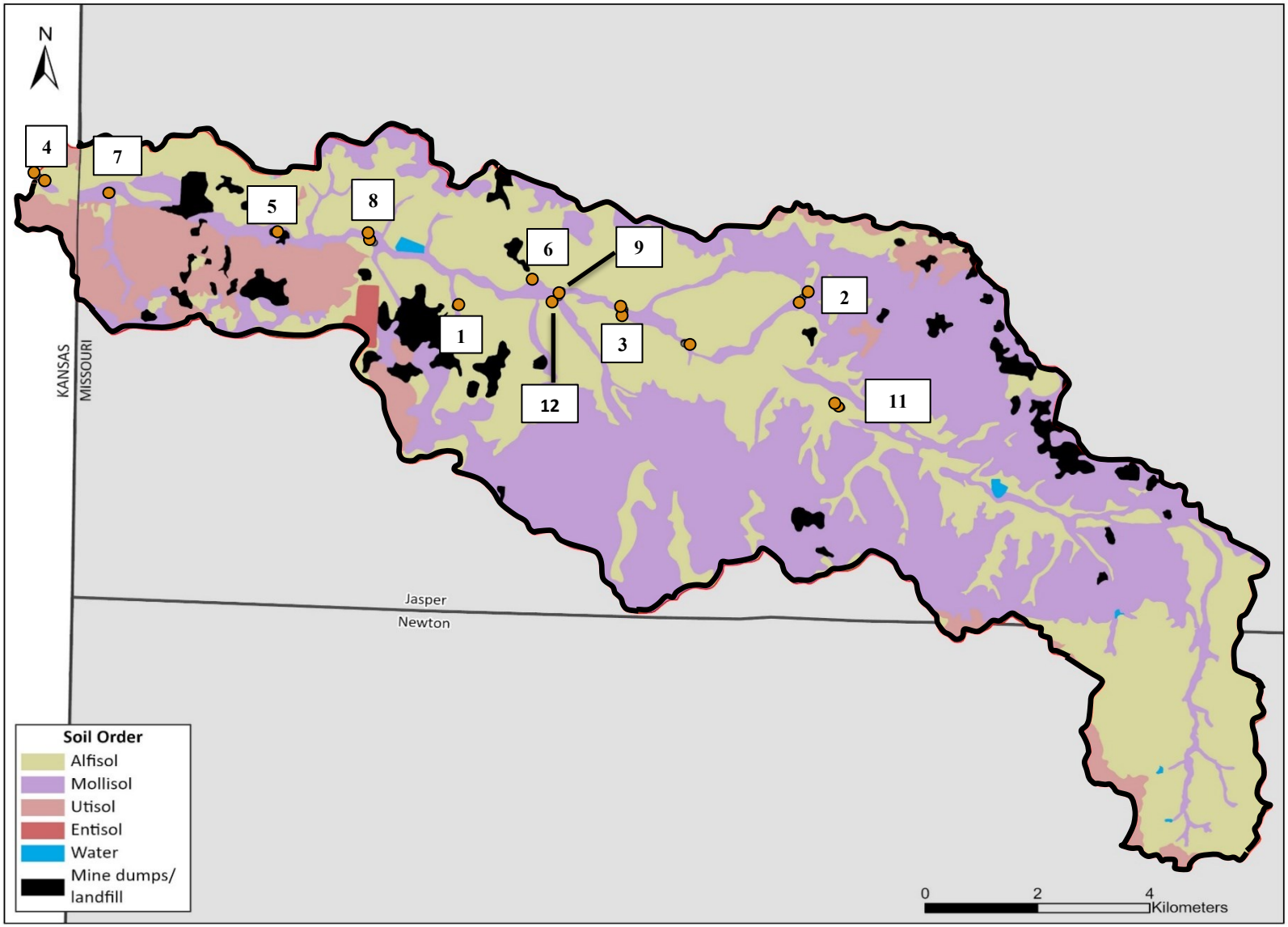

Figure 4. Soil order and site locations (NRCS, 2020).

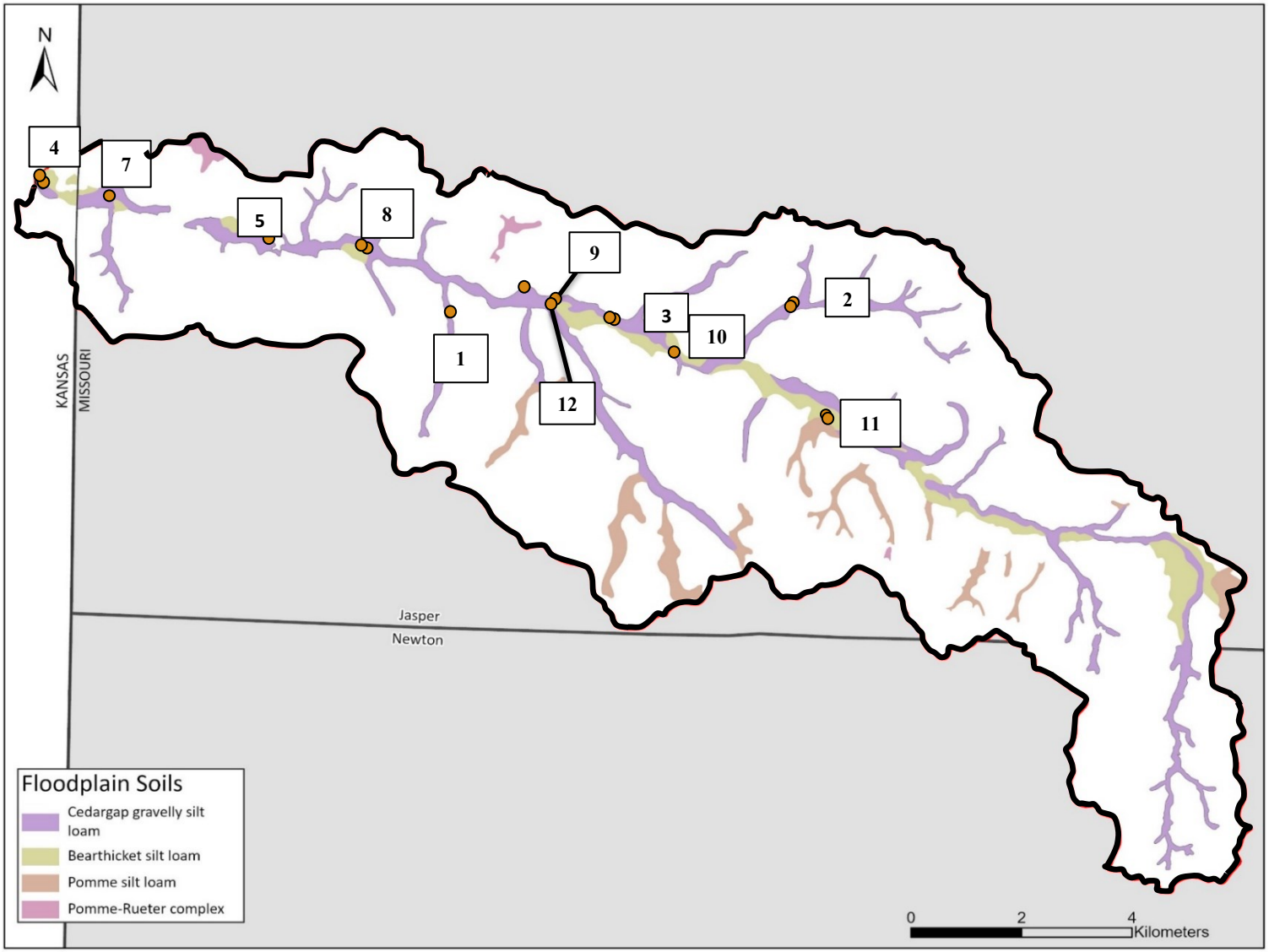

Figure 5. Floodplain soils and site locations (NRCS, 2020).

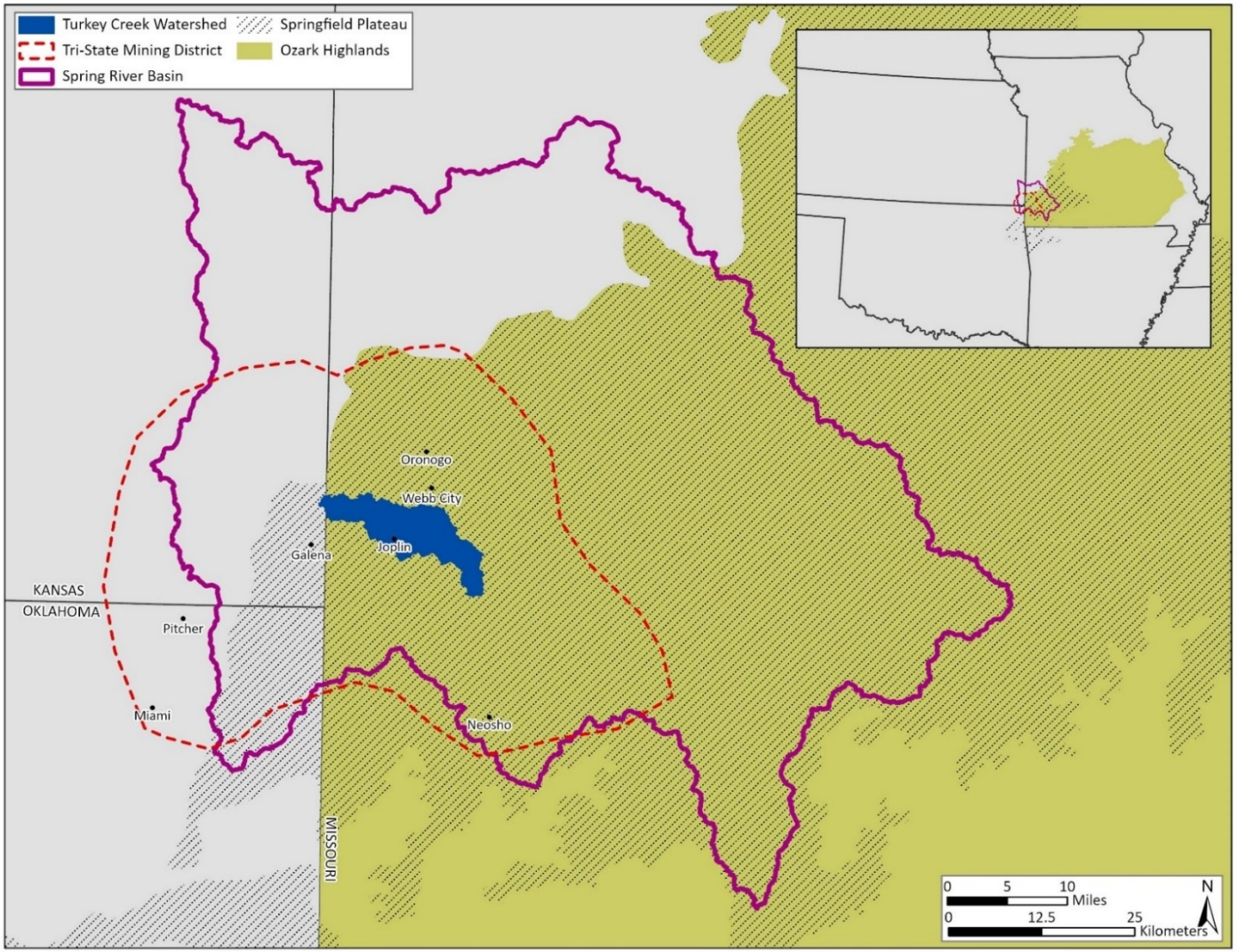

Figure 6. Turkey Creek Watershed and its location within the Spring River Basin and the Tri-State Mining District.

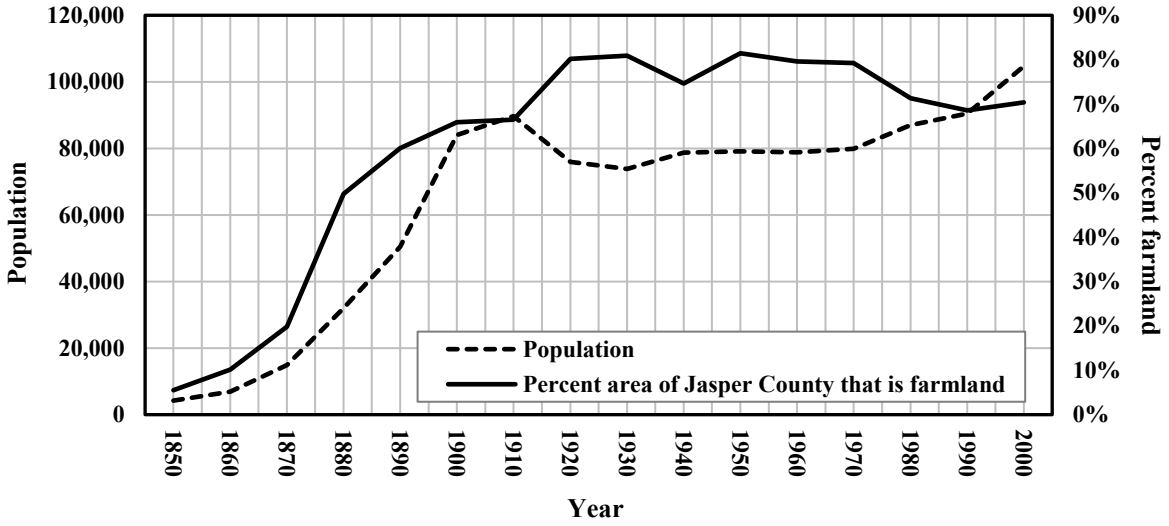

Figure 7. Historical land use records (USDA, 2021) and population data from 1850- 2000 for Jasper County, Missouri (Belby et al., 2019; Manson et al., 2021).

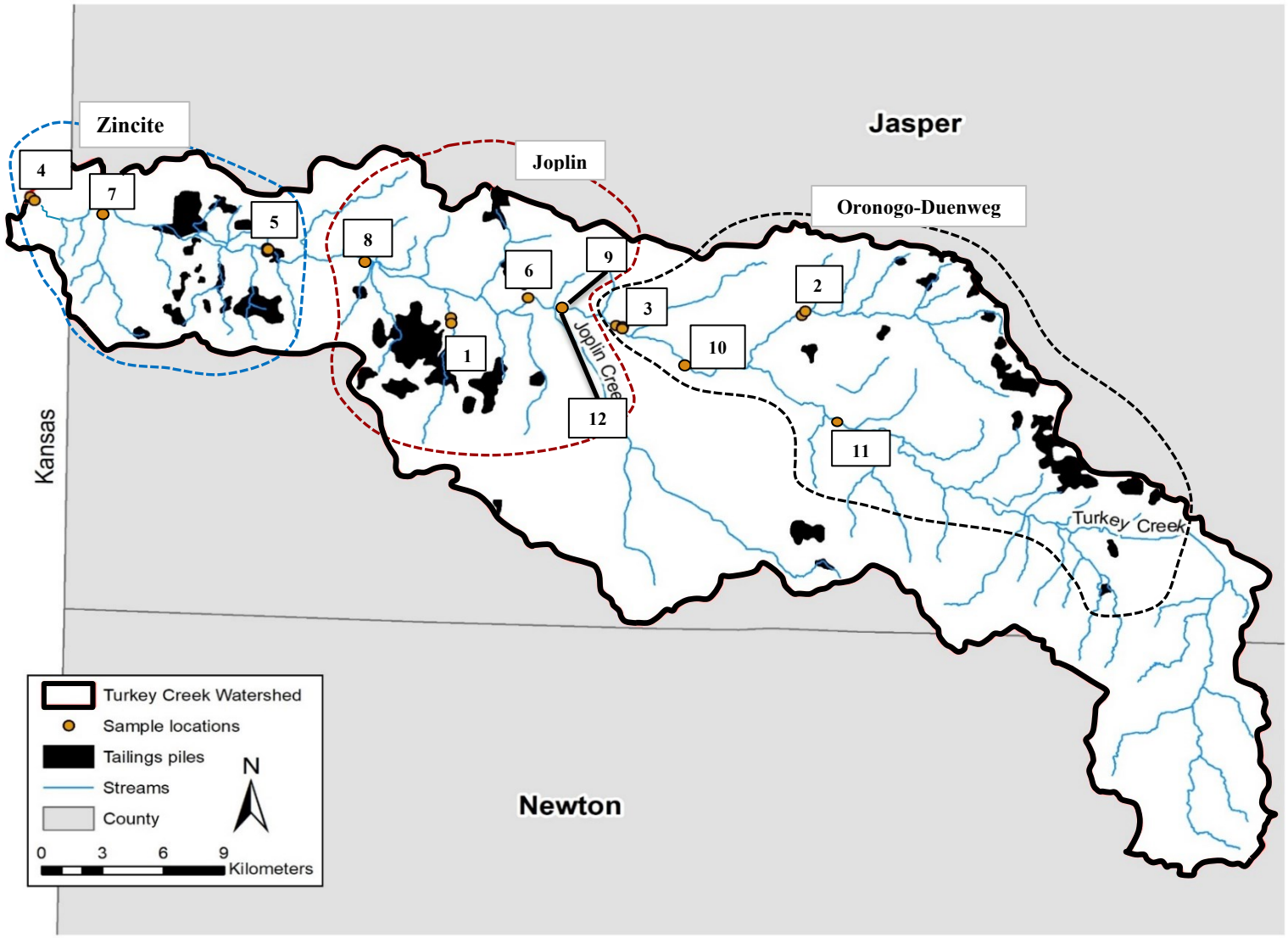

Figure 8. Sample sites and mining sub-district boundaries.

METHODS

Sites were selected according to accessibility and safety was our first priority, as we had to avoid trespassing and find areas where we could safely approach the floodplain and channel. Nevertheless, sampling sites were distributed along tributaries and the upper, middle, and lower segments of the main channel to examine watershed-scale trends in sedimentation. We chose areas containing a variety of valley floor landforms (terraces, floodplains, and benches). Each site has a site number and main channel sites have locations by river kilometer with 0 km at the mouth at Spring River and increasing upstream ending at 30 km. Some sites contain more than one cutbank (sample profile), where this occurred the site number will be accompanied by a bank number as well.

Field Methods

This study sampled cutbanks at a total of 12 sites, three of which were on tributaries (sites 1, 2, and 12) and nine on the main channel (Figure 8). The main channel was grouped into three segments: upper (R-km 19.3 – 13.4) above the confluence of Joplin Creek; middle (R-km 12.5 – 7.9) below Joplin Creek and in the Joplin Sub-district; and lower (R-km 5.6 – 0.1 km) draining the Zincite Sub-district to the Spring River confluence (Figure 8). The upper segment (Sites 11,10, and 3) contains two floodplain, four terrace, and two bench profiles (Table 4). The middle segment (Sites 9, 6, and 8) contains four floodplain, one bench profiles. And the lower segment (Site 5, 7 and 4) contains four floodplain, one terrace and two bench profiles. A total of 340 samples were collected and distributed as follows: tributaries (42); upper segment (88); middle segment (81); and lower segment (129) (Table 4).

Landform Identification. This study sampled three types of alluvial landforms at each study site including terrace, overbank floodplain, and bench deposits. Floodplains were formed during the historical period from initial settlement to present in response to changes in sediment and flood regimes. They typically form to the elevations required for the channel to contain the 1-2 year flood under present conditions (Wolman and Leopold, 1957; Rosgen, 1995). In Turkey Creek below mining areas, overbank deposits accumulating since the mid-1800s are contaminated with Zn and Pb and often overlie pre-settlement floodplains marked by buried soils or older channel bed or bar deposits as channel fills.

Terraces were floodplains active during the late Pleistocene or Holocene Epochs prior to Euro-American settlement, but since then the channel has incised to form a meander belt and new floodplain at a lower elevation so that the terrace is not inundated by annual flood (Wolman and Leopold, 1957). Terrace surfaces sampled for this study are typically covered by a thin (<0.5 m) deposit of historical overbank sediment since they were less frequently over-topped by floods compared to lower elevation floodplain deposits (Wolman and Leopold, 1957; Macklin et al., 1994). It is possible that terrace surfaces represent the primary valley floor or even floodplain prior to Euro-American settlement. Historical channel incision may have occurred during the mining period due to increased upland runoff and larger floods due to soil and vegetation disturbance, artificial channelization, urbanization, or mining disturbances along the main channel and tributaries of Turkey Creek. Tributary floodplains may have been subjected to high rates of sedimentation and associated mining contamination in the middle 1800s. However, channel incision and widening during the historical period may have effectively "terraced" the old floodplains thus preventing them from receiving much contaminated historical overbank sediment during the peak mining period (Knox, 1987; Macklin et al.,1994).

Benches are alluvial features representing relatively recent deposits along the margins of the channel with bank heights below the current floodplain surface (Trimble, 2009). They are generally inset within the bankfull channel, and are assumed to have formed as the result of deposition in over-widened channel due to reduction in flooding and stream power during watershed recovery (i.e., conservation practices and increased vegetation growth) in the post-mining period (Trimble, 2009). However, in some reaches, bank erosion is reducing bench areas possibly due to urban expansion and the related increase in stormwater discharges into Turkey Creek (Trimble, 2009). Typically, benches will be entirely contaminated since they formed after mining began and with previously contaminated sediment eroded from historical deposits or remaining abandoned tailings piles (Trimble, 2009).

Sampling. At each study site, samples were collected at exposed cut-banks from several landforms. Samples were collected in 10 and 20 cm vertical intervals from the top of the bank to the waterline or channel bed. Smaller increments of 10 cm were used in the post-anthropogenic stratigraphy usually in the upper 1-1.5 m of the profile. Larger sampling increments of 20 cm were used in the deeper portions of the profile in terraces since we were not as concerned with vertical variations in background metal concentrations in deposits that were clearly of pre-settlement age. Slumped, loose, or sun-dried sediment or organic matter was cleaned off from the cut using a shovel to reveal a clean surface assumed to represent primary alluvial deposition. The cleaned cut surface was sampled in depth profile from the bank using a 3” square ended trowel next to a hanging tape line with “0” at the surface. A subsample from each trowel grab was collected from portions of the bulk sample not in contact with metal and put into labeled quart size zip-lock bags for transportation and storage until processing in the laboratory at the Ozarks Environmental and Water Resources Institute at Missouri State University.

Cross section surveys using a hand-level and stadia rod along a pulled tapeline were collected at each sampled bank to measure channel width, depth, and bank height in relation to the thalweg of the channel. The locations of cross-sections and sampled banks were recorded using GPS.

Laboratory Methods

All sample processing and analyses occurred in the Ozarks Environmental Water Research Institute's (OEWRI) geomorphology laboratory at Missouri State University. Upon return to the laboratory, sample bags were opened and dried in ovens at 60℃ for approximately 72 hours. Once dry, each sample was disaggregated with a mortar and pestle before being put through a 2 mm sieve, separating the sample into two size fractions of, >2 mm and <2mm. Each size fraction was weighed separately, and a percent total mass was calculated for each size fraction. Once samples were adequately dried, sieved and weighed geochemical analyses could be conducted on the <2mm size fractions.

X-Ray Fluorescence Spectrometer. The <2 mm size fraction was analyzed using a Thermo Scientific Nitron XL3t 500 series handheld X-ray fluorescence (XRF) instrument to determine concentrations in parts per million of Zn, Pb, Ca, and Fe (Appendix A) (OEWRI, 2021). Each sample was put in a lead-free bag and processed for a 90 second run-time in the instrument. A duplicate, blank, and standard were run every tenth sample. Based on the duplicate samples there was a mean percent difference of 4.2% for Pb, 3% for Zn, 1.2% for Fe, 1.5% for Ca and 7.1% for Cd. Besides Cd, all the elements fell under the optimal error (< 5%) and the resulting median error was 0.3% (Appendix B & C).

To ensure the accuracy of the instrument, a subset of samples was sent to a commercial laboratory for inductively coupled plasma mass spectrometry (ICP-MS) analysis of aqua regia extracts using hot concentrated hydrochloric and nitric acids. The results of ICP-MS were used as a standard to calibrate the XL3t XRF through regression analyses (Table 5). Linear regression results indicated strong correlations (r^2= 0.99) between XRF and ICP-MS results. Equivalent aqua regia/ICP-MS concentrations could be calculated by multiplying the pXRF concentration by 0.89 for Zn, and 0.98 for Pb, 0.99 for Ca (Table 5). Comparisons between the two methods were not as strong for Fe. The best-fit conversion equation for Fe was: 0.81 XRF ppm + 8,853 ppm (R^2= 0.82) (Table 5).

Percent Organic Matter. Standard loss on ignition procedures (LOI) were used to determine vertical trends in organic matter in Turkey Creek banks (OEWRI, 2007). Organic content can be used to help determine the presence of buried soils or pre-settlement soils in overbank profiles (Owen et al., 2011). Organic matter content is determined by use of weight loss on ignition of the <2 mm size fraction. Five-gram sub samples were placed in the crucibles and their pre-burn weight was recorded. The samples were then placed in the oven at 105℃ for two hours to remove moisture and their first post-burn weight is recorded. The dried samples are then placed in a muffle furnace for 8 hours at 600℃ to incinerate all organic matter. Once samples are removed from the muffle furnace a final post-burn weight is recorded, and percent organic matter is calculated (Appendix D). To ensure procedure accuracy a duplicate was run every tenth sample and relative percent error was calculated for each sample and duplicate. A less than 5% error is optimal and the median error (1.5%), mean error (1.9%) (Appendix E).

Land Use and Mining Chronology

The mining history of the watershed was determined separately for the Oronogo-Duenweg, Joplin, and Zincite subdistricts to support the higher-resolution analysis of mining-metal profile dating at sampling sites located within the local drainage of each subdistrict (Table 6, Figure 8). Approximate subdistrict boundaries were determined based on written accounts of mine locations as well as a map with known mine locations (Figure 8 & 9) (Winslow et al., 1894). A detailed mining timeline was created based on several different sources that described general history of the watersheds mine production as well as specific mine production records of Pb and Zn ores in tons (Winslow et al.,1894; Martin, 1945; Hagni et al., 1986; Hinrichs, 1996) (Figure 10, 11). Historic land use records (USDA, 2021) and population data (MCDC, 2022; Manson et al., 2021) were also considered in creating this timeline as years of greater population growth and percent area of farmland often aligned with peak metal production (Figure 7).

ArcGIS Analyses

Drainage areas for the Turkey Creek watershed and above each sampling site were delineated using a 1-m LiDAR DEM from the Nation Map as part of the 3D Elevation Program (USGS, 2021b). The sub-basin drainage area was calculated at each site in ArcGIS Pro (3.1) using the hydrology tools. The 1-m DEM was mosaiced into a single dataset then the hydrology tools were used in the following order: fill, flow direction, flow accumulation, con, stream link, stream order, stream to feature. From here pour points were created at each site and snapped (using the snap pour point tool) to the closest flow accumulation cell then the watershed tool was used to calculate the drainage area at each pour point for all sites.

Channel slope and valley width were also derived from GIS analysis. Using the same 1-m DEM (USGS, 2021b). A longitudinal profile was created at each sample site in ArcGIS at a

distance of 20 times the channel width (Rosgen, 1995). Elevation at each end point of the longitudinal profile was obtained from the 1-m DEM and then a rise over run equation was applied to calculate slope.

Cross section data from the field, channel slope and roughness coefficients of the channel (Mannings N) were entered into U.S. Geological Survey Cross Section Analyzer (Version 17) (USGS, 2016) to calculate discharge at bankfull stage. A Mannings N for sections of the cross section within the channel were given a value of 0.035, representing a winding channel with some pools and shoals. While portions of the cross sections on the floodplain surface were given a value of 0.09, representing a floodplain with a very large amount of vegetation including dense brush and timber or mature field crops (Chow, 1959; Arcement and Schneider, 1989). Discharges from this study were used in flood-peak discharge regression equations for streams that drain rural and urban areas in Missouri (USGS, 2001). This provides an estimate of how often these landforms are being overtopped with floods.

Background and Threshold Level Calculations

Background variations in geochemistry were evaluated by both segment location and landform (i.e., terraces, overbank floodplains, and benches). Background was calculated by two methods 1. Average of samples below the thin enriched later (> 30 cm) in terraces and 2. Overbank floodplain deposits were separated by the location of the buried soil into historical (above) and late Holocene (below) units. An average of Zn and Pb in the deepest three samples of each of these profiles was calculated to obtain background values for the main channel and the deepest three samples in terraces were averaged to calculate an upland/general background.

Sedimentation Rates

Mine production records and land use history were compared to overbank profiles that have been receiving consistent sedimentation before, after and during the mining period. We chose to associate Ab horizon depths with the year 1850 as this was when population, agriculture/land clearing, and early mine productivity began to rise. From here inflections in the Zn and Pb concentrations within the profiles were associated with the mining and land use records to create a measuring tool allowing for the calculation of sedimentation rates. This method of calculating sedimentation rates has been successfully used in Europe (Macklin, 1985; Macklin et al., 1994; Parker et al., 2022), the upper Midwest and eastern United States (Knox, 1987; Lecce, 1997; Lecce and Pavlowsky, 2001, 2014), and in the Ozarks (Carlson, 1999; Owen et al., 2011; Jordan, 2018).

Table 4. Sample identification and characteristics.

	Site	Bank	Landform	Profile depth (m)	Number of samples	River km	Drainage Area (km^2)
Tributary	1	b	Floodplain	1.7	17	9.8	3.3
	2	b	Floodplain	1.1	9	16.9	8.8
	2	a	Terrace	1.4	10	16.9	8.8
	12	a	Floodplain	1.6	15	12.4	17.5
Main Channel	11	b	Floodplain	1.6	12	19.3	39.7
		a	Terrace	1.1	9	19.2	
	10	a	Floodplain	1.2	12	15.3	58.0
		b	Bench	1.3	9	15.3	
		c	Terrace	1.0	4	15.4	
	3	b	Terrace	2.3	13	13.8	62.0
		a	Terrace	2.0	15	13.6	
		c	Bench	1.4	14	13.4	
	9	a	Floodplain	2.0	18	12.5	64.8
		b	Bench	1.2	6	12.4	
	6	a	Floodplain	2.1	16	11.7	83.2
	8	a	Floodplain	2.2	18	8.0	101.8
		b	Floodplain	2.3	23	7.9	
	5	b	Bench	1.2	10	5.6	107.5
		a	Floodplain	2.3	19	5.6	
		c	Floodplain	0.8	8	5.5	
	7	b	Bench	1.3	13	1.9	115.5
		a	Terrace	2.5	34	1.9	
	4	b	Floodplain	2.1	18	0.2	121.4
		a	Floodplain	2.8	27	0.1	

Table 5. XRF and Aqua Regia correlations.

		AQR/XRF			XRF to AQR correction	
Metal	XRF DL or range	Ratio	Cv%	n	R^2	Equation to calculate AQR
Cu	30-40 ppm	1.17	24	10	0.87	= (50.5 x ln XRF ppm) - 126.3
Ba	NA	0.39	25	20	0.36	= 67.7 e^ 0.002 XRF ppm
Cd	5-10 ppm	1.02	22	13	0.97	= 1.049 x XRF ppm
Zn	NA	1.13	21	19	0.99	= 0.893 x XRF ppm
Pb	<120 ppm XRF	1.52	18			
Pb	>120 ppm XRF	0.98	10			
Pb	all values			21	0.99	= 0.967 x XRF ppm
Ca	NA	0.89	19	21	0.99	= 1.003 x XRF ppm
Fe	<15K ppm XRF	1.58	17		0.97	= 1.136 x XRF ppm
Fe	>15K ppm XRF	1.10	10			
Fe	all values			18	0.82	= 0.808 XRF ppm + 8,853
Mn	NA	1.30	18	18	0.97	= 1.310 x XRF ppm

Table 6. Sites and locations within the mining sub-districts.

Sample sites and locations		
Upper (Oronogo-Duenweg Sub-district)	Middle (Joplin sub-district)	Lower (Zincite Sub-district)
11	9	5
2	12	7
3	6	4
10	1	
	8	

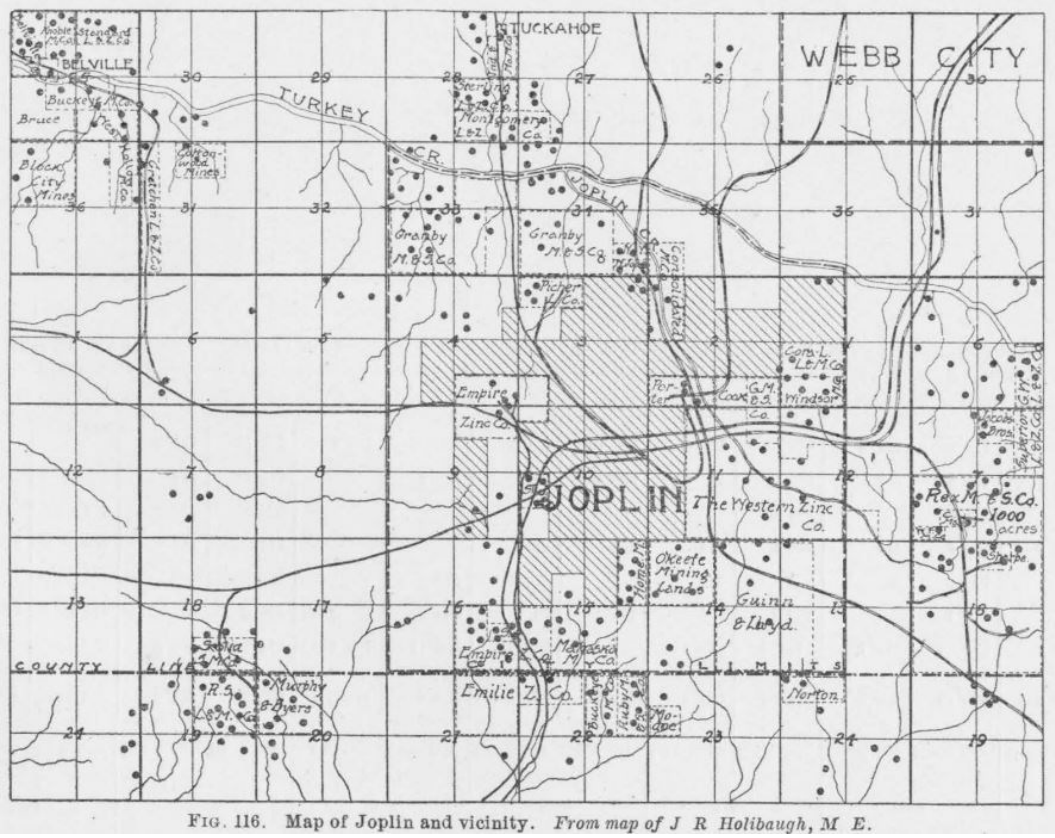

FIG. 116. Map of Joplin and vicinity. *From map of J R Holibaugh, M E.*

Figure 9. Historical map of mine company and camp locations (Winslow et. al., 1894).

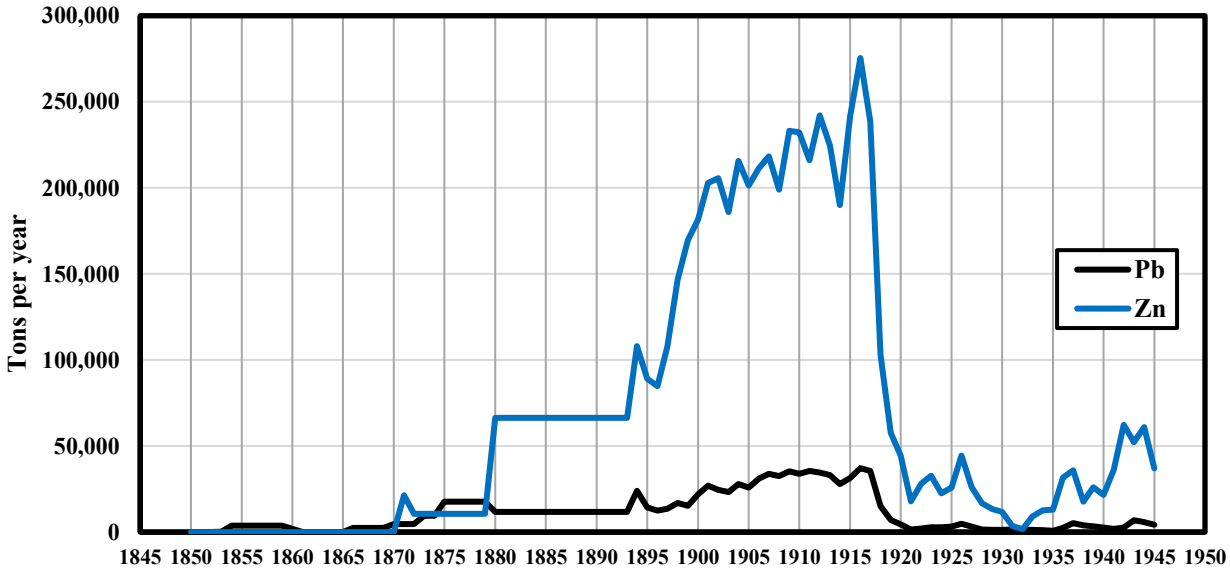

Figure 10. Zinc and Lead production (tons) from all three sub-districts from 1850 – 1940 (Martin, 1945; Winslow et al., 1894).

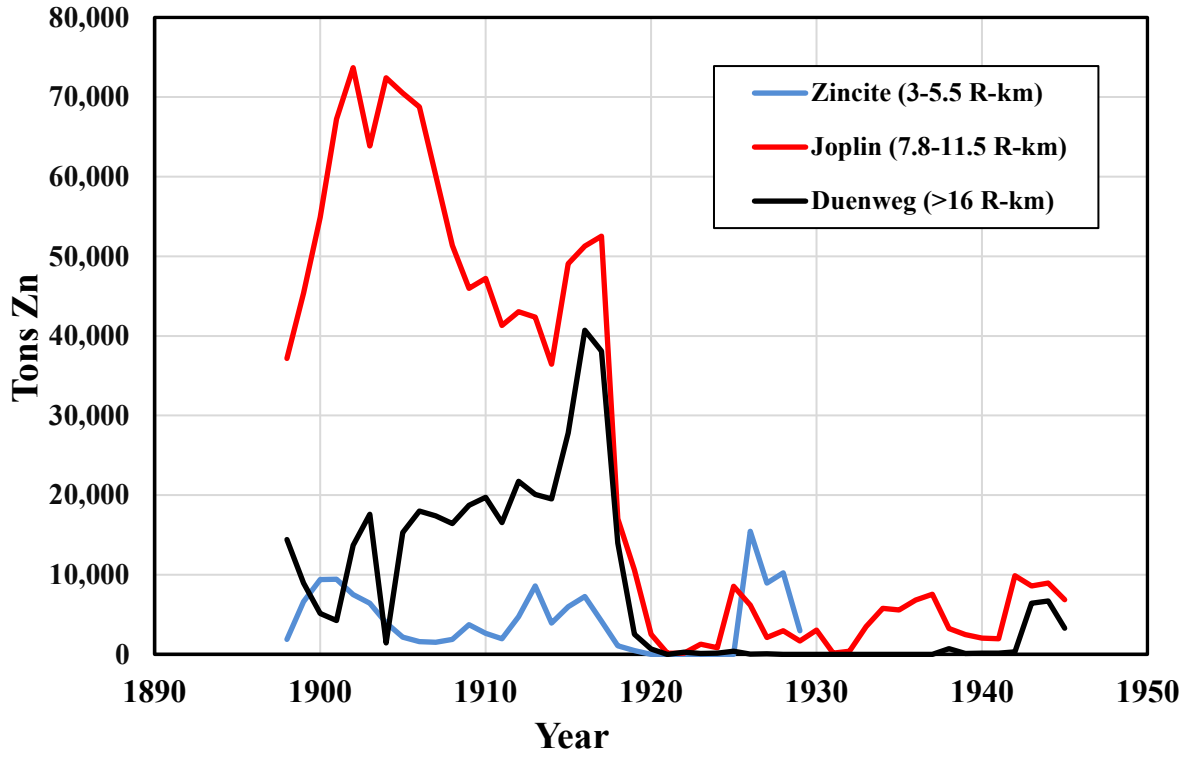

Figure 11. Zinc production at each sub-district from 1898-1945 (Martin, 1945).

RESULTS

The purpose of this chapter is to report hydrologic and geomorphic characteristics and describe stratigraphic relationships in Turkey Creek channel and bank deposits. Geochemical trends for each core are evaluated and compared to the historical mining production records. The combination of core stratigraphy and profile inflections of percent organic matter, Zn, Pb, Ca, and Fe concentrations were used to date the cores and calculate floodplain sedimentation rates since settlement in the 1840's.

Channel Form and Hydrology

Drainage areas for sites on the main channel ranged from 39.6-121.5 km² and tributaries from 1.3-6.7 km² (Table 4). The sampled tributary sites drained to the upper (19.3-13.4 km) and middle (12.5-7.9 km) segments of the watershed. Overall, channel variables showed good relationships with drainage area (Figure 12). Channel slope ($R^2 = 0.669$) decreased with drainage area as expected (Figure 12). The bank-full channel was defined based on field indicators and stratigraphy with flow stage assumed to be at the top elevation of the sampled floodplain banks. Channel ($R^2 = 0.633$) and valley ($R^2 = 0.587$) widths both increased in a similar trend with drainage area (Figure 12). Channel depth also increased downstream for maximum depth ($R^2 = 0.568$) (i.e., height from the channel bed at the thalweg to the top bank elevation of the floodplain) and average depth ($R^2 = 0.378$) (Figure 12). The strongest drainage area correlation among the variables assessed was for cross-sectional area ($R^2 = 0.739$). Overall, velocity showed no trend with drainage area averaging about 1.5 m/s across all sites with a lot of variability, but bank-full discharge ($R^2 = 0.654$) increased at approximately 2/3 power over drainage area

(Figure 12). Bank-full channel variables derived from field data for this study were checked against regional regression equations (USGS, 2001). The published equations were typically based on channel measurements from larger drainage areas compared to this study (USGS, 2001). However, flow frequency analysis for bank-full channels generally yielded an acceptable range from 1 to 5-year recurrence intervals for Turkey Creek (USGS, 2001).

Sedimentology and Stratigraphy

The valley floor landforms sampled along Turkey Creek were classified into four types based on cutbank stratigraphy: (i) Terrace, (ii) Channel fill floodplain-A, (iii) Overbank floodplain-B, and (iv) Bench (Table 7). There were seven terraces sampled in this study, five in the upper segment and two in the lower segment (Table 7). Terraces are typically mapped in the Cedargap alluvial series but often occur in areas mapped as the Bearthicket Series (NRCS, 2020). Terraces sampled along Turkey Creek are better described by the Bearthicket series formed in silty alluvium containing Argillic (Bt) horizons (3a, 3b, 5a) (NRCS, 2020) (Figure 13). Terrace landforms are typically only contaminated with low to moderate levels of heavy metals in the upper 0.3 m of the core.

Floodplain cutbank cores were generally composed of two different floodplain facies: channel-fill and overbank floodplain. The channel-fill facies (Floodplain A) contain a pre-settlement Holocene unit typically about < 1 m thick, composed of fine-grained overbank deposits overlying coarser channel bed or bar deposits with top elevations just above the present-day low flow water line (Figure 14). A thin (<0.1 m) and weakly developed buried soil (Ab) or organic rich bed often occurs in or just above the pre-settlement bench or old channel bed. Field observations of several Floodplain A exposures suggest that overlying legacy sediment may have

been deposited within a multi-channel or anastomosing channel system with wetland characteristics. Clayey residuum is sometimes exposed at the bottom of the Floodplain A cutbanks near the channel bed suggesting that bed incision or channel enlargement has occurred or may be active today. While the selection of sampling sites was affected by logistics and channel scale, bank profiles with channel fill features evaluated for this study were evenly distributed in the upper, middle, and lower segments of the watershed (Table 7).

Overbank floodplain facies (Floodplain B) typically contain a Holocene alluvial unit about 1.6 m thick on top of which is formed a dark and fine-grained Ab horizon typically 0.1 to 0.3 m thick (Figure 15). Compared to the channel-fill facies, the overbank facies usually have a better developed buried soil profile including a thicker and more organic-rich Ab horizon. The relatively dark Ab horizon usually overlies a weak B (Bw) or Bt horizon suggesting the occurrence of a pre-settlement Mollisol or prairie vegetation on the late Holocene floodplain. These profiles were found more often along the Middle segments of the watershed (Table 7). Both the channel fill A and overbank B floodplains are typically contaminated throughout the entire core depth overlying the pre-settlement Ab horizon at depths >1 m (Figure 14 & 15).

Bench deposits are inset within the bank-full channel with bank top elevations <0.7 m below the floodplain surface. They are usually silty deposits interspaced with layers of sand and fine gravel indicating periods coarser sediment transport nearer the bed during flood events. Benches represent stable bar surfaces or places where the channel is filling or narrowing to possibly form future floodplains over time. They lack developed soil horizons except for the occasional surface A-horizon and are contaminated by mining throughout the entire profile indicating they have formed with mining-contaminated sediment beginning about 1900 (Figure 16).

Contamination of Alluvial Deposits

The standards to identify contaminated sediments in this study are based on the EPA PEC threshold for sediment toxicity at 2,083 ppm Zn and 150 ppm Pb (Table 2). They were chosen as the threshold concentration for contaminated sediments in this study because they were determined specifically to indicate ecological toxicity under TSMD conditions (Ingersoll et al. 2009; Juracek, 2013). Therefore, where samples exceed the TSMD PECs in the profile, the sediment is deemed contaminated for the purpose of this study. However, these standards are more stringent than actions levels for remediation at 6,400 ppm Zn and 400 ppm Pb (EPA, 2004, 2010).

The maximum height of terraces generally increases with drainage area and downstream (Figure 17). The overall depth and percent of maximum height of contamination (Zn) in terraces also both generally increase with drainage area (Figure 18). However, terrace banks were not sampled within all segments of the watershed since wider valleys and meander belts downstream limited channel contact with the valley margin. Terraces are typically only contaminated in the upper 0.3 m and usually only 10% or less of the total profile contains samples exceeding the TSMD PEC (Table 8, Figure 18). Depth of contamination in floodplains ranged from 0.3 – 2.8 m (mean = 1.8 m, median = 1.9 m) and usually more than 40% of each core is contaminated (mean = 68%, median = 71%) (Table 9, Figure 18). Floodplains also generally see an increase in bank height with drainage area by up to 1.75 times (Figure 17). Floodplain A – channel fill facies typically have smaller bank heights compared to the Floodplain B – overbank facies (Figure 18). Depth of contamination in floodplains increases with drainage area, percent contamination generally increases as well but with a little more downstream variation (Figure 18). Bench maximum heights remain constant relative to drainage area (km^2). Benches decrease downstream, both in contamination depth and total percent of bank height contaminated (Figure

18). More than 60% of each bench profile is contaminated (mean =71%, median 72%) (Table 10).

In general maximum and average Zn and Pb concentrations from each core increase with drainage area in terrace, floodplain, and bench profiles (Figure 19). Overall terraces contain the lowest average concentrations of Zn (mean = 712 ppm) and Pb (mean = 140 ppm). Floodplain (Zn mean = 8,447 ppm) (Pb=1,349 ppm) and bench profiles (Zn mean = 9,919 ppm) (Pb mean = 980 ppm) have similar average concentrations (Tables 11, 12, & 13). The greatest concentration of Zn (44,072 ppm) in this study occurred in a bench profile at site 7b (1.9 r-km) (Table 13). The greatest concentration of Zn found in terrace profile was also at site 7 (1.9 r-km) (7,171 ppm) (Table 12). Tributary floodplains 1a (Zn = 35,681 ppm) (Pb =9,978 ppm) and 12a (Zn =30,178 ppm) (Pb = 3,993 ppm) contain the greatest Zn concentrations out of all other floodplain cores and the greatest Pb concentrations among all landforms (Tables 11, 12, & 13). This is likely due to their proximity to early active mining areas.

The upper segment (Oronog-Duenweg sub-district) has the lowest overall average and maximum concentrations of Pb and Zn (Figure 20). The middle segment (Joplin sub-district) and tributaries have the greatest average and maximum concentrations of both metals, and two out of three tributary cores (1a and 12a) were located within the middle segment (Figure 20). The Joplin-sub-district was the highest producing district within the watershed, so it is not surprising that sites within the boundary are showing high concentrations of Pb and Zn (Figure 20).

The greatest soil (surface soil) concentrations of Pb and Zn were found in the middle segment of the watershed within or just upstream of the Joplin Sub-district ranging from 3,374-22,019 ppm for Zn and 719-2,713 ppm for Pb (Table 11, Figure 21). The lowest surface concentrations for both Pb (range = 43 – 305 ppm) and Zn (range = 338 - 3,611 ppm) were found

upstream of the Joplin sub-district (13.6 R-km) in the Orongo-Duenweg sub-district (Figure 21). More than 10 sample cores exceed the EPA level of concern for both Zn (6,400 ppm) and Pb (400 ppm), and more than 17 exceed the TSMD PEC both Zn (2,083 ppm) and Pb (150 ppm) (Figure 21). Among all sampled profiles the mean EPA LOC exceedance was 205% for Pb and 75% for Zn (Figure 21). On average floodplains surface concentrations exceed the EPA LOC by 192% Pb and 42% for Zn, benches exceed by 69% (Pb) and 10% (Zn), and terraces 14% (Pb) and 0% (Zn) (Figure 21). The upper segment (Oronogo-Duenweg sub-district) does not have any surface concentrations exceeding the EPA LOC for Zn or Pb (Figure 21). On average tributary sites exceed the EPA LOC by 218% (Pb) and 44% (Zn). The middle segment has average exceedances of 185% (Pb) and 42% (Zn) and the lower segment is 164% (Pb) and 41% (Zn) (Figure 21).

Average depths of peak Pb and Zn in floodplains are 1.02 m (cv% =21) (range = 0.65 – 1.25 m) and 1.04 m (cv% = 24) (range = 0.65 – 1.35 m) respectively (Table 14, Figure 21b). Generally, the depth to maximum concentrations of both Pb (1.05 m) (range = 0.55 – 2.25) and Zn (mean = 0.72 m) (range = 0.25 – 1.25 m) increases with drainage area in floodplains (Table 14, Figure 21b). Typically, Pb peaks at greater depths than Zn, on average there is a 0.4 m difference in depth between these peak concentrations of Zn and Pb, possibly because Pb mining began up to 30 years before Zn mining in Tukey Creek (Table 14, Figure 21b). The depth of maximum concentrations of Pb and Zn for both terraces and benches remain consistent (Tables 15 & 16, Figure 22 a & b). Every terrace core has a depth of maximum Pb and Zn of 0.05 m (cv% <1) (Table 16).

Background Concentrations

Two different background analyses were conducted using: 1) Terrace samples from below the contaminated zone and 2) Holocene or pre-settlement floodplain assumed to represent pre-mining geochemistry. Terrace samples below the mining-enriched zone (>0.5 m depth) from 11 cores (n = 65) yielded a mean background concentration of 229 ppm (Zn) (cv% = 148) and 15 ppm (Pb) (cv% =120) (Table 17). Holocene-age samples from below the buried soil from 10 floodplain cores (n = 55) yielded average concentrations of 2,309 ppm (Zn) (cv% = 27) and 178 ppm (Pb) (cv% = 154) (Table 18). Zinc and Lead concentrations in the historical unit (n = 144) (above the Ab horizon) were also calculated, yielding average concentrations of 3,626 ppm (Zn) (cv% = 41) and 494 ppm (Pb) (cv% = 154) (Table 18). On average Zn (2x) and Pb (3x) concentrations in historical units were greater than in the Holocene units (Table 18). Some Holocene deposits contain concentrations exceeding the EPA LOC for both Zn and Pb (Table 18). It is assumed that deeper Holocene floodplain samples were enriched by groundwater transport of metals from naturally weathering deposits or mining sources such as leaching from overlying contaminated zones or contaminated surface aquifers.

Mining Chronology

The key dates used to interpret geochemical profiles and date floodplain cores were based on settlement and mine production records as follows: 1850 – 1870, Pre-Zn mining; 1870-1890, rise of large-scale Zn mining operations; 1903 and/or 1916, peak production years; 1920 (the first major decline of production); and 1930 (end of significant mining in the watershed) (Table 19). Low levels of Euro-American settlement initially began in Turkey Creek watershed in the late 1830s. However, it is assumed that a critical threshold of land use development would be needed to accelerate deposition on Late Holocene floodplains. The earliest year in the mining

timeline in this study is 1850, this is where crude early Pb mining began (Table 19). The year 1850 is assigned to the pre-settlement surface in the floodplain profiles. There are no profiles in this study that we found to have an Ab horizon occurring before the assigned year of settlement and start of mining in 1850. The depth of the pre-settlement horizon was identified in each profile where Pb concentrations are present but typically low, organic matter is high and where our field observations noted stratigraphic characteristics of an Ab horizon (Appendix F). Between 1850 and 1870 there was an early pre-mining boom peak in Pb production (Table 19). Many profiles contain evidence of this early pre-mining boom Pb peak and can be identified by an inflection in Pb concentrations occurring before Zn concentrations rise 10-30 cm above the Ab horizon (Sites 1a, 2b, 6a, 8a, 4b, and 4a (Figures 22 & 23, Appendix F).

After the early spike in Pb mining, Zn concentrations in floodplain cores begin to rise (Appendix F). We assigned the year 1870 to the lower inflection point where the rise begins since historical documents mark the beginning of Missouri's mining boom at this time (Table 19, Figure 23 & 24). Shortly after the early Pb peak, Zn concentrations start to rise and Pb concentrations either fall or remain constant, this marks the transition into the early Zn period and the beginning of deep shaft mining operations (1870-1890) (Table 19). Large scale operations rapidly increased after 1890 which used more modern milling machinery to extract ores from host rock. During this period, Ca typically increased in core profiles and follows the same vertical trends as Zn, due to inputs of dolomitic tailings composed of coarse and finely-ground limestone and dolomite (i.e., carbonate rock) increased in Turkey Creek and its mined tributaries (Appendix F). A good example of this trend can be seen at floodplain site 8a between 80-100 cm and site 4a between 140-170 cm (Figures 23 & 24, Appendix F). As Zn and Ca begin to rise in the core after 1890, there were one or two Zn peaks. The first was assumed to be

associated with the Joplin sub-district's peak production year in 1903 (Figures 23 & 24). The second Zn peak was assumed to be associated with the overall production peak for the watershed including all mining sub-districts in 1916 (Table 19, Figures 23 & 24). Usually, the geochemical peak in Zn and Ca concentrations occurred at depths where we observed layers of tailings deposits and example of this can be seen in floodplain site 8a between marker B and C (Figure 23).

In Missouri, mining dramatically decreased after 1920, this is when most operations moved in earnest into Oklahoma to the Picher Field or into Kansas to the Galena mines. Then in 1930 the Great Depression finally forced the closing of most of the remaining mines in the watershed (Table 19). Therefore, the first dramatic decline in Zn and Ca concentrations in floodplain cores are associated with 1920 and depths where metals decrease further after that were associated with 1930 (Figures 23 & 24, Appendix F). In some cases, floodplain profiles (2b, 8b, 5c) did not show as much of a decline in Zn concentrations even at shallow depths (<20 cm) (Appendix F). It was assumed that where this occurred the floodplain surface stopped receiving significant amounts of contaminated overbank sediment due to channel enlargement reducing local flood inundation frequency and thereby effectively "terracing" the floodplains (e.g., Knox, 1987; Carlson, 1999; Lecce and Pavlowsky, 2001) (Appendix F).

Sedimentation Rates

On average, terraces were contaminated by Zn (> 2,083 ppm) and Pb (>150 ppm) in the upper 0.1 m of sediment (Table 8). From the depth at which Zn and Pb begin to rise to the top of the floodplain surface is 1850 – 2021 (year of sampling). Sedimentation rates range from 0.06 – 0.16 cm/yr with an average of 0.1 cm/yr in terraces. Benches are the most recently formed

landform and likely started forming as a result of channels adapting to large influx of sediment from agriculture and mining post-settlement. There are no developed soil horizons to mark dates of production years, but they are completely contaminated with mining sediment therefore are assumed to have been deposited between peak mining and the present (1916 – 2021) not accounting for the possibility of large deposition events from floods. Based on this assumption and the measured depths of contamination, benches sedimentation rates ranged 1.0 – 1.3 cm/yr (Table 10).

Floodplain cores contain a sedimentation history spanning from settlement and the start of mining in 1850 to the post-mining era from 1930 to the present (Figures 23 & 24). Sedimentation rates in floodplains were greatest during the peak mining years (1890-1920) (mean = 1.7) and the overall mining period (1870-1930) (mean = 1.6 cm/yr) (range = 0.8 – 2.5 cm/yr) (Table 20). There is an increase from pre-mining (1850-1870) (mean = 1.0 cm/yr), the rise to peak mining (1870-1890) (mean = 1.2 cm/yr) and peak (1890-1920) (1.7 cm/yr) (Table 20). Rates during the pre-mining boom period range from 0.5 – 1.5 cm/yr (Table 20). Post mining rates were the lowest with an average of 0.2 cm/yr (range 0 – 0.7 cm/yr) (Table 20). Pre-mining rates were greatest in tributary (Drainage area < 26 km²) (mean =1.3 cm/yr) and the upper segment of the watershed (Drainage area 26 – 78 km²) (mean = 1.5 cm/yr) (Figure 25). The pre-mining rates decrease with drainage area, 78 – 104 km² (0.9 cm/yr) and 104 – 177 km² (0.8 cm/yr). Mining rates increase with drainage area, < 26 km² (1.0 cm/yr) to 104 – 177 km² (1.9 cm/yr) (Figure 25). Average post mining rates for tributaries, upper and middle segments are 1.0 cm/yr but in the lower segment (largest drainage area) rates increase to 0.4 m/yr (Table 20, Figure 25).

On average overbank floodplain cores (Floodplain B) had higher sedimentation rates than channel fill cores (Floodplain A) during all historical periods other than the peak mining years (1890-1920) (Figure 26). The highest sedimentation rates in the overbank floodplain cores (Floodplain B) occurred during the pre-mining (1.8 cm/yr) and post-mining periods (1.6 cm/yr), these periods also contained the greatest difference in sedimentation rates between floodplain A and B cores (Table 20, Figure 26).

Some sites (2b, 8b and 5c) have zero cm/yr (or small enough values that the 10 cm sampling intervals were not small enough for calculations) and one site that was capped with tailing likely during the end of the major mining period (1930) (site 1a) (Table 20, Appendix F). These floodplain surfaces were terraced most likely due to channels responses (incision and widening) to influx of sediment from agriculture and mining activities. These terraced profiles occur in tributaries (2b), middle segment (8b) and the lower segment (5c) (Table 20, Appendix F).

Table 7. Sample cores and associated landforms by watershed segment.

Stratigraphy type		Segments		
		Upper	Middle	Lower
	Terrace	2a		5c
		11a		7a
		10c		
		3b		
		3a		
Floodplain	Floodplain A: Ab overlying old channel bed	11b	12	4b
		10a	1a	4a
	Floodplain B: Ab overlying finer grain pre-settlement floodplain	2b	9a	5a
			6a	5c
			8a	
			8b	
	Bench	10b	9b	5b
		3c		7b

Table 8. Depth of contamination and percent of the total core that is contaminated in terrace profiles.

River-km	Drainage area (km^2)	Terrace Site ID	Ht to Thalweg (m)	Depth of Contamination (2,083 ppm Zn)	Depth of Contamination (150 ppm Pb)	Total Contaminated (Zn)	Total Contaminated (Pb)
16.9	8.7	2c	1.9	0.0	0.0	0%	0%
19.2	39.7	11a	2.1	0.2	0.2	10%	10%
15.3	58.0	10c	2.7	0.0	0.1	0%	4%
13.8	62.0	3b	3.3	0.0	0.2	0%	6%
13.6	62.0	3a	3.0	0.3	0.0	10%	0%
1.9	115.5	7a	3.2	0.2	0.2	6%	6%
	Mean		2.7	0.1	0.1	0.04%	0.04%
	Median		2.9	0.0	0.2		

Table 9. Depth of contamination and percent of the total core that is contaminated in floodplain profiles.

River-km	Drainage area (km^2)	Site	Ht to Thalweg (m)	Depth of Contamination (Zn)	Depth of Contamination (Pb)	Total Contaminated (Zn)	Total Contaminated (Pb)
9.8	3.3	1a	1.8	1.7	1.7	94%	94%
16.9	8.8	2	1.6	0.3	0.6	19%	37%
12.4	17.5	12a	2.6	1.3	1.6	50%	62%
19.3	39.7	11b	2.1	1.6	1.6	78%	78%
15.4	58	10a	2.0	0.7	0.7	34%	34%

Table 9 continued.

12.5	64.8	9a	3.3	0.7	0.5	21%	15%
11.7	83.2	6a	3.4	2.0	2.0	60%	60%
8.0	101.8	8a	3.4	2.2	2.2	65%	65%
7.9	101.8	8b	3.0	1.4	2.0	46%	66%
5.6	107.5	5a	3.0	2.3	2.3	78%	78%
5.5	107.5	5c	2.1	1.0	1.0	48%	48%
0.2	121.4	4b	3.7	2.1	1.9	57%	51%
0.1	121.4	4a	3.4	2.8	2.7	82%	79%
	Mean		2.7	1.5	1.6	56%	59%
	Median		3.0	1.6	1.7		

Table 10. Depth of contamination and percent of the total core that is contaminated in bench profiles.

River-km	Drainage area (km^2)	Bench Site ID	Ht to Thalweg (m)	Depth of Contamination (2,083 ppm Zn)	Depth of Contamination (150 ppm Pb)	Total Contaminated (Zn)	Total Contaminated (Pb)
15.3	58.0	10b	1.8	1.3	1.3	72%	72%
13.4	62.0	3c	2.0	1.4	1.4	72%	72%
12.4	64.8	9b	1.9	1.5	1.5	80%	80%
5.6	107.5	5b	1.8	1.2	1.2	67%	67%
1.9	115.5	7b	2.1	1.3	1.3	62%	62%
	Mean		1.9	1.3	1.3	71%	71%

Table 10 continued.

	Median	1.9	1.3	1.3			

Table 11. Maximum, surface, and mean concentrations of Zn and Pb in floodplain profiles.

River-km	Drainage area (km^2)	Floodplain Site ID	Zn concentrations (ppm)			Pb concentrations (ppm)		
			Maximum	Surface	Mean	Maximum	Surface	Mean
9.8	3.3	1a	35,681	22,019	14,853	9,978	2,713	2,713
16.9	8.8	2b	2,446	2,316	1,581	239	212	152.47
12.4	17.5	12a	30,178	5,201	13,991	3,993	1,061	2,186
19.34	39.7	11b	18,174	2,339	7,123	1,811	134	623
15.4	58	10a	5,404	3,611	2,752	510	305	228
12.5	64.8	9a	10,081	8,682	2,722	1,198	1,041	318
11.68	83.2	6a	26,632	12,537	12,329	4,562	1,749	1,465
8.02	101.8	8a	18,567	8,625	9,445	1,863	1,318	1,863
7.9	101.8	8b	28,099	12,270	8,336	2,162	1,150	724
5.56	107.5	5a	16,352	6,736	6,833	1,682	800	573
5.5	107.5	5c	14,110	11701	8702.6	1,193	1482	1,192
0.24	121.4	4b	20,620	9,184	10,563	1,349	874	1,349
0.14	121.4	4a	23,394	6,547	10,578	1,555	1,384	1,555

Table 12. Maximum, surface, and mean concentrations of Zn and Pb in terrace profiles.

River-km	Drainage area (km^2)	Terrace Site ID	Zn concentrations (ppm)			Pb concentrations (ppm)		
			Maximum	Surface	Mean	Maximum	Surface	Mean
16.9	8.7	2a	785	338	179	138	43	45
19.2	39.7	11a	2,408	1,773	1,359	306	205	115
15.3	58	10c	1,645	1,175	729	186	142	94
13.8	62	3b	2,935	2,587	183	217	176	59
13.6	62	3a	775	567	803	3,498	1,696	385
1.9	115.5	7a	7,171	3,729	1,020	844	466	143

Table 13. Maximum, surface, and mean concentrations of Zn and Pb in bench profiles.

River-km	Drainage area (km^2)	Bench Site ID	Zn concentrations (ppm)			Pb concentrations (ppm)		
			Maximum	Surface	Mean	Maximum	Surface	Mean
15.3	58	10b	12,933	2,940	6,701	1,669	254	761
13.4	62	3c	8,743	3,511	5,743	1,945	300	627
12.4	64.8	9b	5,530	3,374	3,961	719	445	549
5.6	107.5	5b	24,996	17,032	17,091	3,564	1,577	1,974
1.9	115.5	7b	44,072	8,423	16,099	1,460	800	988

Table 14. Depth to peak concentrations of Zn and Pb in floodplain profiles.

River-km	Drainage area (km^2)	Floodplains	Depth peak Zn (m)	Depth to peak Pb (m)
9.8	3.3	1a	0.75	1.05
12.4	17.5	12a	0.65	1.05
19.34	39.7	11b	0.55	0.75
15.4	58	10a	0.35	0.55
12.5	64.8	9a	0.25	0.45
11.68	83.2	6a	0.75	1.35
8.02	101.8	8a	0.75	1.15
7.9	101.8	8b	0.95	1.05
5.56	107.5	5a	0.85	0.85
5.5	107.5	5c	0.45	0.55
0.24	121.4	4b	1.05	1.6
0.14	121.4	4a	1.25	2.25
	Mean		0.72	1.05
	SD		0.28	0.49
	CV%		38.78	46.09

Table 15. Depth to peak concentrations of Zn and Pb in bench profiles.

River-km	Drainage area (km²)	Bench	Depth peak Zn (m)	Depth to peak Pb (m)
15.3	58	10b	1.25	1.25
13.4	62	3c	1.15	1.35
12.4	64.8	9b	0.9	0.9
5.6	107.5	5b	0.65	0.65
1.9	115.5	7b	1.15	1.05
	Mean		1.02	1.04
	SD		0.22	0.25
	CV%		21.39	24.02

Table 16. Depth to peak concentrations of Zn and Pb in terrace profiles.

River-km	Drainage area (km²)	Terrace	Depth peak Zn (m)	Depth to peak Pb (m)
16.9	8.7	2a	0.05	0.05
19.2	39.7	11a	0.05	0.05
15.3	58	10c	0.05	0.05
13.8	62	3b	0.05	0.05
13.6	62	3a	0.05	0.05
1.9	115.5	7a	0.05	0.05
	Mean		0.05	0.05

Table 16 continued.

SD	< 1.00	< 1.00
CV%	< 1.00	< 1.00

Table 17. Average concentrations of Zn, Pb, Ca, Fe below the thin enriched surface layer of terrace profiles. Used to determine approximate background concentrations for the watershed.

Terrace	Total Samples	n	Mean concentration of samples below enriched surface layer (ppm)			
			Zn	Pb	Ca	Fe
11a	9	7	1,076	66	2,651	17,664
2a	10	9	112	43	2,446	23,690
10c	4	3	424	64	2,952	12,877
3b	13	10	67	24	2,380	14,046
3a	15	11	304	44	4,136	13,365
7a	17	14	439	74	3,565	15,097
Mean			243	16	553	3,036
SD			364	19	696	4,078
Mean ± 2 SD			970	53	1,945	11,192
CV%			150	121	126	134

Table 18. Average concentrations of Zn and Pb in historical legacy sediment and Holocene deposits. Used to evaluate background concentrations by comparing the difference in average concentrations between pre-settlement (below the Ab horizon) and post-settlement (above the Ab horizon) floodplain sediment.

Metal & Deposit Type	Average Concentrations Historical and Holocene (ppm)							
	Tributary	Upper	Middle	Lower	Overall	n	SD	CV%
Zn ppm								
Historical	4,962	1,156	3,846	4,539	3,626	144	1,481	41
Holocene	2,245	3,355	1,800	1,837	2,309	55	629	27
Ratio	2	0	2	2	2			
Pb ppm								
Historical	768	65	532	611	494	144	212	147
Holocene	184	310	134	82	178	55	84	154
Ratio	4	0	4	7	3			

Table 19. General Zn and Pb trends in floodplain profiles and associated historical event in the watershed.

Year/Range	Zn and Pb General Production Trends	Event
2021	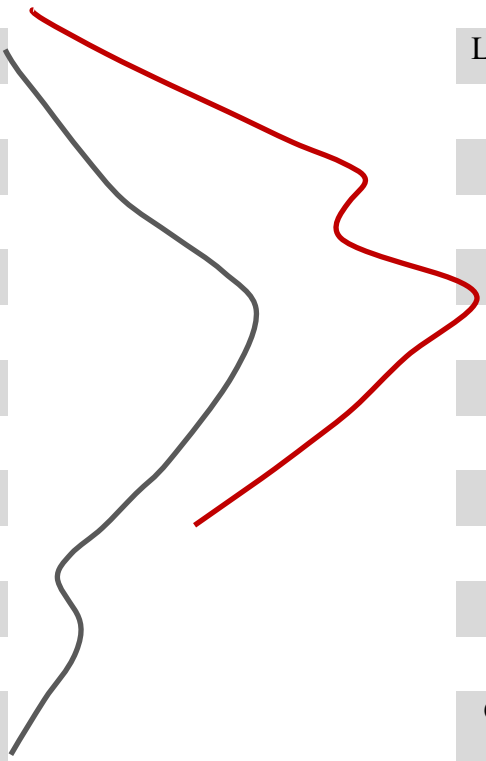	Top of soil surface (year of sampling)
1947		Last operations stopped completely in MO
1930		Great depression
1926		Late Zincite Sub-District Peak Zn
1920		Most production ends in MO
1916		Overall production peak
1900-1910		Population of Jasper County peaks
1903		Peak production in Joplin Sub-District
1880		Railroads and Zn smelter enter MO
1870		Mining boom begins
1861-1865		Civil war
1855-1860		Pre-mining boom Pb peak
1853		Pb smelting begins in Jasper County
1850		Crude early Pb mining begins on Turkey Creek

Table 20. Floodplain sedimentation rates during the pre-mining, rise to peak mining, peak mining, post-mining and the overall mining years.

Sites	Drainage Area km²	Pre-mining (1850-1870)	Rise to peak years (1870-1890)	Peak years (1890-1920)	Overall mining (1870-1930)	Post-mining (1930-2021)
1a*	3.3	1.5	0.5	1.0	0.8	NA
2b*	8.8	1.0	0.5	1.3	0.8	0.0
12a*	17.4	1.5	1.0	1.7	1.5	0.2
11b	39.6	1.0	0.5	1.0	1.2	1.0
10a	58.0	2.0	0.5	1.0	1.0	0.1
9a	64.8	1.5	1.5	0.8	1.0	0.1
6a	83.1	0.5	2.0	2.3	2.0	0.1
8a	101.8	1.0	1.0	2.0	1.7	0.2
8b	101.8	0.5	1.5	3.0	2.5	0.0
5c	107.5	0.5	0.5	1.3	1.0	0.0
5a	107.5	1.0	2.0	2.0	2.2	0.3
4b	121.5	0.5	2.0	2.0	2.0	0.4
4a	121.5	1.0	2.0	2.7	2.5	0.7
Average rate (cm/yr)		1.0	1.2	1.7	1.6	0.2

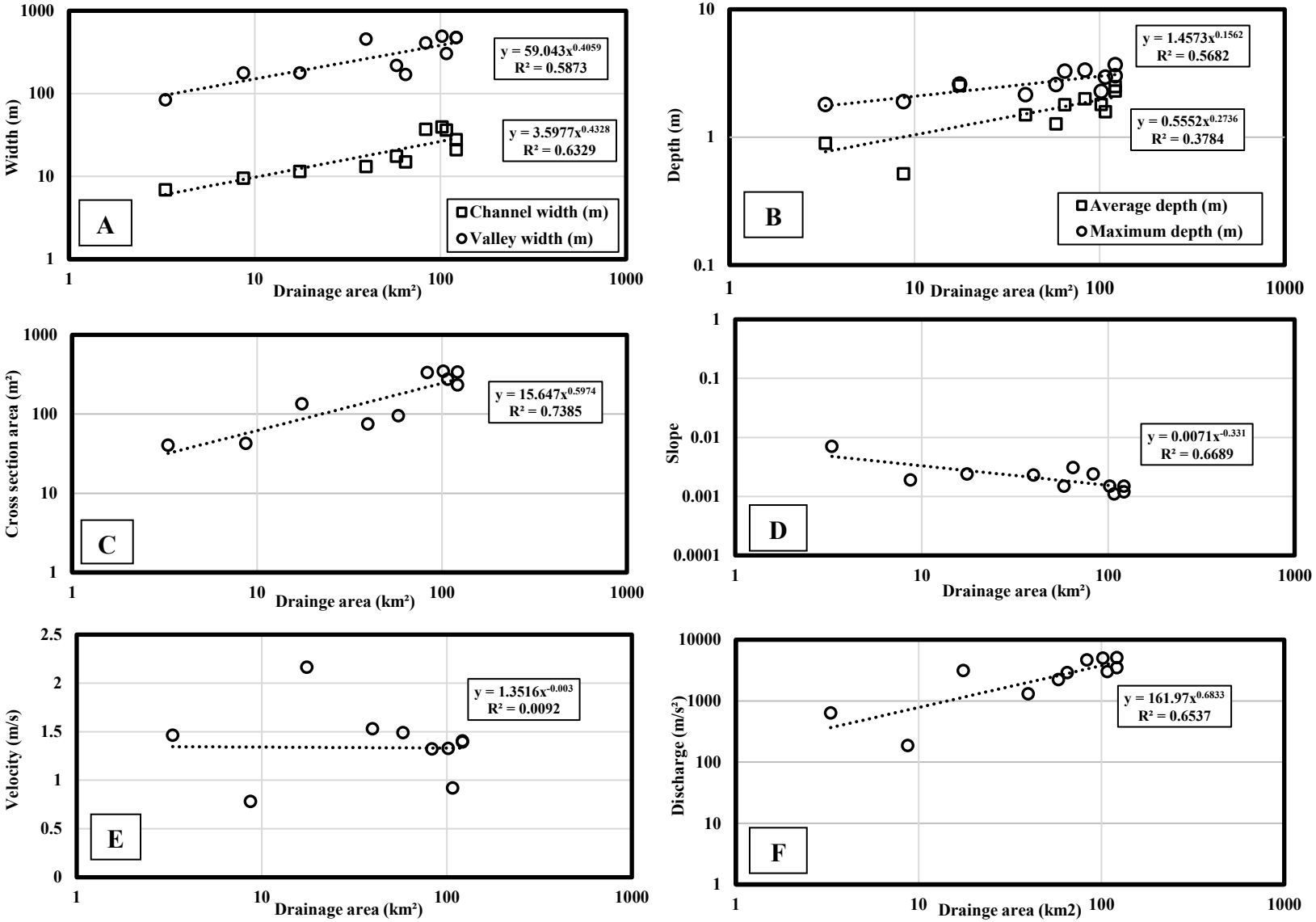

Figure 12. Channel hydrology and drainage area relationships. Trends are shown above for: (A) Channel and valley width; (B) Average and maximum depth; (C) Cross section area; (D) Slope; (E) Velocity; and (F) Discharge.

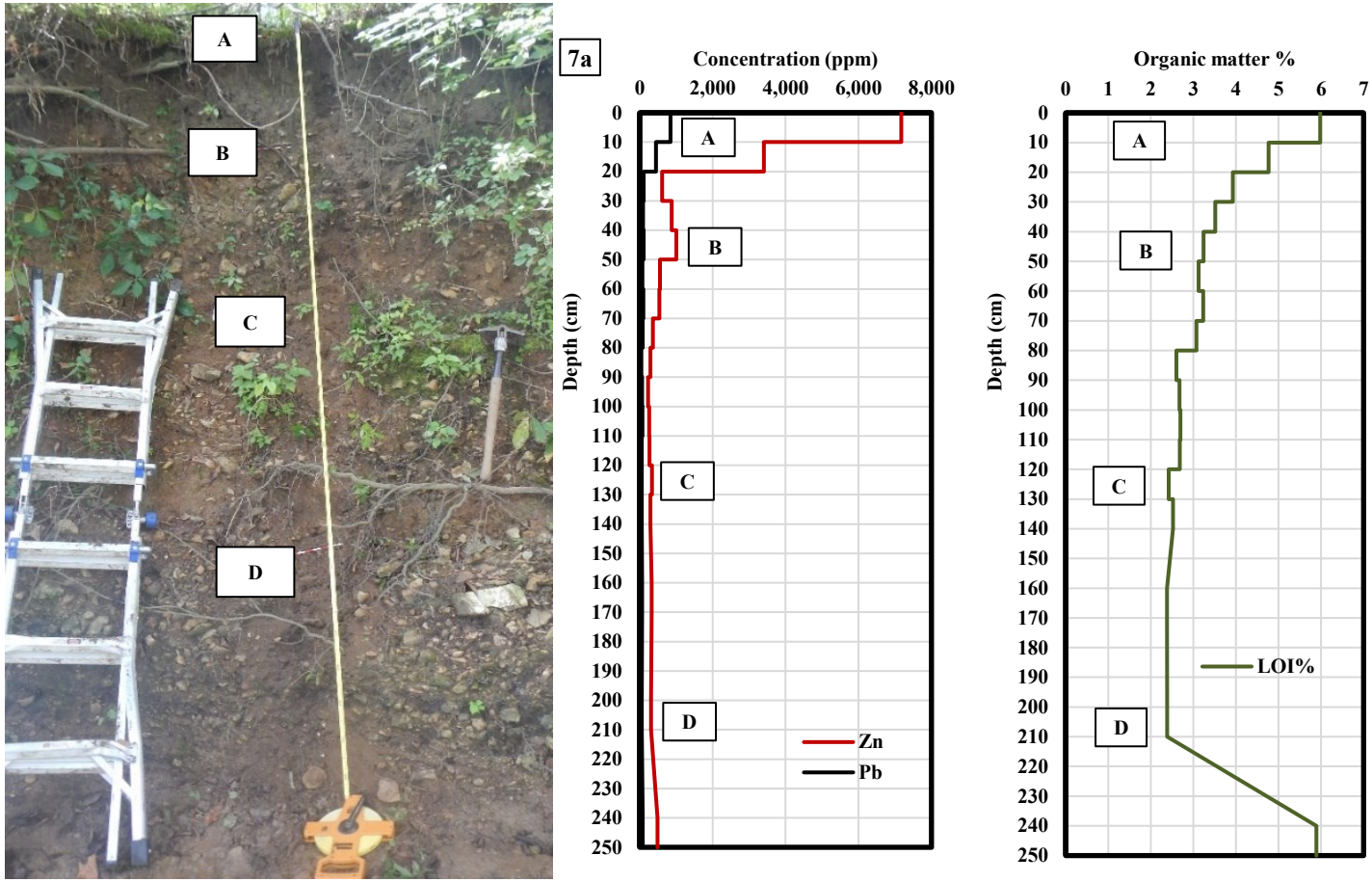

Figure 13. Example of terrace stratigraphy and geochemical trend. Trends are shown above for: (A) 0-20 cm dark organic rich A-horizon; (B) top of a light tan chert gravel layer; (C) top of a fine gravel unit; and (D) top of a coarse gravel/cobble layer (Site 9a).

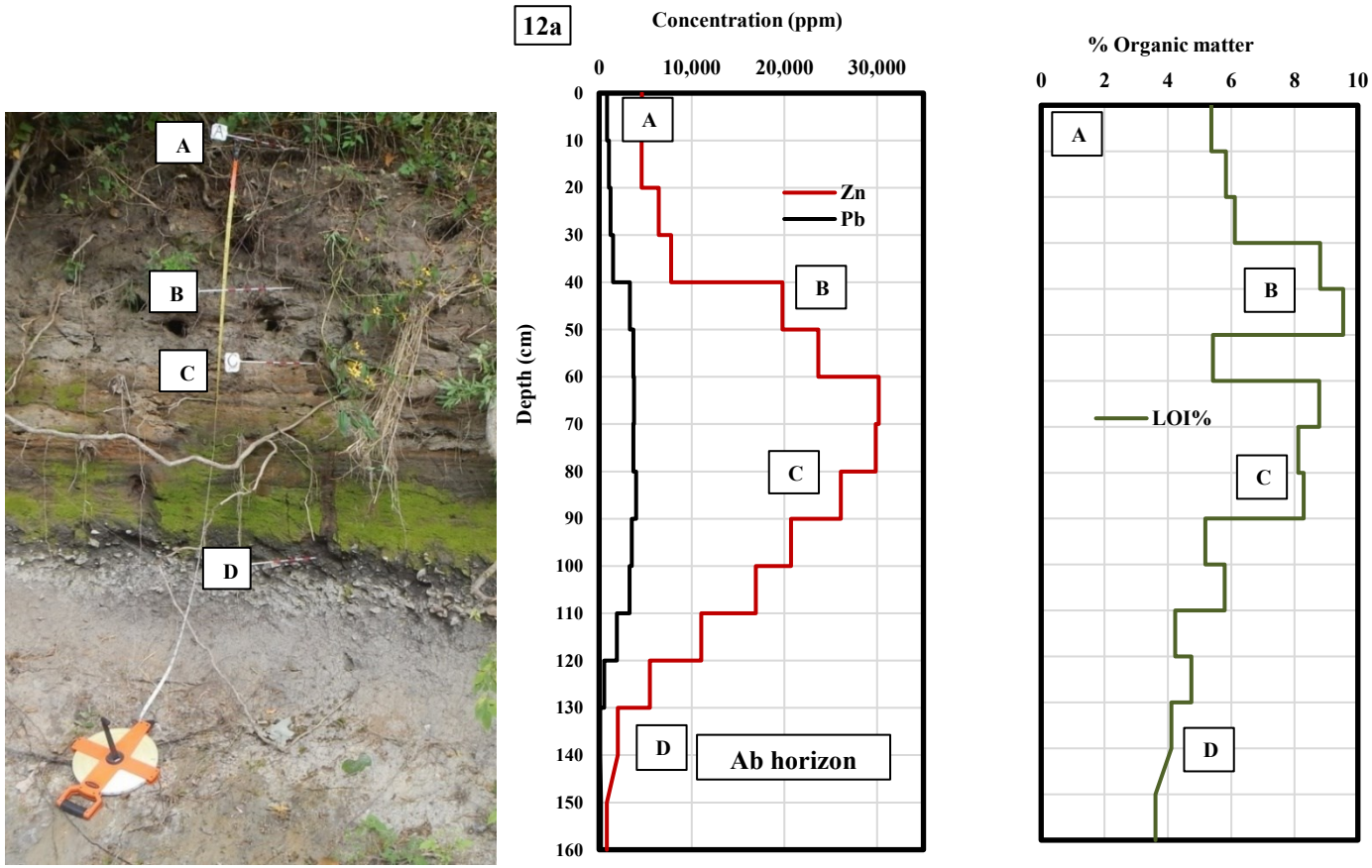

Figure 14. Example of channel fill floodplain A stratigraphy and geochemical trends. Trends are shown above for: (A) 0-10 cm A-horizon; (B) top of a grey sandy silt loam with some tailings; (C) top of a grey tan sandy silt loam; and (D) dark silt loam, Ab horizon (Site 12a).

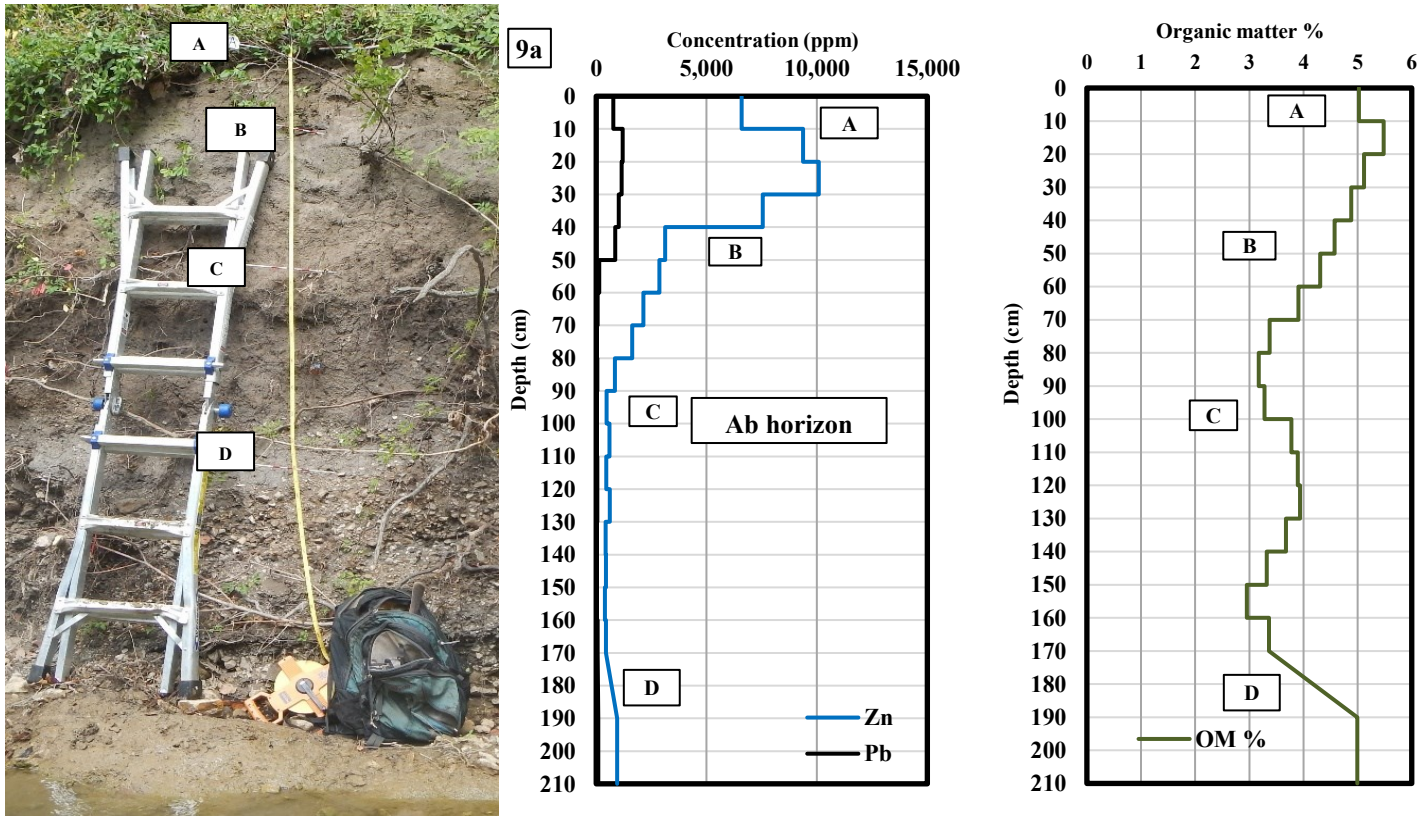

Figure 15. Example of overbank floodplain B stratigraphy and geochemical trends. Trends are shown above for: (A) 0-20 cm A-horizon above a light brown silt loam; (B) top of a grey/brown sandy loam; (C) dark brown/grey silt loam Ab horizon; and (D) top of a grey/brown gravel layer from 180-200 cm (Site 9a).

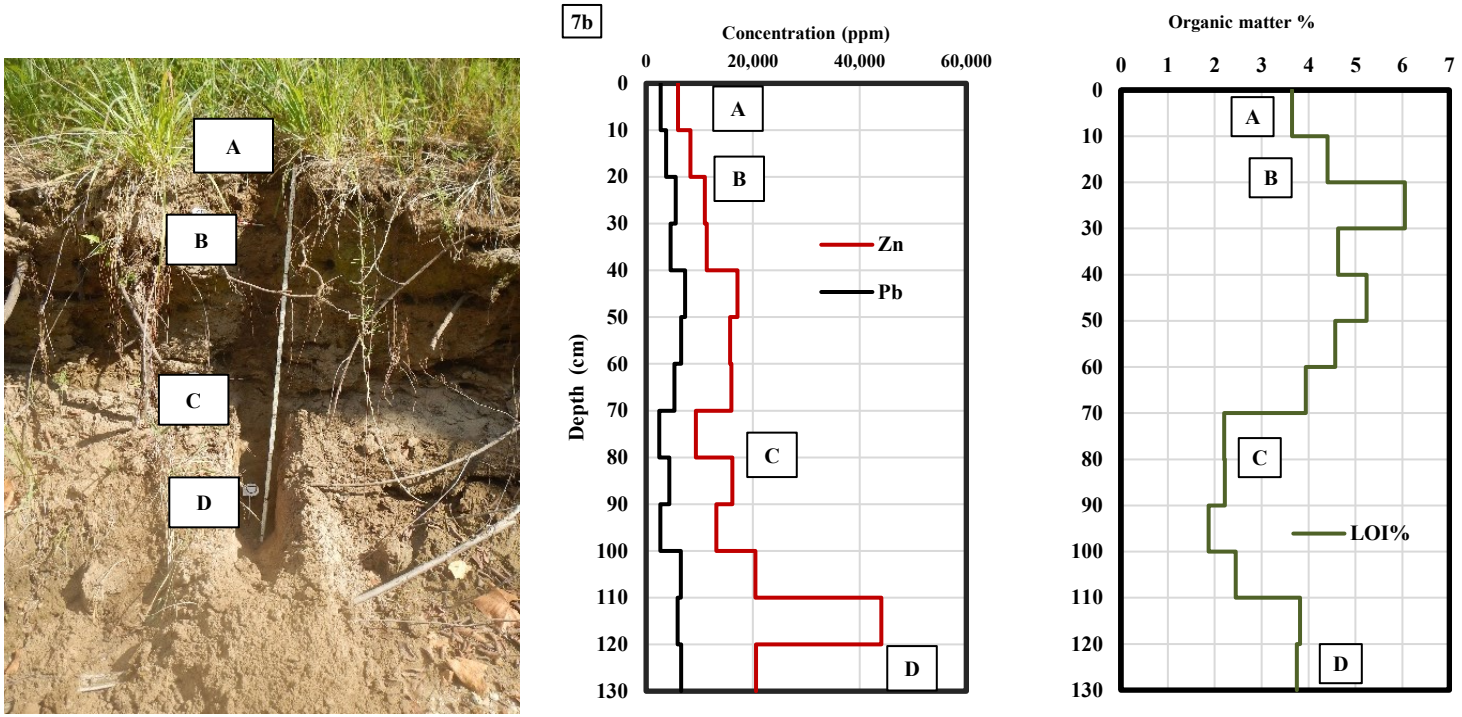

Figure 16. Example of bench stratigraphy and geochemical trends. Trends are shown above for: (A) weak A-horizon; (B) top of a brown silt loam made up of >10% chat from 20-80 cm; (C) top of a light grey sandy loam; and (D) bottom of the sampled profile overlying a silty mud (Site 7b).

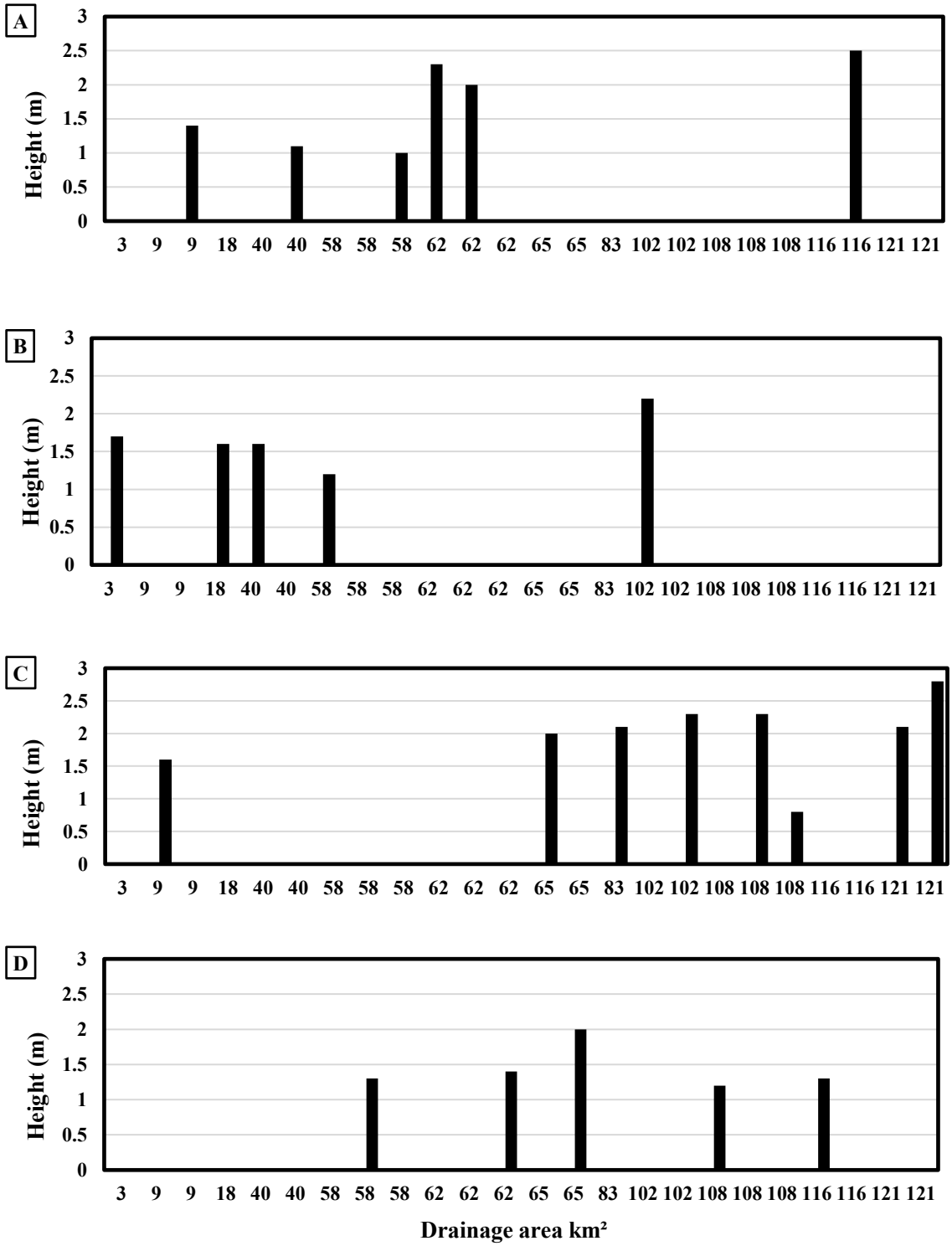

Figure 17. Maximum height of sampled cutbanks by drainage area and landform. Trends are shown above for: (A) Terrace; (B) Floodplain – Channel Fill; (C) Floodplain – Overbank; and (D) Bench.

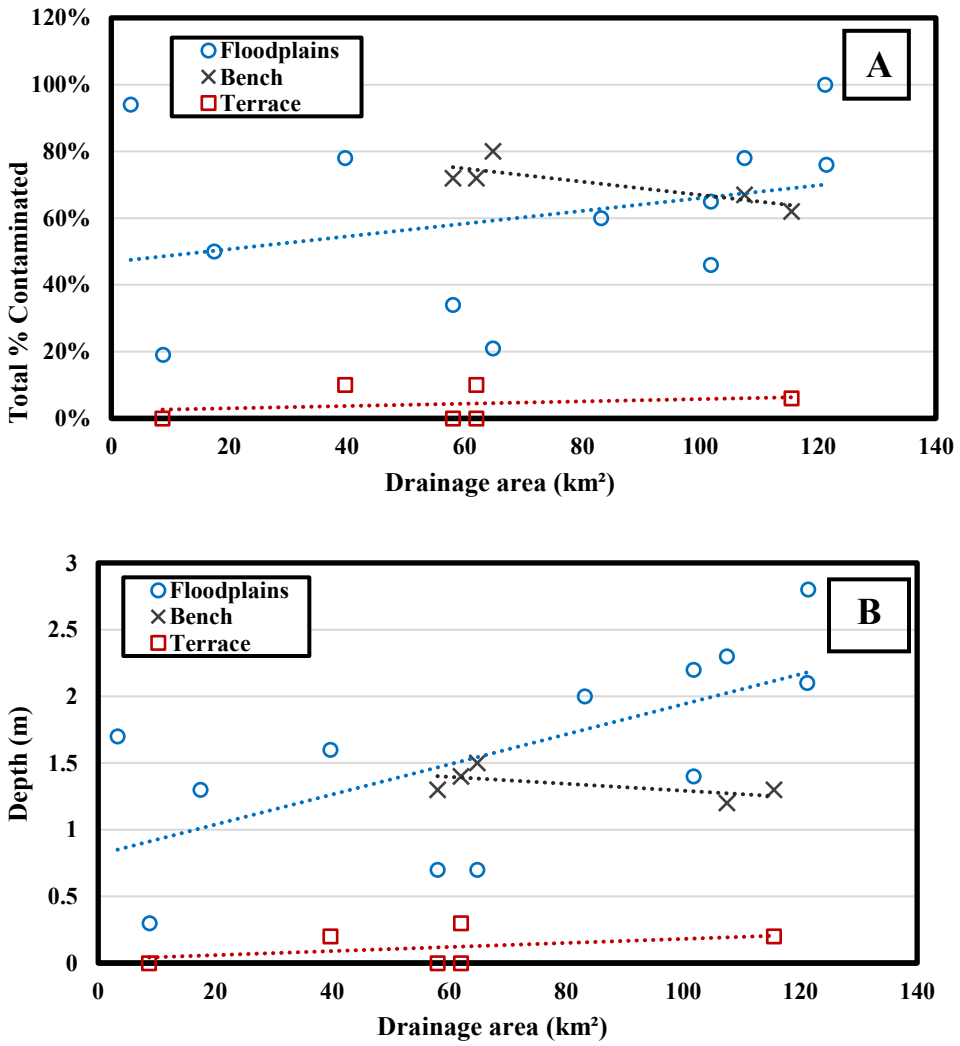

Figure 18. Extent of contamination in terrace, floodplain, and bench profiles. Trends are shown above for: (A) Percent of the core that is contaminated and (B) Depth of contamination by landform.

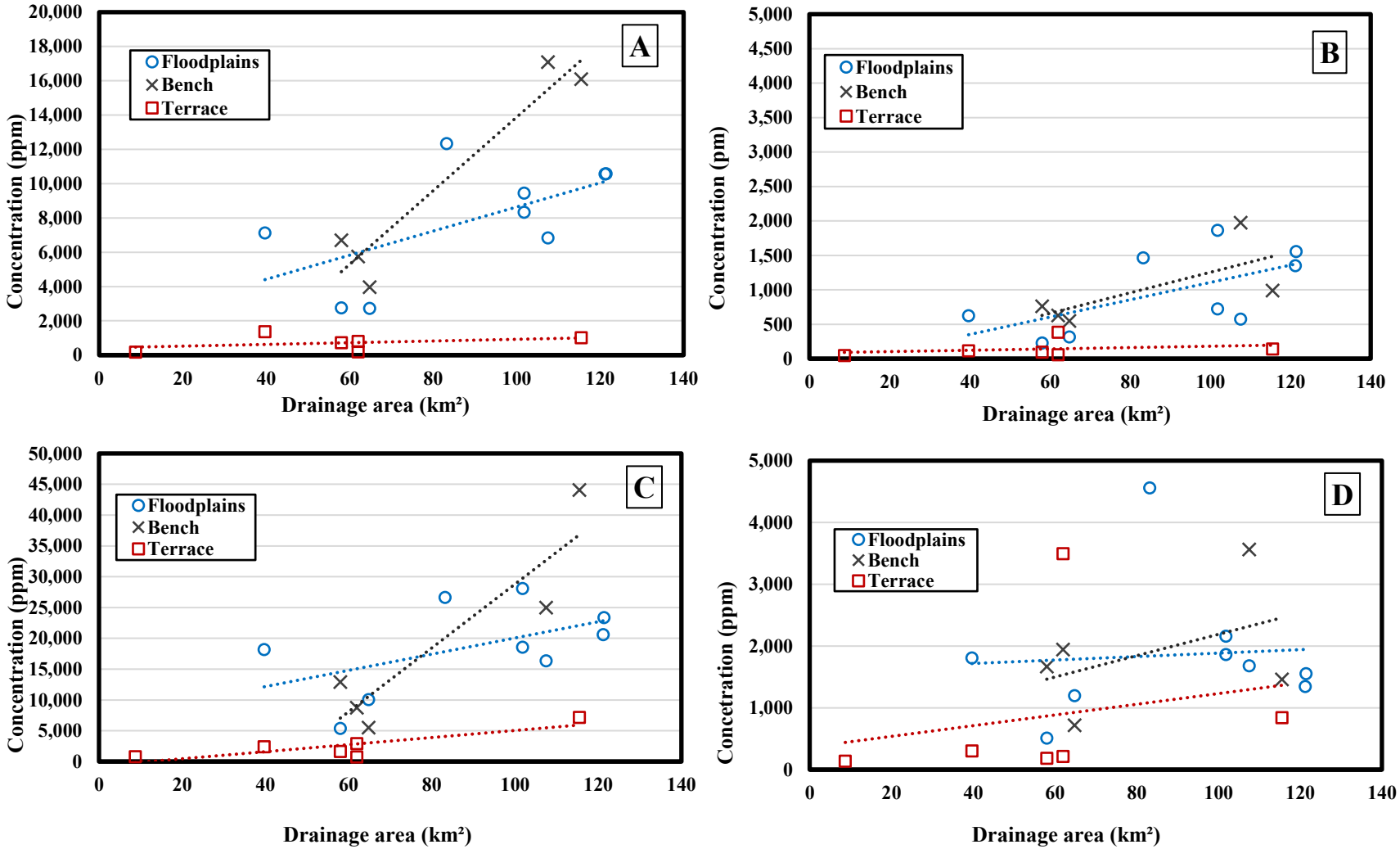

Figure 19. Average and maximum concentrations of Pb and Zn by landform and drainage area. Trends are shown above for: (A) Average Zn; (B) Average Pb; (C) Maximum Zn; and (D) Maximum Pb.

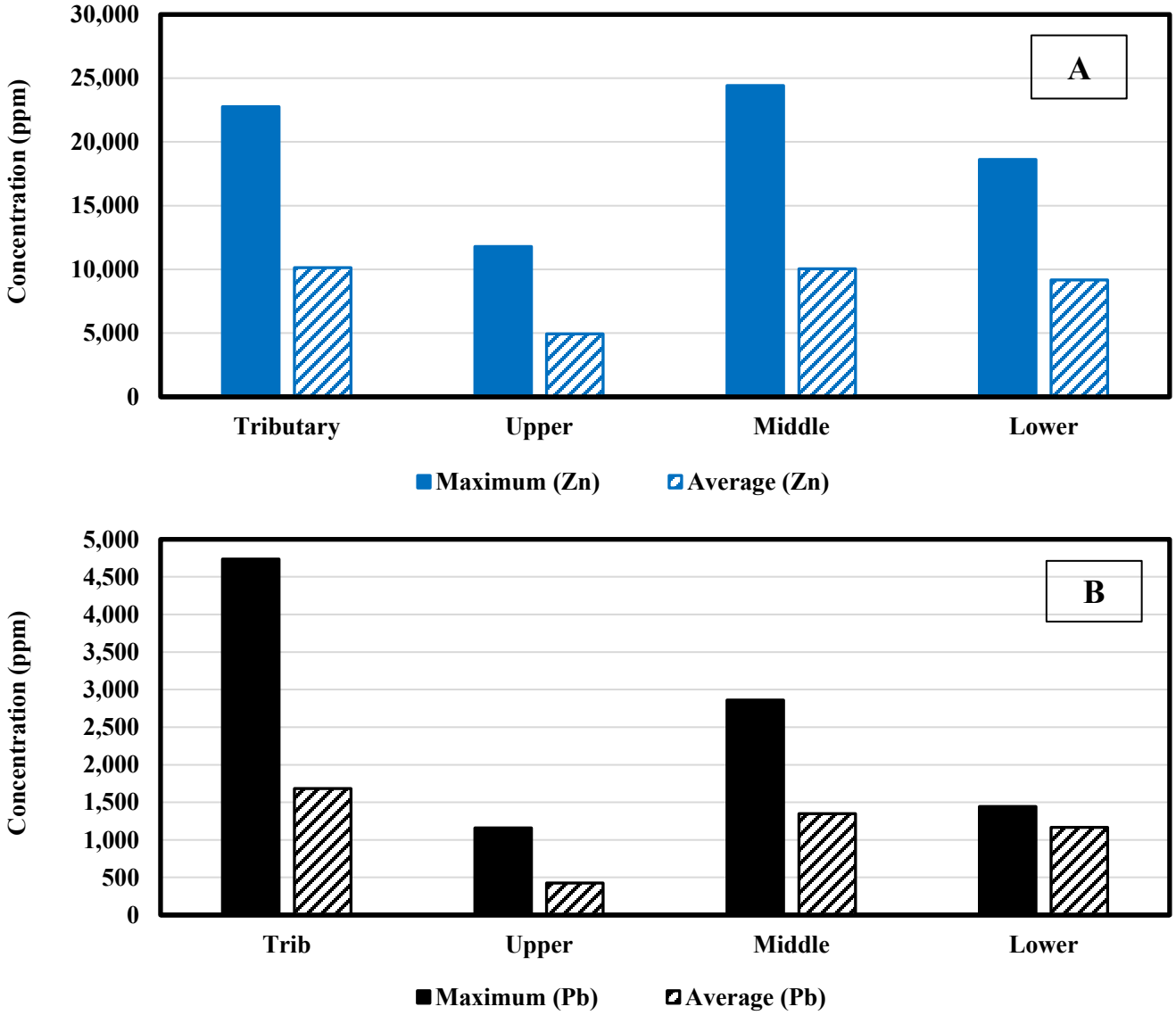

Figure 20. Average and maximum Pb and Zn concentrations by watershed segment. Trends are shown above for: (A) Zn and (B) Pb.

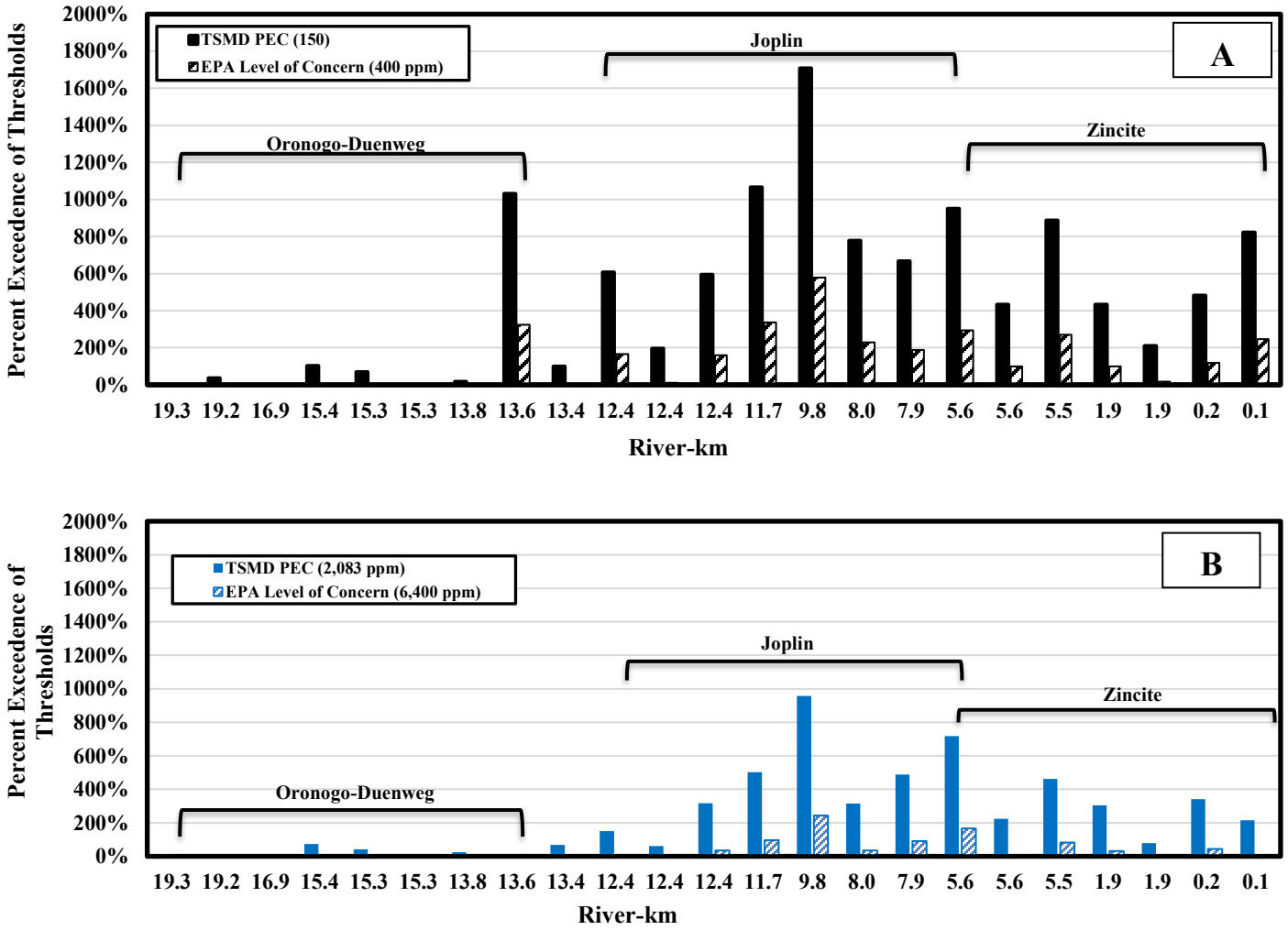

Figure 21. Surface concentrations exceedance of EPA contamination thresholds for Pb and Zn by drainage area. Trends are shown above for: (A) Threshold exceedance for Pb and (B) Threshold exceedance for Zn

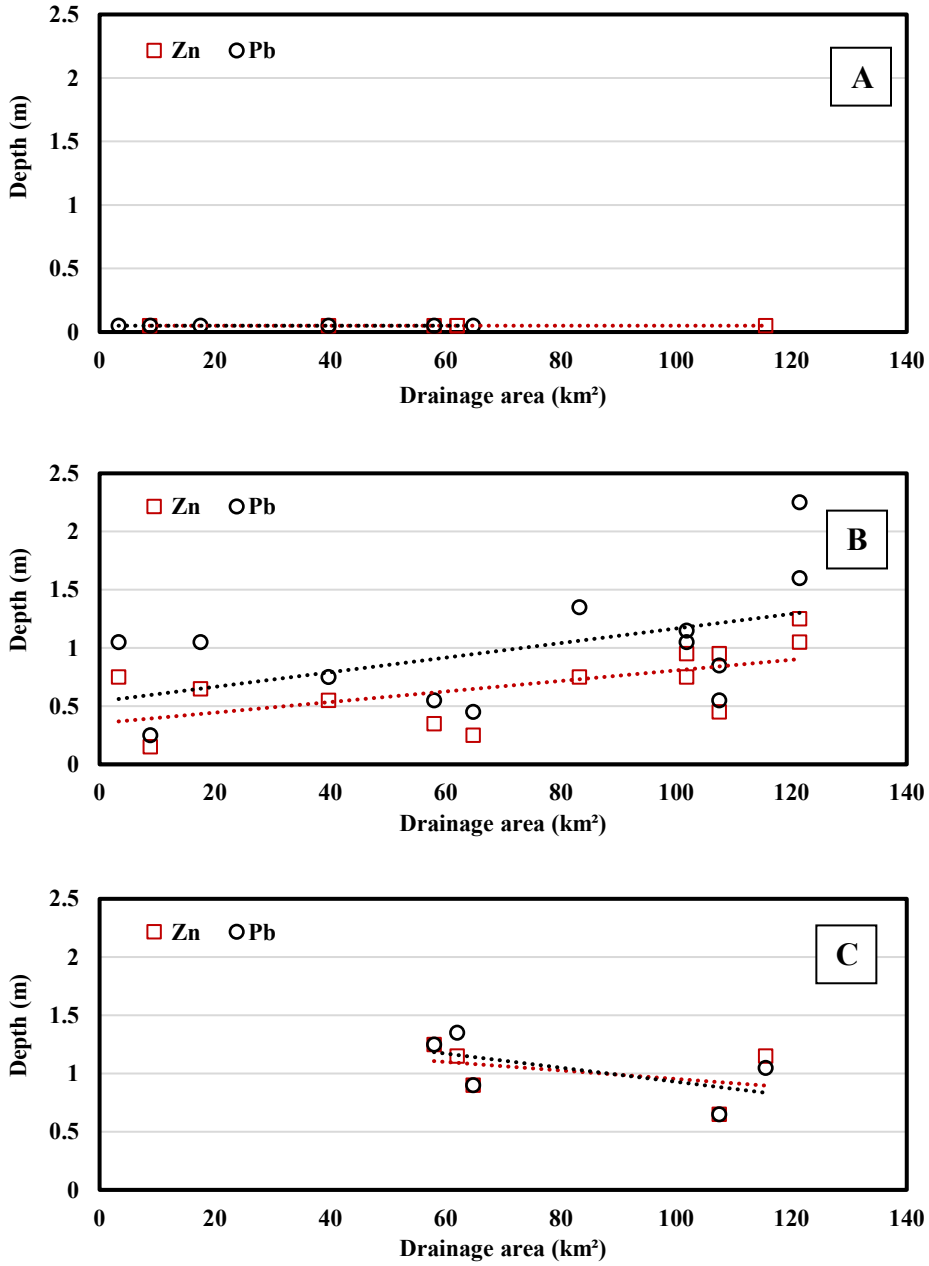

Figure 22. Depth to maximum Zn and Pb concentrations by landform. Trends are shown above for :(A) Terrace; (B) Floodplain; and (C) Bench.

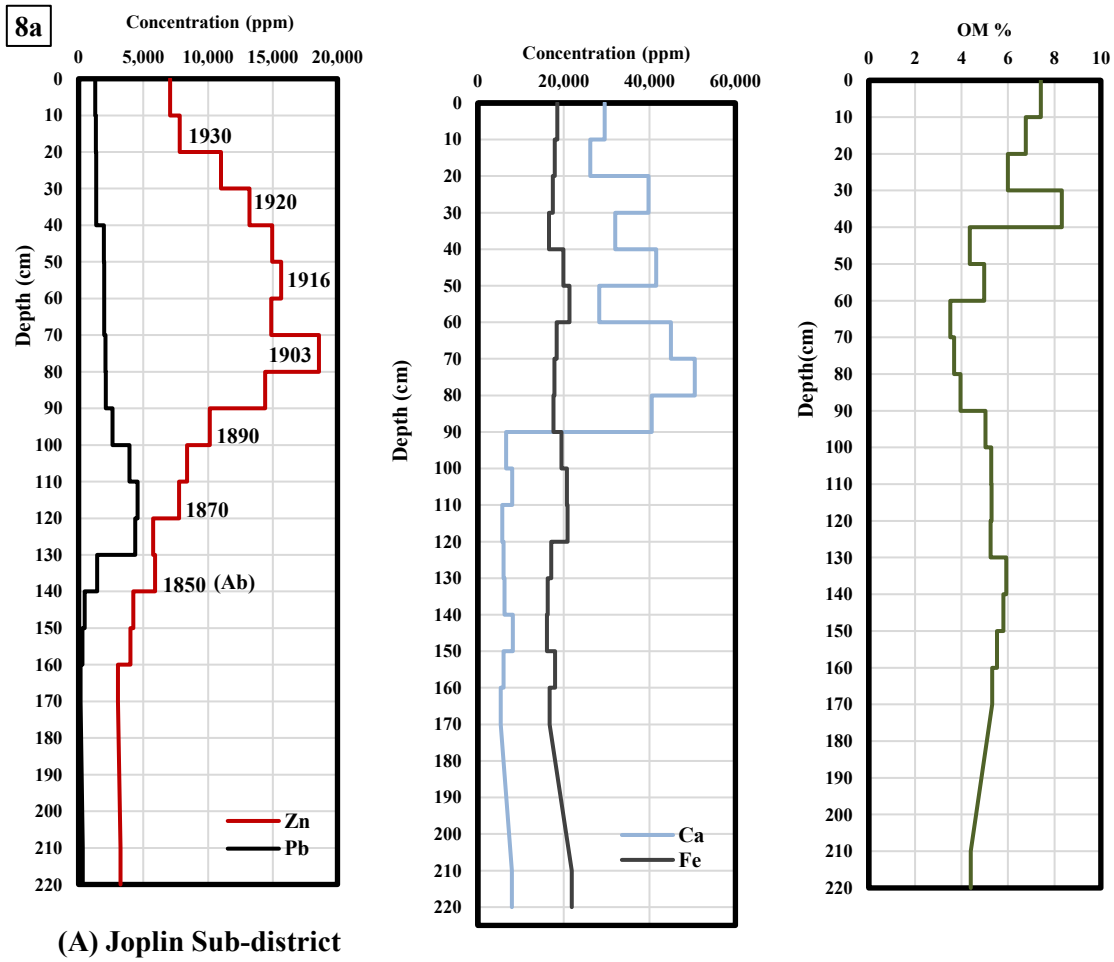

Figure 23. Example of core dating using Pb, Zn, Ca, Fe, and organic matter in the Joplin sub-district (Site 8a - Joplin-subdistrict).

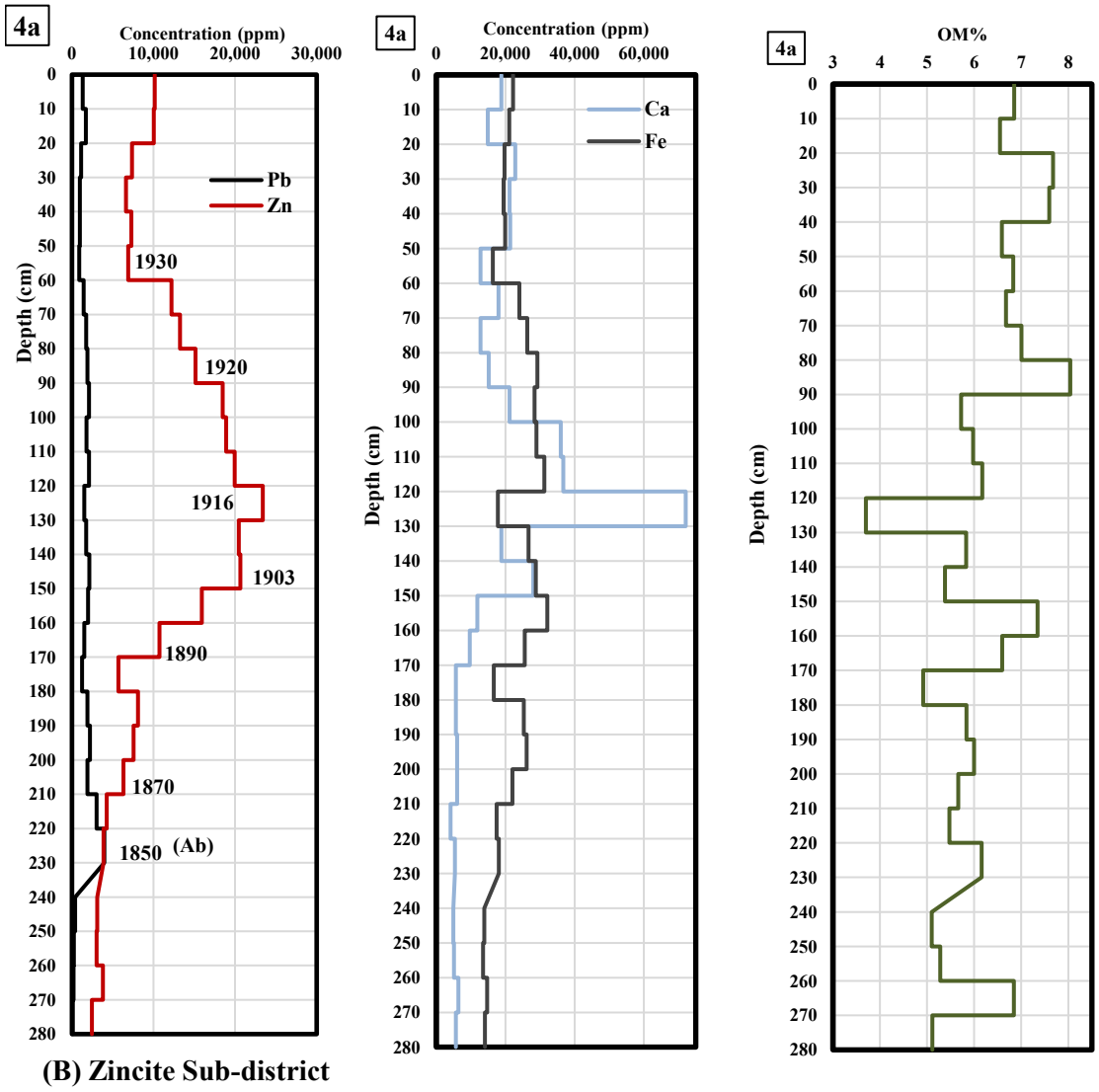

Figure 24. Example of core dating using Pb, Zn, Ca, Fe, and organic matter in the Zincite sub-district (Site 4a - Zincite sub-district).

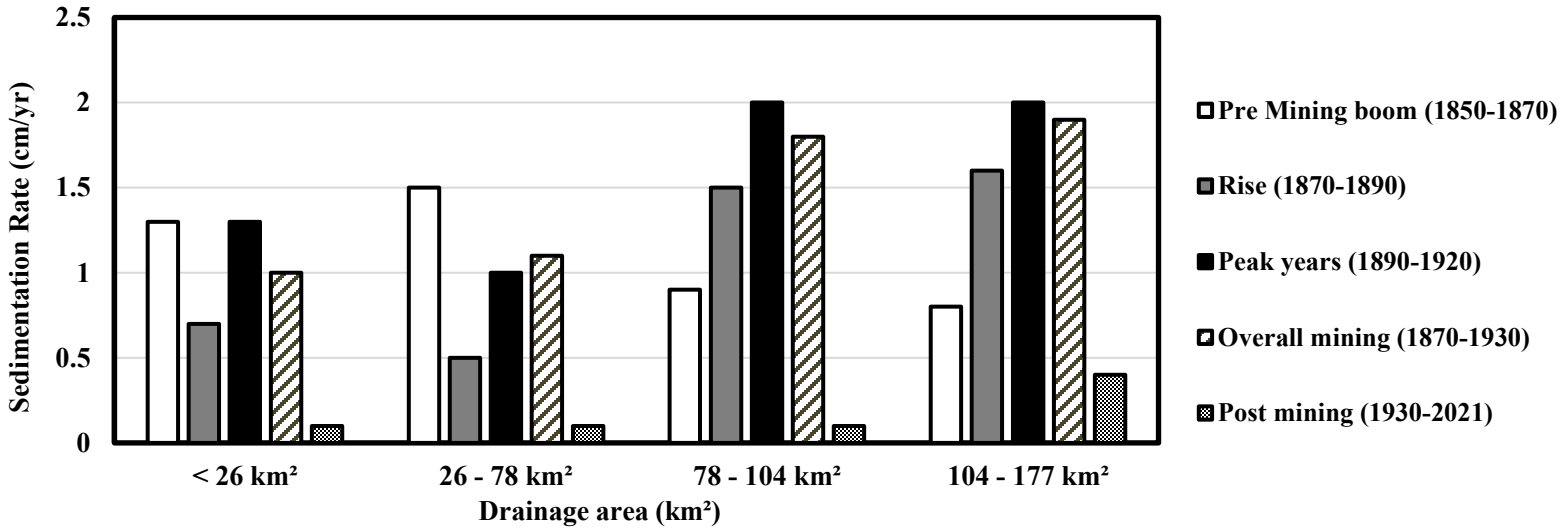

Figure 25. Sedimentation rates by historical period and drainage area.

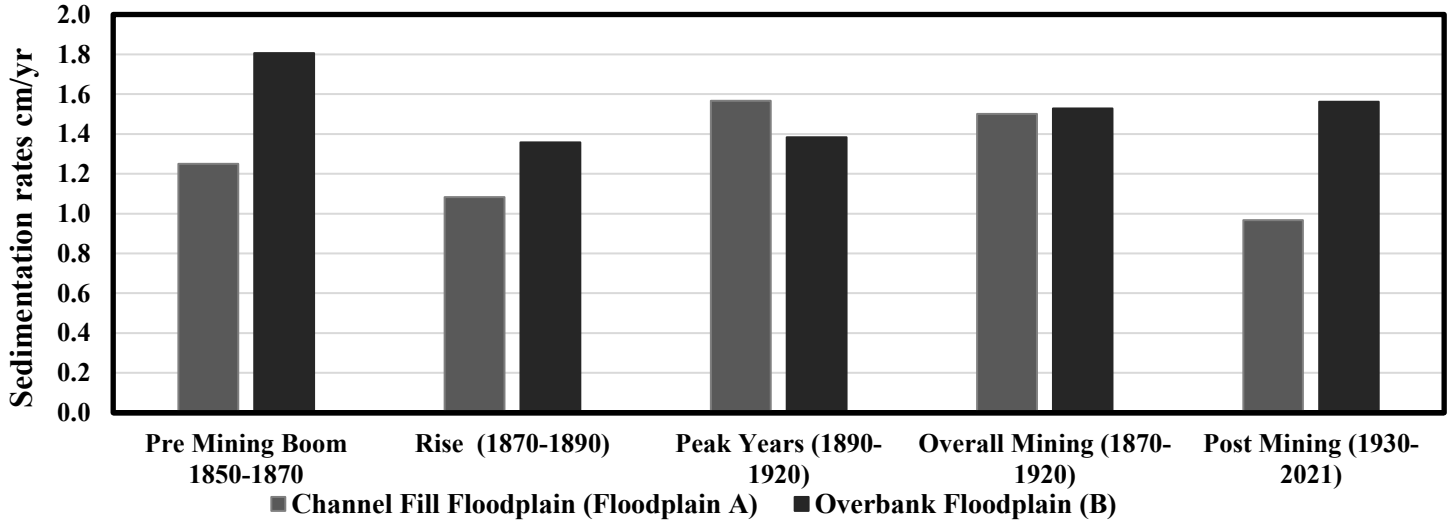

Figure 26. Floodplain facies average sedimentation rates by historical period.

DISCUSSION

The results chapter analyzed the spatial and stratigraphic relationships of contaminated deposits within terrace, floodplain, and bench features in Turkey Creek. This chapter will interpret the results to broaden our scientific understanding of the following: (i) nature of contamination; (ii) background levels; (iii) floodplain stratigraphy, (iv) downstream variations in historical floodplain sedimentation rates and the significance of legacy deposits in Turkey Creek. Results and patterns of contamination and sedimentation will be compared to similar studies in the region and any relationships found will be described. Finally, suggestions for future work to advance understanding will be provided and environmental concerns described.

Degree of Contamination

On average within the bench and overbank profiles, more than 60% of the total core depth is contaminated by both Zn and Pb. The depth of contamination in floodplains ranges from 0.7-2.8 m and tends to increase downstream (Table 9, Figure 18). Tributary sites contained contaminated profiles up to 1.7 m deep (Table 9). The upper segment of the watershed has the shallowest average contamination depths at 1.3 m for Zn and Pb compared to the middle segment at 1.8 m for Zn and 1.9 m for Pb and the lower segment at 1.9 m for Zn and Pb (Figure 27). Depths of contamination for Zn and Pb are similar and usually contaminated to the same depth or within 10 cm (Table 9, Figure 18). The highest concentrations of mining-metals are found in tributary site 1a in the Joplin sub-district (Pb maximum = 9,978 ppm and Zn maximum = 35,681) (Table 11). The middle segment contains the greatest maximum and average concentrations for both metals (Pb maximum = 4,562 ppm and Zn maximum = 28,099 ppm)

(Figure 20). Both tributary sites also drain to the middle segment, so by far the middle segment contains the greatest contamination threat in the watershed. This segment also includes the Joplin mining sub-district where mining in the area began and it had the longest running and highest ore production compared to the Oronogo-Duenweg and Zincite sub-districts (Winslow, 1894; Martin, 1945). The lower augment probably received direct tailings inputs the from mines near Turkey Creek in Zincite subdistrict but still has lower contamination levels compared to the middle segment (Zn Maximum = 18,619 ppm and Zn mean =9,169 ppm; Pb maximum = 1,445 ppm and Pb mean= 1,167 ppm) but all the floodplain samples still exceeded the TSMD PEC and the EPA LOC (Tabe 11, Figure 20). Remediation efforts should focus first on the Joplin sub-district segment and then the Zincite sub-district. The upper segment contains the lowest concentrations for both metals (Zn maximum = 11,789 ppm and Zn mean = 4,938 ppm; Pb maximum =1,161 ppm and Pb mean = 426 ppm), but average and maximum values all still exceed the TSMD PECs (Table 11, Figure 20). All Turkey Creek segments are contaminated by both Zn and Pb with Joplin sub-district of greatest concern, followed by Zincite, and then Oronogo-Duenweg.

This study has assessed the presence and depth of contamination of floodplains along the channel. Further sampling using soil coring across the valley floor would provide more information about the lateral extent of floodplain contamination. A rough estimate of contaminated sediment storage using an average floodplain width of 40 m, average depth of contamination by sub-district, and channel length of each sub-district resulted in volumes of contaminated sediment as follows: 960,000 m^3 (Duenweg-Oronogo), 448,000 m^3 (Joplin), and 544,000 m^3 (Zincite) (Table 21).

The Smith (2016) and Juracek (2013) floodplain studies limit the understanding of floodplain contamination to one single transect. Even so, these studies present a case for continued work based on the significant Zn and Pb concentrations at each of their transects. For example, Smith (2016) found significant Zn concentrations (> TSMD PEC) up to 5 m deep, approximately 200 m from Turkey Creek. Further, this study measured Zn and Pb concentrations that greatly exceeded those found in the Smith study, presenting another cause for concern that Turkey Creek is more contaminated than previously thought. Remediation targets are less stringent, so possibly only half of the contaminated amount or about 1 million cubic meters of contaminated sediment would need to be removed or contained for long-term management purposes.

High levels of contamination are found within the floodplain banks and benches exposed to erosion by relatively frequent floods (i.e., <5-year RI) so the risk of Zn and Pb remobilization may be high in Turkey Creek. The profiles with the most potential for remobilization are the benches (10b, 3c, 9b, 5b, 7b). All but one out of five of these profiles contain Zn concentrations exceeding the EPA level of concern and all of them also exceed it for Pb (Table 13). As benches represent the youngest landform sampled by this study, additional landform change studies could determine the risks of remobilization. As flooding continues to increase in magnitude and frequency due to the changing climate, the likelihood of remobilization of contaminated legacy sediment in the watershed may rise (Foulds et al., 2014). Continued studies on the hydrology, channel evolution, and sediment transport in relation to flood capacity of the Turkey Creek channel system will be necessary for predicting the risk of metals being remobilized from floodplain storage to be transported further downstream (Foulds et al., 2014).

Background Levels

The background concentrations calculated by this study for deep terraces deposits (229 ppm Zn and 15 ppm Pb) and Holocene units (2,309 ppm Zn and 178 ppm Pb) produced values higher than what other studies used for regional background levels (Pope, 2005; Smith, 2016; Juracek, 2013). Concentrations can be higher especially in the Holocene floodplain units due to naturally mineralized soils. Much of Turkey Creek was mined in the early 1850s by pulling Pb ores directly from the bank indicating very high background levels prior to the start of mining in the region (Winslow et al., 1894; Martin, 1945). Groundwater flows in alluvial aquifers, karst seeps, and old mine drains can transport high concentrations of dissolved metals such as Zn and Pb to for binding and co-precipitation with fine sediment and organic matter in Holocene and modern floodplain deposits (Carroll et al., 1998). The downward leaching of dissolved metals from the above highly contaminated legacy sediment is highly likely, many cores contained units composed of mostly pure tailings (Carroll et al., 1998; Hudson-Edwards et al., 1998).

Floodplain Stratigraphy

Other studies have recognized that Holocene channel systems in the Mid-West may have alluviated during the post-Euro American settlement period in response to increased flooding and soil erosion due to vegetation clearing and soil disturbances for the agricultural development of the region (Happ et al., 1940; Trimble, 2009, 1999). Increased runoff led to larger peak floods and increased stream power that could cause incision into pre-existing bed elevations (Trimble, 2009, 1999). The formation of higher banks due to historical legacy deposition across the valley floor led channels to adapt by lateral erosion and widening (Knox, 1987; Trimble, 1999). This resulted in contemporary channels taking on a single-channel form compared to lower energy

anastomosing channel systems with wetland attributes present at the time Euro-American settlement (Sauer, 1920; Knox, 1987).

The geomorphic history of the Turkey Creek follows a similar story, with high and steep stream banks up to 3.5 m in height, and single channel forms. Fine grained, contaminated legacy sediment accounts for the majority of channel banks in overbank floodplains in this watershed. These large volumes of young fine-grained contaminated sediment indicate geomorphically recent deposition in the post-settlement and mining periods. The two floodplain facies (A and B) observed in Turkey Creek suggest two forms of legacy deposition (Knox, 1987; Trimble, 1999). Floodplain A-channel fill facies suggest the deposition of fine-grained sediment on the bed of a multi-channel system, or a more intricate and lower energy single channel system compared to today. It is possible multi-channel reaches occurred interspaced with single channel reaches. This finding adds to our understanding of the heterogenous patterns of deposition of legacy sediment and how channels adapted to the influx of sediment by creating a single channel system. Floodplain B- overbank facies have post-settlement sediment overlying on older developed soil typically having a thick Ab horizon and Bw or Bt horizons indicating a late Holocene mollisol within a prairie landscape at some sites. This finding suggests a shift from grassland and dispersed native forests to an agricultural landscape with small villages and mixed hardwoods in wooded patches.

Although the USDA does not map Ab horizons within the Turkey Creek watershed, field and laboratory data indicates these floodplains contain young pre-settlement alluvium (<200 years) with few pedogenic features except those related to hydromorphic effects or anthropic tailings deposits (NRCS, 2020). Like with the channel-fill facies, overbank sedimentation occurred on the historical floodplains at relatively high rates since the mid-1800's. Elevated rates

of suspended sediment deposition are still occurring today but at lower rates since weak A-horizons have formed along most of the present-day floodplain surfaces. Historical floodplain units contain the highest concentration of Pb and Zn in overbank deposits since they were contaminated during the peak mining period.

Legacy Deposition and Sedimentation Rates

Legacy sediment in the Turkey Creek watershed, has an overall average depth of 1.3 m. Terraces have an average of 0.3 m and floodplain and bench averaged 1.3 m (Tables 22, 23, & 24). There is a wide range of legacy sediment depths in overbank floodplain deposits along Turkey Creek (0.6 – 2.3 m) which generally fall in the middle range of those measured in other regional studies (Tables 22 & 25). Honey Creek is a smaller stream located about 40 mi southeast of Turkey Creek with a mining history in the TSMD (Carlson, 1999) (Table 25). The maximum depth of contamination for Honey Creek was 1.15 m less than in Turkey Creek (Tables 25, Figure 27). In Turkey Creek the largest volumes of legacy sediment occurred in the lower segment but varied from 0.6 m at site 5c to 2.3 m at site 4a (Table 22, Figure 27).

Tributaries tend to have higher stream power to transport legacy sediment downstream to where the channel widened, and slope decreased which was more conducive for overbank sedimentation. The tributaries and upper segment of the watershed contain the largest depths of pre-mining storage of historical sediment (0.1-0.5 m) and thicknesses tend to decrease with drainage area (Figure 28). This is likely the result of early accumulation of legacy sediment during the initial phases of settlement and mining in tributary valleys, but as increasing runoff led to higher stream power, tributary channels were incised and widened, and sediment transport capacity increased sediment loads to downstream segments (Knox, 1987). Therefore, legacy

sediment deposition decreased in tributaries and upstream reaches by the 1900s and the locus of deposition progressively shifted downstream (Figure 28). Accordingly, terraces had the lowest sedimentation rates overall from 1850 to the present day (range = 0.06 – 0.16 m) assuming they were still receiving overbank sediment up until present-day. However, sedimentation rates increase to an average of 0.8 cm/yr ranging from 0.3 – 1.3 cm/yr if only the period of active sedimentation is considered since terraces were likely cut off from active sedimentation by around 1900. This was likely caused by channel enlargement in response to larger floods after 1850 caused by land use disturbances.

The greatest rates of sedimentation occurred during mining periods which also coincided with peak agricultural expansion in Turkey Creek with average sedimentation rates of 1.2 cm/yr during 1870-1890 and1.7 cm/yr during 1890-1920. (Table 20). The average sedimentation rate in the pre-mining period before 1850 (1.0 cm/yr) was slightly lower than that of the mining periods with the post-mining period between 1930 to the present, rate being over five-times lower (0.2 cm/yr) (Table 20). Similar studies in the region found highest rates of sedimentation during the peak mining and agricultural development periods, with average values at each site ranging from 0.55 – 3.4 cm/yr (Table 25). The post mining rates in this study are lower than those found in similar studies (Table 20 & 25). For example, a study on the larger Big River Watershed in southeast Missouri reported a maximum post-mining period rate almost two times greater than Turkey Creek (Jordan, 2018) (Table 25). However, it is possible that land use driven sedimentation rates have remained high along reaches with larger drainage areas (Lecce and Pavlowsky, 2001). Even in Turkey Creek, recent sedimentation at downstream sites were 3-4 times greater than those on the upper or middle segment floodplains (Figure 25).

Elevated Pre-mining rates (0.5 – 2.0 cm/yr) indicate that historical sedimentation rates increased due to early settlement before large scale mining occurred. More evidence of this early sedimentation is that pre-mining rates are greatest in tributaries and the upper segment of the watershed and decrease downstream (Figure 25). Average sedimentation rates during the post-mining period (1930-2021) in the tributaries, upper, and middle segments are all about 0.1 cm/yr and rates increased greatly to 0.4 cm/yr in the lower segment (Table 20, Figure 25). These higher rates downstream could indicate that these sites are still currently accumulating reworked contaminated sediment that has been transported downstream even after large scale mining in the area ended almost a hundred years ago (Lecce and Pavlowsky, 2001). These findings contribute to our understanding of the extent to which legacy has affected floodplains, although this study only focuses on one watershed, the patterns of sediment and mining-metal dispersal and rates of legacy sedimentation found in Turkey Creek are similar to other studies in the regions. Thus, these results can be applied to other watersheds with a similar land use history in the Ozark Highlands.

Table 21. Approximate volume of contaminated sediment in floodplains in each mining sub-district.

Sub-district	Mean Width of Floodplain (m)	Mean Depth of Contamination (m)	Length of Sub-District (m)	Volume of Contaminated Sediment (m^3)
Duenweg-Oronogo	40	1.2	20,000	960,000
Joplin	40	1.4	8,000	448,000
Zincite	40	1.7	8,000	544,000

Table 22. Pre-settlement and post-settlement sediment thicknesses in overbank floodplain deposits.

Drainage area (km^2)	River-km	Floodplain	Pre-settlement (Holocene) thickness (m)	Post-Settlement (legacy) thickness (m)
3.3	9.8	1a	0.4	0.8
8.8	16.9	2b	0.4	0.7
17.5	12.4	12a	0.2	1.4
39.7	19.3	11b	0.6	0.7
58.0	15.4	10a	0.1	1.1
64.8	12.5	9a	1.1	1
83.2	11.7	6a	0.7	1.4
101.8	8.0	8a	0.8	1.4
101.8	7.9	8b	0.7	1.6
107.5	5.6	5a	0.6	1.7
107.5	5.5	5c	0.4	0.6

Table 22 continued.

0.2	0.2	4b	0.4	1.7
0.1	0.1	4a	0.5	2.3

Table 23. Post-settlement sediment thicknesses in bench deposits.

Drainage area (km²)	River-km	Bench	Pre-settlement (Holocene) thickness (m)	Post-Settlement (legacy) thickness (m)
58.0	15.3	10b	-	1.3
62.0	13.4	3c	-	1.4
64.8	12.4	9b	-	1.2
107.5	5.6	5b	-	1.1
115.5	1.9	7b	-	1.3

Table 24. Pre-settlement and post-settlement thicknesses in terrace deposits.

Drainage area (km²)	River-km	Terrace	Pre-settlement (Holocene) thickness (m)	Post-Settlement (legacy) thickness (m)
8.8	16.9	2a	1.1	0.2
39.7	19.2	11a	0.8	0.3
58.0	15.3	10c	0.7	0.3
62.0	13.8	3b	2.2	0.1
62.0	13.6	3a	1.5	0.4
115.5	1.9	7a	2.2	0.2

Table 25. Legacy sediment depths and rates in areas with a history of large-scale mining operations.

Legacy Sediment depth (m)	Mining rates (cm/yr)	Post mining (cm/yr)	Overall rates (cm/yr)	Location	Source	Method
3.0 - 4.0	(1.29 = mean) (1890-1925)	(0.30 = mean) (1925-1985)	(0.40 = mean) (0.30 - 5.0 = range) (1890-1985)	Mississippi River, Wisconsin/ Illinois	Knox (1987)	metals
0.08 - 1.25	(0.82 = mean) (1886-1916)	(0.6 = mean) (1916-1988)	NA	Honey Creek Watershed, Southwest Missouri	Carlson Thesis (1999)	metals
NA	(0.59 = mean) (1900-1920)	(0.53 = mean) (1920-1997)	(0.89= mean) (1830-1997)	Blue River Watershed, Wisconsin	Lecce and Pavlowsky (2001)	metals
0.5 - 1.0	(0.55 = mean) (0.17-1.27 = range) (1885-1920)	(0.3 = mean) (0.27-0.31 = range) (1920-1963)	NA	James River, Springfield Missouri	Owen et al. (2011)	metals
NA	(1.1-7.2 = range) (1842-1856)	NA	(0.9 = mean) (1842-2007)	Gold Hill Mining District, North Carolina	Lecce and Pavlowsky (2014)	metals
2.2 - 4.0	(3.4 = mean) (1896-1942)	(1.2 = mean) (1942-2018)	(2.0 = mean) (1896-2018)	Big River Watershed, Southeast Missouri	Jordan (2018)	C- and metals

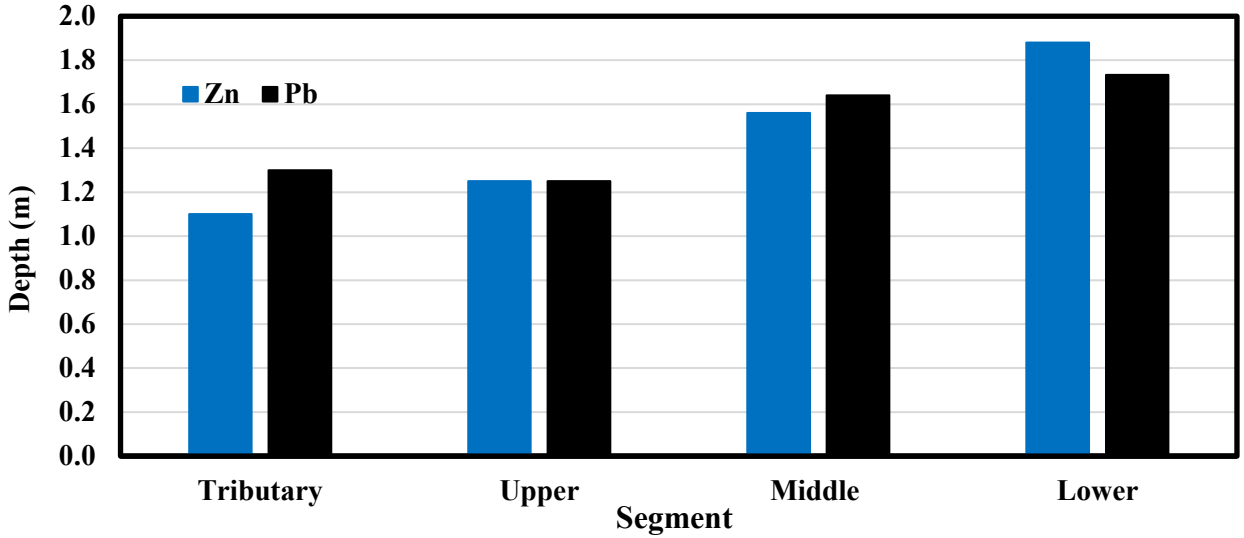

Figure 27. Average depth of contamination by watershed segment.

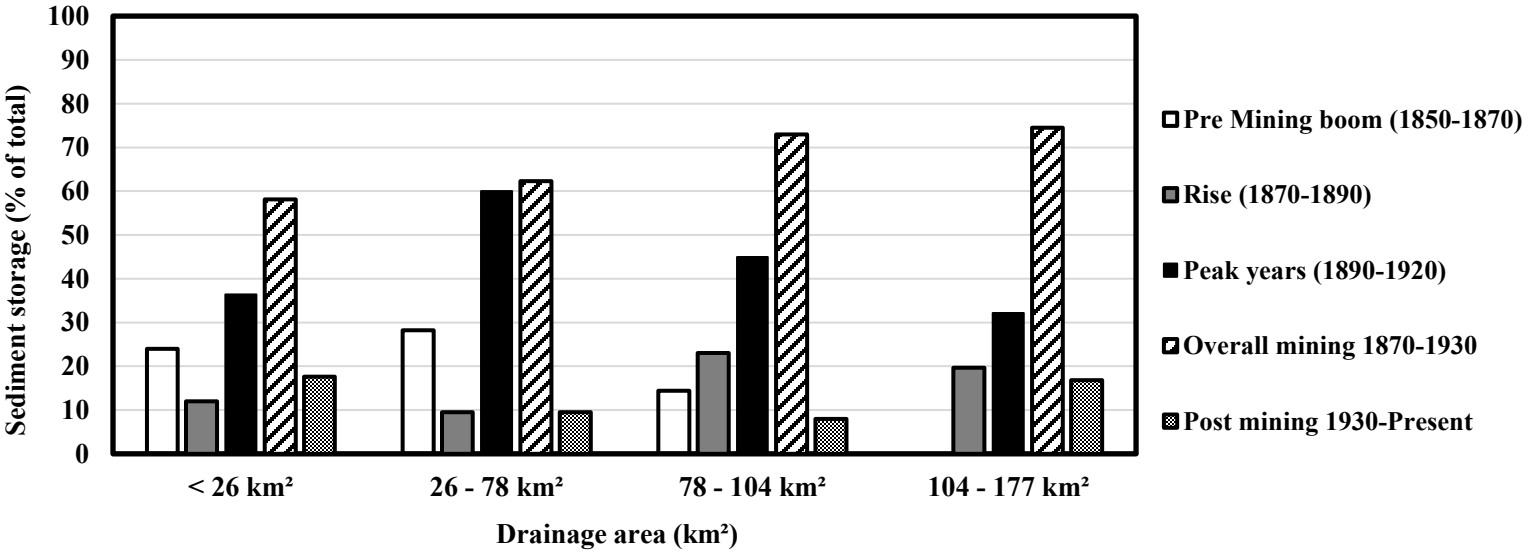

Figure 28. Sediment storage apportioned as a percentage of total post-settlement core depth within a given historical period.

CONCLUSION

This study offers a more focused look on the extent and history of floodplain soil contamination within a watershed resulting from a century of mining in the TSMD. Detailed assessments of the geomorphic responses of watersheds to extensive land alteration from early settlement and large-scale mining operations can help to better understand changes in stream systems as imposed by human activities including such characteristics as geochemical patterns and legacy deposits. This study is the first to recognize legacy deposits in Turkey Creek and their relationship to historical sedimentation rates and contamination patterns. Published soil surveys report on the relatively large-scale distribution of soil-landform relationships therefore the presence of buried soils and legacy sediments were not previously documented for the Turkey Creek watershed as well as other surrounding watersheds in southwestern Missouri along the western border of the Ozarks Highlands.

The results of this study indicate that legacy deposits are probably found throughout the region where agricultural settlement began in the mid-1800s and accelerated dramatically after the Civil War. Further, legacy deposits in mining areas such as the TSMD indicate the long-term storage of metal-contaminated sediment leading to the high probability of remobilization and continued toxic risk in the future. Floodplains represent a significant sink and source of sediments and mining-metal contamination along Turkey Creek and its tributaries. Legacy deposits on floodplains of Turkey Creek average 1.3 m thick and range from 0.6-2.3 m. Floodplain and bench deposits contain average Zn and Pb concentrations exceeding both the TSMD Probable effect threshold and the EPA's Remedial action levels (Table 3). Therefore, the results of this study can be a useful resource to inform Superfund managers for the continued

work of remediating mining impacts. For example, rough estimates indicate that upwards of one-million cubic yards of contaminated floodplain soil may require remediation in Turkey Creek.

The sedimentation history of Turkey Creek reflects the intensity of land use since the early 1800's. With the use of mining records, detailed stratigraphic mapping, and mining-metal profiles we calculated sedimentation rates for five historical periods, pre-mining (1850-1870), rise to large scale mining (1870-1890), peak mining (1890-1920), overall mining (1870-1930) and post mining (1930-2021). The greatest rates of sedimentation occurred during the mining periods, with the peak years (1890-1920) being the highest (1.7 cm/yr). The pre-mining period (1850-1870) had an average rate of 1.0 cm/ys and the post-mining period (1930-2021) had an average rate of 0.2 cm/yr. Rates and storage of the pre-mining deposits decrease with drainage area while those of mining and post mining deposits increase with drainage area. This depicts a shift in overbank deposition from upstream to downstream reaches, with downstream reaches actively receiving contaminated overbank deposition today.

Although this is a focused study in a small area, we can see how greatly land disturbances such as land clearing and large-scale mining operations impact fluvial environments. The findings in this study offer important insights into understanding the dynamic processes of floodplain development and evolution. Not only does it contain work that can further the understanding of sediment as a pollutant but as well as the extent to which floodplains can be contaminated by heavy metal mining. The value of floodplains to the biologic and physical health of a watershed is still gaining recognition and increasingly being studied in environmental assessments. This study presents supporting evidence for the importance of more floodplain studies in other areas that can be used to assess the longer-term influence of fluvial processes on water quality impairments and geomorphic instability. This is particularly important since recent

climate change and ongoing urbanization are predicted to increase flooding and potentially bank erosion rates in streams draining the Ozarks Highlands.

REFERENCES

Arcement, G.J., Schneider, V.K., 1989. Guide for selecting mannings roughness coefficients for natural channels and floodplains. U.S. Geological Survey Water Supply Paper 2339.

Barks, J.H., 1977. Effects of abandoned Lead and Zinc mines and tailings piles on water quality in the Joplin Area, Missouri. U.S. Geological Survey Water-Resources Investigations 77-75.

Belby, C.S., Spigel, L.J., Fitzpatrick, F.A., 2019. Historic changes to floodplain systems in the Driftless Area. The Physical Geography and Geology of the Driftless Area: The Career and Contributions of James C. Knox: Geological Society of America Special Paper 543, 119-145.

Bradley, S.B., 1989. Incorporation of metalliferous sediment from historic mining into river floodplains. GeoJournal 19, 5-14. https://doi.org/10.1007/BF00620544.

Brosius, L., Sawin, R.S., 2001. Lead and Zinc mining in Kansas: Kansas Geological Survey Public Information Circular 17, 6.

Carlson, J.L.,1999. Zinc mining contamination and sedimentation rates of historical overbank deposits, Honey Creek Watershed, Southwest Missouri. Missouri State University Graduate Theses. 784.

Carroll, S.A., O'Day, P.A., Piechowski, M., 1998. Rock-water interactions controlling Zinc, Cadmium, and Lead concentrations in surface waters and sediments, U.S. Tri-State Mining District. Environmental Science and Technology 32(7) 956-957.

Chow, V.T., 1959. Open channel hydraulics. New York, McGraw-Hill Book Co, 680.

Dennis, I.A., Coulthard, T.J., Brewer, P., Macklin, M.G., 2008. The role of floodplains in attenuating contaminated sediment fluxes in formerly mined drainage basins. Earth Surface Processes. Landforms 34, 453-466.

Donovan, M., Miller, A., Baker, M., Gellis, A., 2015. Sediment contributions from floodplains and legacy sediments to Piedmont streams of Baltimore County, Maryland. Geomorphology 235, 88-105. https://doi.org/10.1016/j.geomorph.2015.01.025.

Foulds, S.A., Brewer, P.A., Macklin, M.G., Haresign, W., Betson R.E., Rassner, S.M.E., 2014. Flood-related contamination in catchments affected by historical metal mining: An unexpected and emerging hazard of climate change. Science of the Total Environment 476-477, 165-180. https://doi.org/10.1016/j.scitotenv.2013.12.079.

Garvin, E.M., Bridge, C.F., Garvin, M.S., 2017. Screening level assessment of metal concentrations in streambed sediments and floodplain soils within the Lake Watershed in Northeastern Oklahoma, USA. Arch Environmental Contamination Toxicology.

Gilbert, G., 1917. Hydraulic-mining debris in the Sierra Nevada: Professional Paper. https://doi.org/10.3133/pp105.

Gutierrez, M., Collette, Z.J., McClanahan, A.M., Mickus, K., 2019. Mobility of metals in sediments contaminated with historical mining wastes: Example from the Tri-State Mining District, USA. Soil Systems 3(22) 1-11.

Gutierrez, M., Qiu, X., Collette, Z.J., Lurvey, Z.T., 2020. Metal content of stream sediments as a tool to assess remediation in an area recovering from historic mining contamination. Minerals 10(247). http://dx.doi.org/10.3390/min10030247.

Gutiérrez, M., Wu, S.S., Peebles, J.L., 2015. Geochemical mapping of Pb-and Zn-contaminated streambed sediments in southwest Missouri, USA. Journal of Soils and Sediments 15(1), 189-197.

Hagni, R.D., Saadallah, A.A., 1965. Alteration of host rock limestone adjacent to zinc-lead ore deposits in the Tri-State District, Missouri, Kansas, Oklahoma. Economic Geology 60(8), 1607-1619. doi:10.2113/gsecongeo.60.8.1607.

Hagni, R.D, Stewart, R. D., Brown, J. C., Dressel, W. M., McFarland, M. C., Fuerst, A. C., 1986. Guidebook to the geology and environmental concerns in the Tri-State Lead-Zinc District, Missouri, Kansas, Oklahoma. Association of Missouri Geologists 33rd annual meeting.

Happ, S.C., Rittenhouse, G., Dobson, G.C., 1940. Some principles of accelerated stream and valley sedimentation. U.S. Department of Agriculture Technical Bulletin 695, 133.

Heimann, D.C., Holmes, R.R., Jr., and Harris, T.E., 2018, Flooding in the southern Midwestern United States, April–May 2017: U.S. Geological Survey Open-File Report 2018–1004, 36 https://doi.org/10.3133/ofr20181004.

High Plains Regional Climate Center (HPRCC), 2022. Station Data Explorer – MOJS0034. https://hprcc.unl.edu/stationtool/explore.php?sid=MOJS0034 (Retrieved October 2022).

Hillerman M.Q., 2022. Mining-contaminated sediment and metal storage in channel deposits in Turkey Creek, Tri-State Mining District, Missouri and Kansas. MSU Graduate Theses. 3756. https://bearworks.missouristate.edu/theses/3756.

Hinrichs, D.R., 1996. Surface Waste of the Tri-State Mining District. Tailing and Mine Waste Conference Proceedings 16-19.

Hudson-Edwards, K.A., Macklin, M.G., Curtis, C.D., Vaughn, D.J., 1998. Chemical remobilization of contaminant metals within floodplain sediments in an incising river system: implications for dating and chemostratigraphy. Earth Surface Processes and Landforms 8(23) 671-684.

Ingersoll, C.G., Ivey, C.D., Brumbaugh, W.G., Besser, J.M., Kemble, N.E., 2009. Toxicity assessment of sediments from Grand Lake O' the Cherokees with the amphipod Hyalella azteca. Administrative Report CERC-8335-FY09-20-01. U.S. Geological Survey, Columbia, Missouri.

James, A.L, 1989. Sustained Storage and Transport of Hydraulic Gold Mining Sediment in the Bear River, California. Annals of the Association of American Geographers 79, 570–592. https://doi.org/10.1111/j.1467-8306.1989.tb00277.x.

James, A.L., 2013. Legacy Sediment: Definitions and processes of episodically produced anthropogenic sediment. Anthropocene 2, 16-26.

Johnson, A.W., Gutierrez, M., Gouzie, D., McAliley, L.R., 2016. State of remediation and metal toxicity in the Tri-State Mining District, USA. Chemosphere 144, 1132-1141.

Jordan, M.M., 2018. Historical floodplain sedimentation rates using mining contaminant profiles, Cesium-137, and sediment source indicators along the Lower Big River, Jefferson County, Missouri. Missouri State University Masters Theses, 3408.

Juracek, K.E., 2013. Occurrence and Variability of Mining-related lead and zinc in the Spring River Flood Plain and Tributary floodplains, Cherokee County, Kansas, 2009-11. U.S. Geological Survey Scientific Investigations Report 5028(70).

Klager, B.J., Juracek, K.E., 2017. Evaluation of Streambed-Sediment Metals Concentrations in the Spring River Basin, Cherokee County Superfund Site, Kansas, 2017. U.S. Geological Survey Scientific Investigations Report 5046, 25. https://doi.org/10.3133/sir20195046.

Knox, J.C., 1977. Human Impacts on Wisconsin Stream Channel. Annals of the Association of American Geographers 67(3), 323-342.

Knox, J.C., 1987. Historical valley floor sedimentation in the Upper Mississippi Valley. Annals of the Association of American Geographers 77(2), 224-244.

Knox, J.C., 1989. Long and short-term episodic storage and removal of sediment in watersheds of southwestern Wisconsin and northwestern Illinois. International Association of Hydrological Sciences (184), 157-164.

Knox, J.C., 2006. Floodplain sedimentation in the Upper Mississippi Valley: Natural versus human accelerated. Geomorphology 79, 286-310.

Lecce, S.A., 1997. Spatial patterns of historical overbank sedimentation and floodplain evolution, Blue River, Wisconsin. Geomorphology 18, 265-277.

Lecce, S.A., Pavlowsky, R.T., 1997. Storage of Mining-Related Zinc in Floodplain Sediments, Blue River, Wisconsin. Physical Geography 18, 424-439.

Lecce, S.A., Pavlowsky, R.T., 2001. Use of mining-contaminated sediment tracers to investigate the timing and rates of historical flood plain sedimentation. Geomorphology 38, 85-108.

Lecce, S.A., Pavlowsky, R.T., 2014. Floodplain storage or sediment contaminated by mercury and copper from historic gold mining at Gold Hill, North Carolina, USA. Geomorphology 206, 122-132. http://dx.doi.org/10.1016/j.geomorph.2013.10.004.

Lewin, J., Macklin, M.G., 1987. Metal mining and floodplain sedimentation, in Gardiner, V. (Ed). International Geomorphology Part 1. Chichester: John Wiley and Sons 1009-1027.

MacDonald, D.D., Ingersoll, C.G., and Berger, T.A., 2000, Development and evaluation of consensus-based sediment quality guidelines for freshwater ecosystems: Archives of Environmental Contamination and Toxicology 39, 20–31.

Macklin, M.G., 1985. Flood-plain sedimentation in the Upper Axe Valley, Mendip, England. Transactions of the Institute of British Geographers 10(2), 235-244.

Macklin, M.G., Brewer, P.A., Hudson-Edwards, K.A., Bird, G., Coulthard, T.J., Dennis, I.A., Lechler, P.J., Miller, J.R., Turner, J.N., 2006. A geomorphological approach to the management of rivers contaminated by metal mining. Geomorphology 79, 423-447.

Macklin, M.G., Hudson-Edwards, K.A., Dawson, E.J., 1997. The significance of pollution from historic metal mining in the Pennine orefields on river sediment contaminant fluxes to the North Sea. The Science of Total Environment 194, 391-397.

Macklin, M.G., Klimek, K., 1992. Dispersal, storage, and transformation of metal-contaminated alluvium in the upper Vistula basin, southwest Poland. Applied Geography 12, 7-30

Macklin, M.G., Ridgway, J., Passmore, D.G., Rumsby, B.T., 1994. The use of overbank sediment for geochemical mapping and contamination assessment: results from selected English and Welsh floodplains. Applied Geochemistry 9, 689-700.

Magilligan, F.J., 1985. Historical floodplain sedimentation in the Galena River Basin, Wisconsin, and Illinois. Annals of the Association of American Geographers 75(4), 583-594.

Manson, S., Schroeder, J., VanRiber, D., Kugler, T., Ruggles, S., 2021. IPUMS National Historical Geographic Information System Dataset. Version 17.0 (Retrieved May 2022).

Martin A.J., 1945. Summarized statistics of production of lead and zinc in the Tri-State (Missouri-Kansas-Oklahoma) Mining District. U.S. Department of Interior – Bureau of Mines Information Circular 7383.

McCauly, J.R., Brady, L.L., Wilson, F.W., 1983. A study of stability problems and hazard evaluation of the Kansas portion of the Tri-State Mining Area. Kansas Geological Survey, Open-file report 83-2.

Meade, R.H., 1982. Sources, sinks, and storage of river sediment in the Atlantic drainage of the United States. Journal of Geology 90(2), 235-252.

Miller, J.R., 1997. The role of fluvial geomorphic processes in the dispersal of heavy metals from mine sites. Journal of Geochemical Exploration 58, 101–118. https://doi.org/10.1016/s0375-6742(96) 00073-8.

Missouri Census Data Center (MCDC), 2022. https://www.census.gov/programs-surveys/decennial-census/decade.h (Retrieved August 2022).

Missouri Department of Natural Resources (MDNR), 2022. GeoStrat Application. https://modnr.maps.arcgis.com/apps/webappviewer/index.html?id=3ac3a61da4af4834811503a24a3cb935 (Retrieved May 2022).

Natural Resources and Conservation Service (NRCS), 2020. Web Soil Survey. United States Department of Agriculture. http://websoilsurvey.sc.egov.usda.gov/ (Retrieved October 2021).

Neary, D., Riekerk, H., 1988. An overview of nonpoint source pollution in the southern United States. Proceedings of the symposium: Forested Wetlands of the Southern United States 1214, 50.

Nigh, T.A. and Schroeder, W.A., 2002. Atlas of Missouri ecoregions. Missouri Department of Conservation, Jefferson City, Missouri.

Owen, M.R., Pavlowsky, R.T., Womble, P.J., 2011. Historical disturbance and contemporary floodplain development along an Ozark River, southwest Missouri. Physical Geography 32(5), 423-444.

Ozarks Environmental and Water Resources Institute (OEWRI), 2007. Standard operating procedure: Loss on ignition method.

Ozarks Environmental and Water Resources Institute (OEWRI), 2021. Standard operating procedure for: X-MET3000TXS Handheld XRF Analyzer.

Parker, A.J., Milan, D.J., McEwen, L.J., 2022. Correlating floodplain geochemical profiles with archival historical mining records to establish depositional chronologies of river sediment. Catena, 218.

Pavlowsky, R.T., Lecce, S.A., Owen, M.R., Martin, D.J., 2017. Legacy sediment, lead, and zinc storage in channel and floodplain deposits of the Big River, Old Lead Belt Mining District, Missouri, USA. Geomorphology 299, 54-75.

Pizzuto, J., Skalak, K., Pearson, A., Benthem, A., 2016. Active overbank deposition during the last century, South River, Virginia. Geomorphology 257, 164-178. https://doi.org/10.1016/j.geomorph.2016.01.006.

Pope, L.M., 2005. Assessment of contaminated streambed sediment in the Kansas part of the historic Tri-State Lead and Zinc Mining District, Cherokee County, 2004. U.S. Geological Survey Scientific Investigations 61, Report 5251.

Rosgen, D., 1995. A classification of natural rivers. Catena 22, 169-199.

Rowan, J.S., Barnes, S.J.A., Hetherington, S.L., Lambers, B., Parsons, F., 1995. Geomorphology and pollution: the environmental impacts of lead mining, Leadhills, Scotland. Journal of Geochemical Exploration 52, 57-65.

Sauer, C.O., 1920. The Geography of the Ozark Highland of Missouri. The Geographic Society of Chicago Bulletin 7.

Smith, 2016. Occurrence, distribution, and volume of metals-contaminated sediment of selected streams draining the Tri-State Mining District, Missouri, Oklahoma, and Kansas, 2011-2012. USGS Scientific Investigations Report 2016-5144.

Taggart, A.F., 1945. Handbook of mineral dressing: Ores and industrial minerals. New York, NY: John Wiley and Sons.

Thayer, J. B., Ashmore, P., 2016. Floodplain morphology, sedimentology, and development processes of a partially alluvial channel. Geomorphology 269, 160–174. doi:10.1016/j.geomorph.2016.06.040

Trimble, S.T., 1983. A sediment budget for Coon Creek Basin in the Driftless Area, Wisconsin, 1853-1977. American Journal of Science 283, 454-474.

Trimble, S.T., 1999. Decreased rates of alluvial sediment storage in the Coon Creek Basin, Wisconsin, 1975-1993. Science 28(5431), 1244-1246.

Trimble, S.T., 2009. Fluvial processes, morphology and sediment budgets in the Coon Creek Basin, WI, USA, 1975-1993. Geomorphology 108, 8-23. doi:10.1016/j.geomorph.2006.11.015.

United States Department of Agriculture Historical Archive (USDA), 2021. http://agcensus.mannlib.cornell.edu/AgCensus/homepage.do. (Retrieved August 2021).

United States Environmental Protection Agency (USEPA), 1997. The incidence and severity of sediment contamination in surface waters of the United States. National sediment quality survey: Report 823–R–97–006.

United States Environmental Protection Agency (USEPA), 2004. Incidence and severity of sediment contamination in surface waters of the United States - National sediment quality survey. Report to Congress EPA823-R-04-007.

United States Environmental Protection Agency (USEPA), 2010. Record of decision for Newton County mine tailings superfund site Newton County, Missouri, mine waste remediation operable units 1 and 2.

United States Environmental Protection Agency (USEPA), 2013. Record of decision amendment plan for Orongo-Duenweg Mining Blet Superfund Site Jasper County. Missouri, mine, and mill waster operable unit 1.

United States Geological Survey (USGS), 2001. The national flood-frequency program – methods for estimating flood magnitude and frequency in rural and urban areas in Missouri, 2000. USGS Fact Sheet 015-01.

United States Geological Survey (USGS), 2016. Cross Section Analyzer, Version 17-2016.

United States Geological Survey (USGS), 2021a. USGS Water Data for the Nation. https://waterdata.usgs.gov/nwis/inventory/?site_no=07187000 (Retrieved April 2021).

United States Geological Survey (USGS), 2021b. 3D Elevation Program. https://apps.nationalmap.gov/downloade/#/ (Retrieved October 2021).

U. S. Fish and Wildlife Service (USFWS), 2013. Tri-State Transition Zone Assessment Study. U.S. Fish and Wildlife Service, Tulsa, Oklahoma.

Walling, D.E., He, Q., 1998. The spatial variability of overbank sedimentation on river floodplains. Geomorphology 24, 209-223.

Winslow, A. J., Keyes, C. R., Robertson, J. D., 1894. Lead and Zinc deposits. U.S. Geological Survey 7(2).

Wolman, G., and L. Leopold., 1957. River flood plains: Some observations on their formation. U.S. Geological Survey Professional Paper 282-C.

APPENDICES

Appendix A. XRF Results – Zn, Pb, Ca, Fe, and Cd Concentrations (ppm).

Sample	Site/Bank	Depth	Zn	Pb	Ca	Fe	Cd
he1	1a	0-10	17227.8	1016.7		12961.8	81.3
he2	1a	10-20	26421.1	1096.5		8086.4	147.9
he3	1a	20-30	22409.9	1273.7		5840.9	112.9
he4	1a	30-40	31046.7	982.4		7673.8	231.7
he5	1a	40-50	35680.8	1083.4		14672.9	173.1
he6	1a	50-60	15577.2	2394.2	64581.5	8712.2	95.3
he7	1a	60-70	24068.5	6159.1	31874.7	15527.6	238.8
he8	1a	70-80	33314.2	9978.5	52637.9	12696.6	185.5
he9	1a	80-90	6980.4	1714.1	2522.8	11929.7	29.2
he10	1a	90-100	5036.5	3121.7	3733.8	14657.4	32.2
he11	1a	100-110	8071.6	9777.5	10814.6	11599.0	33.9
he12	1a	110-120	5233.6	4745.0	4705.6	13469.0	30.5
he13	1a	120-130	2675.7	1657.2	5043.3	14978.6	11.3
he14	1a	130-140	5096.7	249.6	6854.2	17155.6	24.0
he15	1a	140-150	5564.3	279.0	5742.9	26721.1	38.3
he16	1a	150-160	4434.3	286.3	6041.7	20243.6	19.9
he17	1a	160-170	3655.2	298.4	6230.3	19425.1	13.4
Standard			95.7	16.9	23353.5	29035.4	<LOD
Blank			<LOD	<LOD	103.8	55.0	13.8
he22	2a	0-10	784.7	67.0	2608.9	11134.9	<LOD
he23	2a	10-20	122.4	28.3	2446.2	12774.1	<LOD
he24	2a	20-30	107.6	33.0	2181.2	15691.7	<LOD
he25	2a	30-40	65.5	26.4	2254.9	16356.0	<LOD
he26	2a	40-50	67.6	24.5	1942.3	21495.6	<LOD
he27	2a	50-60	66.8	22.7	2137.8	20139.3	<LOD
he27	2a	50-60	92.4	45.3	2138.2	22549.6	<LOD

Appendix A Continued.

Sample	Site/Bank	Depth	Zn	Pb	Ca	Fe	Cd
Standard			97.5	16.8	23548.6	28341.5	<LOD
Blank			<LOD	<LOD	367.6	141.2	14.1
he28	2a	60-80	93.1	42.4	2139.8	25293.1	<LOD
he29	2a	80-100	115.9	137.6	2228.2	44600.7	<LOD
he30	2a	100-120	160.0	40.0	2943.5	28823.2	<LOD
he31	2a	120-140	208.5	30.9	3736.5	28040.8	<LOD
he32	2b	0-10	2084.6	179.9	4202.7	16094.6	22.3
he33	2b	10-20	2446.5	218.5	4250.3	19661.1	23.9
he34	2b	20-30	2417.2	238.7	3872.2	18367.0	24.3
he35	2b	30-40	1998.5	199.9	4172.0	19513.2	15.2
he36	2b	40-50	785.9	60.8	4231.2	27632.0	<LOD
he37	2b	50-60	2095.9	164.3	4971.5	21609.7	9.9
he37	2b	50-60dup	1979.7	148.0	4549.3	22904.2	14.6
Standard			109.7	11.1	23119.3	27995.5	<LOD
Blank			<LOD	<LOD	431.5	158.1	<LOD
he38	2b	60-70	686.4	83.4	3980.1	47775.5	<LOD
he39	2b	70-90	847.1	136.8	4762.2	42836.4	14.4
he40	2b	90-110	834.8	86.7	5863.0	44492.6	<LOD
he41	3a	0-10	2934.7	3497.6	12353.9	15960.9	17.9
he42	3a	10-20	2685.0	1240.8	5838.5	14196.1	28.8
he43	3a	20-30	2143.5	350.4	4065.0	12022.6	17.5
he44	3a	30-40	933.0	201.0	3990.7	10093.1	<LOD
he45	3a	40-50	484.0	93.8	3690.7	10612.9	<LOD
he46	3a	50-60	203.3	42.0	3771.3	10349.4	<LOD
he47	3a	60-70	244.7	35.6	3947.2	11665.7	<LOD
he47	3a	60-70dup	243.3	35.4	3843.9	11801.0	<LOD
Standard			104.3	19.3	23717.0	29003.0	11.1
Blank			<LOD	<LOD	428.6	196.2	16.7
he48	3a	70-80	271.5	38.7	4029.5	11560.9	<LOD

Appendix A Continued.

Sample	Site/Bank	Depth	Zn	Pb	Ca	Fe	Cd
he49	3a	80-90	321.2	40.5	3795.9	12187.9	<LOD
he50	3a	90-100	341.5	35.4	4004.4	12105.5	<LOD
he51	3a	100-120	345.6	45.8	4371.8	13070.0	<LOD
he52	3a	120-140	328.1	36.4	4048.6	14076.9	<LOD
he53	3a	140-160	319.6	38.3	4133.1	13998.1	<LOD
he54	3a	160-180	268.7	39.4	4497.6	20683.7	<LOD
he55	3a	180-200	219.7	34.5	5203.9	16707.5	<LOD
Standard			86.0	14.8	23166.5	28463.1	14.2
Blank			<LOD	<LOD	150.7	72.7	<LOD
he56	3b	0-10	775.5	217.4	6895.7	8780.3	<LOD
he57	3b	10-20	631.4	197.8	4561.6	7733.3	<LOD
he58	3b	20-30	294.5	112.9	3064.8	7489.5	<LOD
he59	3b	30-40	115.6	43.2	2589.5	9176.2	<LOD
he60	3b	40-50	72.7	22.8	2163.1	11278.4	<LOD
he61	3b	50-60	63.0	19.3	1928.9	12496.1	<LOD
he62	3b	60-70	50.6	19.5	1366.5	13133.9	9.6
he63	3b	70-80	51.1	17.4	1635.7	14482.8	<LOD
he64	3b	80-90	56.8	29.3	1554.8	15167.9	<LOD
he65	3b	90-100	39.0	17.6	1754.3	14212.0	<LOD
he65	3b	90-100	57.2	22.5	1693.4	14216.1	<LOD
Standard			95.7	12.4	23281.5	27857.4	<LOD
Blank			<LOD	<LOD	251.8	60.8	<LOD
he66	3b	130-140	62.7	22.8	3149.3	15877.1	<LOD
he67	3b	150-160	65.3	15.9	3454.5	17218.4	<LOD
he68	3b	220-230	95.0	30.8	4203.8	17419.2	<LOD
Standard			92.2	17.8	22738.5	28182.4	12.5
Blank			<LOD	<LOD	148.7	68.1	<LOD
he69	3c	0-10	3461.0	291.4	17907.6	16881.1	21.7
he70	3c	10-20	3632.6	312.5	17568.6	17818.0	23.0

Appendix A Continued.

Sample	Site/Bank	Depth	Zn	Pb	Ca	Fe	Cd
he71	3c	20-30	3440.2	295.4	12588.6	18179.7	25.8
he72	3c	30-40	3290.4	308.5	15477.2	18039.0	28.9
he73	3c	40-50	4362.2	338.3	11226.6	17962.7	38.7
he74	3c	50-60	4735.5	374.7	8238.9	16955.5	44.2
he75	3c	60-70	5848.7	447.2	7022.4	18853.9	47.4
he76	3c	70-80	5530.7	500.2	5607.0	16804.8	48.6
he77	3c	80-90	6642.3	627.9	5486.2	19715.8	50.8
he78	3c	90-100	7188.5	591.0	4977.6	21454.8	55.2
he78	3c	90-100	7098.6	605.5	5124.1	21191.7	55.2
he79	3c	100-110	7871.5	666.6	5432.7	20857.8	74.9
he80	3c	110-120	8708.6	886.2	6217.1	22003.9	75.0
he81	3c	120-130	8744.0	1196.7	10979.7	25281.9	91.7
he82	3c	130-140	6942.3	1944.7	6450.6	25266.0	79.9
Standard			83.7	10.0	22893.0	28200.4	<LOD
Blank			<LOD	<LOD	131.0	112.0	<LOD
he83	4a	0-10	10137.0	1329.1	18785.1	22170.8	70.6
he84	4a	45585	10046.6	1703.6	14879.1	21075.1	80.0
he85	4a	20-30	7369.6	1118.0	22813.6	19703.5	51.3
he86	4a	30-40	6622.4	949.1	21174.2	19465.0	45.9
he87	4a	40-50	7289.6	978.0	21334.1	19939.0	44.9
he88	4a	50-60	6905.0	886.7	12761.6	16362.5	58.0
he89	4a	60-70	12203.0	1420.6	18001.5	24060.9	60.1
he90	4a	70-80	13249.9	1755.0	12829.6	26274.8	69.5
he91	4a	80-90	15160.7	1898.9	15160.1	29263.8	103.5
he92	4a	90-100	18480.1	2103.6	21223.0	28403.4	120.8
he92	4a	90-100	18162.6	2105.1	21055.8	28280.8	128.2
Standard			183.8	25.5	23707.7	27964.1	<LOD
Blank			43.5	<LOD	1226.8	236.8	<LOD
he93	4a	100-110	18892.2	1780.3	36006.7	28940.3	128.8

Appendix A Continued.

Sample	Site/Bank	Depth	Zn	Pb	Ca	Fe	Cd
he94	4a	110-120	19950.4	2089.8	36748.2	31257.5	143.4
he95	4a	120-130	23393.9	1502.7	72098.4	17789.8	235.5
he96	4a	130-140	20447.2	1729.6	18852.3	26643.1	128.6
he97	4a	140-150	20654.7	2118.3	28085.6	28758.0	133.5
he98	4a	150-160	15902.3	1968.6	11911.4	32099.5	78.5
he99	4a	160-170	10734.3	1508.8	9683.3	25570.1	59.1
he100	4a	170-180	5704.6	1240.0	5694.6	16612.7	52.4
he101	4a	180-190	8102.3	1912.2	5686.5	25310.2	54.0
he102	4a	190-200	7550.1	2219.2	5994.2	26105.6	56.8
he102	4a	190-200	7637.2	2267.3	5960.5	26327.0	52.0
Standard			168.8	24.5	24496.6	28318.7	11.6
Blank			57.7	<LOD	1706.4	231.6	<LOD
he-103	4a	200-2110	6309.0	1881.6	6054.9	22029.7	55.2
he104	4a	210-220	4275.6	3017.6	4133.3	17437.8	34.4
he105	4a	220-240	3891.5	3970.3	5361.8	18058.2	45.2
he106	4a	240-250	3083.7	377.8	4942.5	13863.2	46.4
he107	4a	250-260	3015.4	229.6	5146.0	13529.0	45.5
he108	4a	260-270	3798.6	207.6	6356.3	14682.3	58.9
he109	4a	270-280	2445.6	97.0	5661.1	14055.7	33.9
he110	4b	0-10	6473.3	872.7	25028.5	18093.5	39.2
he111	4b	10-20	6571.4	876.9	19177.3	18044.1	39.3
he112	4b	20-30	6596.6	872.4	22265.4	17669.9	44.1
Standard			167.4	23.7	24220.6	27847.7	<LOD
Blank			72.5	<LOD	1810.8	273.5	<LOD
he113	4b	30-40	6418.4	899.9	19318.6	18780.5	48.8
he114	4b	40-50	15950.0	1877.6	26129.8	25090.2	100.8
he115	4b	50-60	13532.3	1466.3	19755.3	22360.4	91.2
he116	4b	60-70	19226.3	1718.7	35032.1	25709.0	122.3
he117	4b	70-80	17817.9	1472.9	46178.3	20632.5	118.6

Appendix A Continued.

Sample	Site/Bank	Depth	Zn	Pb	Ca	Fe	Cd
he118	4b	80-90	19399.7	1791.8	30417.2	30133.0	121.2
he119	4b	90-100	19397.3	2039.6	52083.5	25556.7	142.2
he120	4b	100-110	20620.0	1897.8	39555.0	27119.8	128.2
he121	4b	110-120	9091.3	1475.8	6567.4	21143.4	54.5
he122	4b	120-130	5738.3	1117.8	6184.1	15330.7	46.2
he122	4b	120-130	6248.1	1238.0	6678.2	16825.0	46.5
Standard			208.2	24.7	24789.7	28253.2	<LOD
Blank			74.2	<LOD	2301.6	303.7	<LOD
he123	4b	130-140	4703.1	1024.0	6053.8	14315.2	53.5
he124	4b	140-150	5965.4	1392.4	5586.5	15541.0	59.9
he125	4b	150-170	7513.8	2346.6	5988.3	24687.9	52.8
he126	4b	170-190	2740.0	1048.6	6202.3	14500.5	44.7
he127	4b	190-210	2377.9	88.3	5987.6	13867.0	29.5
he128	5a	0-10	6582.1	1023.5	22456.6	17765.8	34.7
he129	5a	10-20	7650.0	929.5	19211.6	16033.9	45.1
he130	5a	20-30	5978.4	447.4	38247.3	12886.0	47.1
he131	5a	30-40	7503.0	428.4	52364.5	13181.9	36.2
he132	5a	40-50	7089.2	406.0	35888.3	11080.3	26.7
he132	5a	40-50	7024.1	391.0	36909.2	11466.1	30.2
Standard			204.9	27.4	24708.4	27943.8	14.3
Blank			92.9	<LOD	2527.2	390.3	<LOD
he133	5a	50-60	6556.0	611.3	36884.1	11640.2	36.6
he134	5a	60-70	12856.7	1441.2	20747.7	19865.6	71.2
he135	5a	70-80	12763.6	1604.3	24489.8	19316.6	72.6
he136	5a	80-90	16352.2	1682.4	46077.3	22464.2	103.0
he137	5a	90-100	15114.9	1067.2	35480.7	17757.3	110.1
Standard			121.8	22.0	23354.2	28482.3	<LOD
Blank			22.6	<LOD	475.4	121.6	<LOD
he138	5a	100-110	6307.9	82.2	4331.3	15844.4	41.7

Appendix A Continued.

Sample	Site/Bank	Depth	Zn	Pb	Ca	Fe	Cd
he139	5a	110-120	5022.2	75.3	4944.0	15800.1	41.5
he140	5a	120-130	3316.8	59.5	4227.2	13870.7	35.2
he141	5a	130-140	2066.5	66.4	3464.3	13049.1	15.8
he142	5a	140-150	1386.3	65.6	4935.6	13816.2	<LOD
he143	5a	150-160	686.2	65.8	4989.9	13940.5	<LOD
he144	5a	160-170	4697.7	348.6	15373.8	42339.1	22.0
he145	5a	170-180	4388.0	276.9	14285.4	84164.9	27.3
he146	5a	210-230	3506.0	210.4	10198.3	66802.5	14.7
he146	5a	210-230	3529.6	238.7	10640.5	65842.2	17.0
Standard			120.6	18.2	23497.8	28495.7	<LOD
Blank			29.9	<LOD	542.6	172.2	<LOD
he147	5b	0-10	12511.9	1239.2	66632.1	14618.5	57.5
he148	5b	10-20	18613.8	1793.9	46400.1	20493.7	94.0
he149	5b	20-30	19972.9	1698.1	59493.9	23659.0	111.5
he150	5b	30-40	19646.0	2067.3	26585.5	31865.0	124.9
he151	5b	40-50	15901.9	1736.8		13788.1	126.2
he152	5b	50-60	16885.6	2555.9	35583.2	20384.8	97.7
he153	5b	60-70	25154.0	3419.0	19755.6	27765.3	157.6
he152	5b	50-60	15431.2	2253.8	32580.6	18371.1	90.8
he153	5b	60-70	24995.6	3564.3	20585.5	26839.2	175.5
he154	5b	70-80	18788.2	2576.3	13063.0	20591.8	113.3
he155	5b	80-100	19049.2	2551.5	10891.3	59504.5	108.7
he156	5b	100-120	5999.5	255.2	5548.5	11162.8	81.6
he156	5b	100-120	5998.2	252.9	5730.3	11319.0	88.0
Standard			253.8	12.7	24751.4	28705.8	12.0
Blank			92.7	<LOD	1919.3	381.4	<LOD
he157	5c	0-10	10326.6	1205.3	27796.6	17867.8	60.3
he158	5c	10-20	13060.1	1624.0	26973.3	20559.8	60.2
he159	5c	20-30	11718.9	1615.3	29256.0	21098.8	72.7

Appendix A Continued.

Sample	Site/Bank	Depth	Zn	Pb	Ca	Fe	Cd
he160	5c	30-40	14096.2	1563.2	43992.7	18982.2	94.4
he161	5c	40-50	14110.2	1927.4	24609.4	21008.9	92.2
he162	5c	50-60	5353.1	1996.8	4493.2	16179.2	43.1
he163	5c	60-70	3748.3	363.5	4625.2	13749.3	22.6
he164	5c	70-80	2817.2	92.6	4059.6	13717.9	26.5
he165		grab	3092.6	344.2	10449.8	20708.9	19.0
he166	6a	0-10	4883.9	1097.3	12727.2	36937.8	19.7
he166	6a	0-10	4977.7	1096.4	12477.4	36876.1	21.9
Standard			182.5	23.2	23452.0	28123.7	10.8
Blank			77.6	<LOD	1093.3	412.4	<LOD
he167	6a	10-20	12760.1	2012.8	16184.7		43.5
he168	6a	20-30	19968.9	2136.9	67550.4	24855.1	79.9
he169	6a	30-40	15904.5	1015.3		7984.4	52.9
he170	6a	40-50	13688.5	907.5		8560.5	48.6
he171	6a	50-60	14930.8	974.8		10312.0	51.5
he172	6a	60-70	19623.6	1657.5	81554.8	29991.0	197.8
he173	6a	70-80	26632.9	1003.3	61952.5	34787.7	185.5
he174	6a	80-90	14060.6	2111.4	11811.0	24743.9	78.2
he174	6a	90-100	11676.8	1662.2	8939.4	18779.4	56.1
Standard			167.1	26.5	23843.2	28587.5	<LOD
Blank			76.3	9.4	659.4	345.2	<LOD
he176	6a	100-110	8719.0	1253.8	3772.5	15870.4	37.1
he177	6a	110-120	2426.6	225.7	1519.5	5234.2	33.0
he178	6a	120-130	16850.2	1436.9	4016.3	13634.1	88.9
he179	6a	130-140	11070.8	4561.6	4886.2	17610.9	92.0
he180	6a	160-170	2547.7	1315.0	3903.4	10491.7	23.8
he181	6a	200-210	1518.3	62.2	5501.3	13918.9	9.5
Standard			126.2	20.0	23424.0	28753.1	<LOD
Blank			40.9	<LOD	359.1	226.4	<LOD

Appendix A Continued.

Sample	Site/Bank	Depth	Zn	Pb	Ca	Fe	Cd
he182	7a	0-10	7171.9	844.4	16835.4	14292.6	45.0
he183	7a	10-20	3403.5	443.0	6210.1	11635.1	26.8
he184	7a	20-30	612.1	110.3	3738.0	9832.2	<LOD
he185	7a	30-40	874.2	92.2	6683.0	11691.3	<LOD
he186	7a	40-50	1003.2	107.8	7298.1	11526.8	<LOD
he187	7a	50-60	552.6	75.4	4597.7	13084.4	<LOD
he188	7a	60-70	537.2	96.2	4300.0	14079.7	<LOD
he189	7a	70-80	362.0	82.6	3332.0	13093.9	<LOD
he190	7a	80-90	292.8	44.5	3433.4	14478.6	<LOD
he191	7a	90-100	229.8	68.9	2797.0	12645.1	<LOD
he192	7a	100-110	261.7	74.7	2186.0	14612.1	<LOD
he193	7a	110-120	270.7	61.4	2009.4	13741.5	<LOD
he194	7a	120-130	339.8	56.7	1701.5	14369.7	<LOD
he195	7a	130-140	295.7	57.5	2013.8	12825.9	<LOD
he196	7a	160-170	331.0	69.9	2267.1	14493.6	10.1
he196	7a	160-170	350.6	65.6	2298.6	14657.4	10.0
Standard			129.1	19.4	23525.9	28006.6	14.5
Blank			35.0	<LOD	400.5	255.5	<LOD
he197	7a	200-210	308.4	59.4	1794.0	11051.3	<LOD
he198	7a	240-250	490.1	84.5	5498.2	39666.1	<LOD
Standard			119.7	18.6	23713.5	27850.5	<LOD
Blank			25.9	<LOD	481.0	221.2	<LOD
he1000	7b	0-10	5970.5	539.9	50537.9	13922.4	51.5
he1001	7b	10-20	8290.7	748.0	35349.9	14277.7	46.2
he1002	7b	20-30	11010.7	1111.4	30202.7	18564.0	66.2
he1003	7b	30-40	11380.6	915.3	56427.9	16602.9	71.2
he1004	7b	40-50	17136.1	1459.7	34747.8	21416.1	82.9
he1005	7b	50-60	15758.9	1317.8	34175.9	21780.5	110.6
he1006	7b	60-70	15976.2	1065.5	33706.2	20552.4	85.1

Appendix A Continued.

Sample	Site/Bank	Depth	Zn	Pb	Ca	Fe	Cd
he1007	7b	70-80	9331.3	491.8	69593.2	9667.0	72.0
he1008	7b	80-90	16142.5	871.5	71326.7	12746.6	113.3
he1009	7b	90-100	13153.6	527.9	76086.8	8317.7	117.1
he1009	7b	90-100	13212.6	578.7	75157.1	8363.6	123.8
Standard			178.0	18.0	23565.6	28105.7	12.6
Blank			62.3	<LOD	1493.2	269.6	<LOD
he1010	7b	100-110	20478.8	1301.7		13372.2	123.3
he1011	7b	110-120	44072.4	1182.5	95623.2	15532.8	268.0
he1012	7b	120-130	20589.1	1310.9	56928.3	16517.7	138.7
Standard			103.2	20.5	24431.6	27783.4	11.9
Blank			20.4	<LOD	589.3	199.2	<LOD
he205	8a	0-10	7079.1	1273.0	29514.5	18556.5	52.9
he206	8a	10-20	7807.2	1324.6	26194.0	17943.2	40.1
he207	8a	20-30	10989.4	1355.7	39752.2	17482.2	55.1
he208	8a	30-40	13212.8	1366.0	31998.5	16594.6	55.6
he209	8a	40-50	14952.5	1944.5	41525.7	19915.2	87.0
he210	8a	50-60	15650.1	1987.1	28269.7	21324.8	101.9
he211	8a	60-70	14874.5	1984.2	44970.9	18374.9	99.7
he211	8a	60-70	15058.4	1971.5	44722.1	18472.1	94.9
Standard			162.8	13.2	23100.0	28532.5	<LOD
Blank			89.8	<LOD	914.4	384.1	<LOD
he212	8a	70-80	18567.4	2084.0	50538.4	17823.6	123.4
he213	8a	80-90	14417.2	2096.5	40541.3	17641.0	90.6
he214	8a	90-100	10136.3	2613.7	6611.7	19509.2	63.4
he215	8a	100-110	8376.5	3928.1	8048.5	20762.8	41.7
he216	8a	110-120	7752.2	4556.7	5710.7	20915.8	46.6
he217	8a	120-130	5766.9	4372.0	6003.8	17075.2	62.1
he218	8a	130-140	5912.8	1422.6	6200.5	16294.7	56.0
he219	8a	140-150	4233.9	469.2	4330.8	14862.7	43.1

Appendix A Continued.

Sample	Site/Bank	Depth	Zn	Pb	Ca	Fe	Cd
he220	8a	150-160	3840.0		8133.8	16105.1	29.7
he221	8a	150-160	3814.9		8233.7	15997.4	30.5
Standard			148.4	26.4	27590.1	27941.4	<LOD
Blank			477.6	<LOD	4688.5	3032.4	<LOD
he222	8a	200-230	3276.7	416.0	13996.8	21107.4	20.4
he223	8b	0-10	12074.8	1091.7	42128.2	15998.1	68.0
he224	8b	10-20	15868.3	1348.1	48032.3	19082.9	84.3
he225	8b	20-30	8867.0	1008.8	38293.2	17759.7	49.1
he226	8b	30-40	11376.5	1001.7	50478.9	17844.2	71.3
he227	8b	40-50	15343.7	1243.1	42628.0	20250.9	73.3
he228	8b	50-60	14858.0	1175.9	76615.0	15254.9	82.3
he229	8b	60-70	16035.7	1382.0	68152.3	17291.0	84.4
he230	8b	70-80	15439.6	1790.6	51092.1	21487.3	85.0
Standard			108.7	16.2	23377.3	28230.1	14.2
Blank			18.7	<LOD	459.8	165.4	<LOD
Standard			109.5	11.3	23903.4	27676.8	12.1
Blank			<LOD	<LOD	343.6	104.8	<LOD
he231	8b	80-90	18487.6	2162.4	61361.7	24626.5	112.5
he232	8b	90-100	28099.0	1714.3	79991.1	21214.8	200.3
he233	8b	100-110	10498.4	1439.2	11914.7	19526.0	49.4
he234	8b	110-120	6156.9	183.9	6036.5	16545.1	38.0
he235	8b	120-130	3344.5	96.1	4675.6	17780.8	22.6
he236	8b	130-140	2501.1	103.9	4491.8	16633.5	17.9
he237	8b	140-150	2052.7	88.6	4886.0	17432.1	20.2
he238	8b	150-160	1771.3	82.5	5059.2	17889.1	9.2
he239	8b	160-170	1421.2	66.5	5432.2	13210.8	<LOD
he240	8b	170-180	1331.2	74.4	5935.9	8748.5	<LOD
he240	8b	170-180	1337.8	79.5	6049.5	8918.2	<LOD
Standard			142.4	22.5	23711.9	27642.3	<LOD

Appendix A Continued.

Sample	Site/Bank	Depth	Zn	Pb	Ca	Fe	Cd
Blank			23.0	<LOD	400.9	84.2	<LOD
he241	8b	180-190	1409.8	98.8	4522.5	15387.7	17.8
he242a	8b	190-200	1606.2	191.0	6081.9	25301.7	29.6
he242b	8b	200-210	1470.0	142.6	7463.0	26193.5	17.8
he243	8b	210-220	883.5	75.3	4882.4	20227.0	9.5
he244	8b	220-230	839.7	81.6	4723.5	19139.1	<LOD
he245	9a	0-10	6589.2	781.1	3384.3	18826.9	50.0
he246	9a	10-20	9375.7	1198.5	3399.5	22123.2	60.3
he247	9a	20-30	10081.5	1144.1	2898.1	29185.1	69.3
he248	9a	30-40	7547.2	1027.6	2722.2	21253.5	64.9
Standard			108.2	14.0	23894.4	28564.7	<LOD
Blank			<LOD	<LOD	110.3	75.2	<LOD
he249	9a	40-50	3123.4	857.4	2601.6	11120.6	42.2
he250	9a	50-60	2863.3	137.2	2149.5	12063.3	28.1
he251	9a	60-70	2139.4	64.5	2792.6	11246.1	19.7
he252	9a	70-80	1626.0	35.3	2784.4	10812.7	<LOD
he253	9a	80-90	851.6	51.8	2882.7	12097.6	<LOD
he254	9a	90-100	476.6	35.2	3132.7	12099.7	<LOD
he255	9a	100-110	597.1	33.7	3115.5	12338.9	<LOD
he256	9a	110-120	458.7	44.2	3289.0	12120.4	<LOD
he257	9a	120-130	616.6	44.8	2750.7	13203.4	<LOD
he258	9a	130-140	424.2	41.4	3912.5	13673.3	<LOD
he259	9a	140-150	444.7	38.7	4075.1	19040.3	11.5
he260	9a	150-160	394.5	37.5	3822.7	14475.0	<LOD
he260	9a	160-170	363.6	34.0	3145.3	12994.9	10.1
Standard			94.7	22.6	23696.5	28456.9	<LOD
Blank			<LOD	<LOD	148.5	90.6	<LOD
he261	9a	190-210	435.2	58.4	3935.9	11038.0	<LOD
he262	9a	190-210	953.0	86.5	4340.1	21154.4	<LOD

Appendix A Continued.

Sample	Site/Bank	Depth	Zn	Pb	Ca	Fe	Cd
he264	9b	0-20	3042.8	390.2	15852.9	16799.6	24.1
he265	9b	20-40	3372.6	499.1	19458.0	18297.6	22.4
he266	9b	40-60	3709.0	553.1	18196.7	18235.7	26.3
he267	9b	60-80	3911.5	718.5	12079.1	19593.0	32.0
he268	9b	80-100	5529.9	690.6	11061.1	19050.7	38.8
he269	9b	110-130	4202.3	442.5	5814.3	21061.5	22.9
he270	12a	0-10	4609.4	864.0	19166.6	20450.5	26.7
he271	12a	10-20	4571.1	1071.8	11401.4	21995.3	23.9
he271	12a	10-20	4717.6	1102.1	11398.4	22074.0	30.9
Standard			114.1	13.2	24002.8	28064.6	14.3
Blank			12.9	<LOD	420.5	185.5	<LOD
he272	12a	20-30	6424.0	1248.6	14566.7	22969.3	34.9
he273	12a	30-40	7759.8	1516.4	10326.8	27581.7	43.0
he274	12a	40-50	19771.7	3317.9	28979.6	40930.2	93.4
he275	12a	50-60	23662.0	3700.2	33702.0	34402.9	146.3
he276	12a	60-70	30177.8	3758.2	39468.3	57212.0	170.4
he277	12a	70-80	29840.0	3701.6	23682.9	53951.3	138.2
he278	12a	80-90	26079.8	3993.4	28920.5	53314.7	104.0
he279	12a	90-100	20714.6	3531.5	29216.5	42262.8	119.1
he280	12a	100-110	16905.1	3286.0	17194.7	35200.0	106.6
he281	12a	110-120	11016.6	1917.8	12697.3	22140.7	53.6
he282	12a	120-130	5481.5	554.0	4018.3	15764.1	16.4
he283	12a	130-140	2015.2	117.3	4507.8	17300.2	11.9
he284	12a	140-160	833.7	217.5	4944.4	15628.5	<LOD
Standard			110.8	18.8	22890.9	28250.6	<LOD
Blank			11.9	<LOD	311.6	127.5	<LOD
he500	10a	0-10	3173.1	282.1	18572.4	19284.2	29.5
he501	10a	10-20	3792.3	298.7	12570.4	20072.1	22.2
he502	10a	20-30	3869.4	332.8	14848.4	20618.4	29.6

Appendix A Continued.

Sample	Site/Bank	Depth	Zn	Pb	Ca	Fe	Cd
he503	10a	30-40	5403.9	410.2	9849.9	22110.5	39.2
he504	10a	40-50	4770.3	391.4	11865.2	20649.7	32.9
he505	10a	50-60	5211.4	510.1	7326.2	19781.8	41.1
he506	10a	60-70	2417.4	241.5	4044.9	13401.1	25.0
he507	10a	70-80	1303.9	86.6	3722.3	11270.9	16.5
he508	10a	80-90	844.0	53.9	4638.0	15653.1	<LOD
he509	10a	90-100	716.9	43.1	4089.1	12552.9	11.1
he510	10a	100-110	674.2	44.6	3622.2	13008.6	<LOD
he511	10a	110-120	851.6	43.9	4220.3	14916.4	14.0
he512	10a	230-260	2919.4	117.1	4033.4	20972.0	<LOD
he512	10a	230-260	2918.7	124.5	3903.7	20114.1	<LOD
Standard			114.5	15.3	23474.0	28251.2	12.7
Blank			<LOD	<LOD	369.9	95.8	<LOD
he513	10b	0-10	2164.7	210.2	6117.3	16765.4	20.0
he514	10b	10-20	3128.8	257.8	5785.3	19298.3	20.2
he515	10b	20-30	3527.8	294.5	5510.2	18497.4	27.3
he516	10b	30-40	2115.1	150.8	3935.9	13405.2	18.9
he517	10b	80-90	7890.7	1033.9	4867.9	22303.8	40.0
he518	10b	90-100	7090.3	1016.8	3934.2	21826.3	50.2
he519	10b	100-110	9579.6	1043.4	4129.8	24968.4	56.7
he520	10b	110-120	11875.9	1175.2	3838.9	28875.8	63.2
he521	10b	120-130	12933.3	1668.6	5023.8	34133.4	65.6
he522	10c	0-10	1645.5	185.6	5614.5	12491.5	13.4
he522	10c	0-10	1615.2	195.5	5768.9	12279.3	20.3
Standard			95.8	13.3	22931.6	28583.9	12.8
Blank			<LOD	<LOD	350.2	432.2	<LOD
he523	10c	30-40	705.8	99.3	3252.4	9626.0	<LOD
he524	10c	60-70	196.3	35.7	2495.1	10850.9	<LOD
he525	10c	90-100	370.4	56.9	3108.1	18153.8	11.7

Appendix A Continued.

Sample	Site/Bank	Depth	Zn	Pb	Ca	Fe	Cd
he600	11a	0-10	2408.4	271.8	5136.4	15967.0	11.4
he601	11a	10-20	2293.5	306.0	4687.7	15222.5	17.0
he602	11a	20-30	619.1	36.9	2382.1	11018.4	9.5
he603	11a	30-40	728.9	64.1	2235.6	19121.0	12.4
he604	11a	40-50	1543.7	79.8	2919.3	17252.7	<LOD
he605	11a	50-60	1538.3	84.3	2523.2	17637.4	17.0
he606	11a	60-70	1329.9	71.5	2728.9	30424.4	17.7
he607	11a	70-80	464.3	43.0	2859.1	11348.1	<LOD
he607	11a	70-80	450.2	35.4	2564.9	12592.0	<LOD
Standard			119.5	19.3	23124.3	27898.3	12.8
Blank			<LOD	<LOD	439.4	200.7	<LOD
he608	11a	100-110	1306.8	79.6	2907.8	16843.7	10.5
he608	11a	100-110	1313.1	76.1	3403.8	19658.0	<LOD
he609	11b	0-10	1466.8	244.9	5411.7	14353.7	13.3
he610	11b	10-20	2043.1	279.5	6269.5	14739.6	17.8
he611	11b	20-30	3509.8	427.3	4216.4	14967.5	29.8
he612	11b	30-40	3810.1	430.4	3353.9	14724.6	26.4
he613	11b	40-50	4423.8	539.9	3038.2	13759.6	28.0
he614	11b	50-60	18174.1	1247.4	3116.4	20537.2	39.6
he615	11b	60-70	12333.0	998.0	2724.4	16904.9	40.1
he616	11b	70-80	5015.0	575.8	2785.6	14726.1	49.2
he617	11b	80-90	6329.8	764.8	3165.3	18054.4	64.6
he618	11b	90-100	10386.5	1810.6	3471.0	22782.5	83.8
he618	11b	90-100	9864.9	1752.1	3252.3	22406.5	91.3
Standard			111.7	19.7	22950.4	28366.6	<LOD
Blank			27.8	<LOD	404.9	207.5	<LOD
he619	11b	110-120	6035.2	579.9	2759.4	11760.0	45.4
he620	11b	150-160	11949.9	8311.4	2982.1	10574.3	22.8

Appendix B. XRF Duplicate Errors of Pb, Zn, Fe and Ca.

Sample	Pb Error	% Difference	Zn Error	% Difference	Fe Error	% Difference	Ca Error	% Difference
27	7.5	-66.5	13.9	-32.2	360.6	-11.3	204.5	0.0
27 dup	9.8		16.0		388.3		207.6	
37	17.0	10.5	66.1	5.7	385.6	-5.8	283.4	8.9
37 dup	16.2		63.8		394.5		272.9	
47	8.5	0.5	22.6	0.6	269.9	-1.2	238.0	2.7
47 dup	8.6		22.7		272.7		234.5	
65	7.0	-24.3	12.0	-37.8	301.2	0.0	185.2	3.5
65 dup	7.5		13.2		304.3		181.8	
78	31.5	-2.4	122.3	1.3	386.6	1.2	298.7	-2.9
78 dup	32.0		122.0		385.5		304.4	
92	66.7	-0.1	221.6	1.7	502.6	0.4	579.0	0.8
92 dup	66.6		219.1		500.0		577.5	
102	62.8	-2.1	130.1	-1.1	441.7	-0.8	342.8	0.6
102 dup	63.8		131.4		445.5		334.5	
122	43.2	-10.2	109.5	-8.5	327.9	-9.3	304.9	-7.7
122 dup	45.4		114.1		342.8		323.0	
132	27.5	3.8	127.4	0.9	292.4	-3.4	603.9	-2.8
132 dup	26.6		125.0		293.3		608.4	
146	20.8	-12.6	92.5	-0.7	732.5	1.4	489.5	-4.2
146 dup	21.9		92.4		724.6		492.8	
156	20.2	0.9	106.9	0.0	267.1	-1.4	281.9	-3.2
156dup	20.2		107.4		270.3		290.3	
166	45.0	0.1	106.4	-1.9	533.0	0.2	457.3	2.0
166 dup	45.0		107.5		532.6		459.2	
196	11.2	6.4	26.2	-5.8	304.8	-1.1	178.7	-1.4
196 dup	10.9		26.9		306.7		180.8	

Appendix B Continued.

Sample	Pb Error	% Difference	Zn Error	% Difference	Fe Error	% Difference	Ca Error	% Difference
1009	31.9		176.8		259.6		909.5	
1009 dup	33.3	-9.2	177.1	-0.4	260.2	-0.5	904.6	1.2
211	61.2		188.0		382.9		803.9	
211 dup	61.3	0.6	189.9	-1.2	385.5	-0.5	809.3	0.6
240	11.1		49.2		229.2		270.1	
240 dup	11.4	-6.7	49.1	-0.5	230.2	-1.9	273.7	-1.9
260	8.8		28.4		302.7		240.0	
260 dup	8.7	9.8	28.1	8.1	294.8	10.8	193.3	19.4
271	42.1		97.5		390.0		418.7	
271 dup	42.9	-2.8	99.5	-3.2	392.8	-0.4	425.9	0.0
512	14.6		77.6		379.5		244.4	
512 dup	14.9	-6.1	77.2	0.0	369.8	4.2	241.3	3.3
522	17.2		55.8		280.1		279.8	
522 dup	17.5	-5.2	55.0	1.9	276.2	1.7	275.4	-2.7
607	9.2		30.3		265.6		203.7	
607 dup	8.5	19.3	29.7	3.1	278.9	-10.4	200.9	10.8
618	56.4		151.5		410.7		262.3	
618 dup	55.9	3.3	148.6	5.2	409.8	1.7	250.5	6.5
Mean:		-4.2		-3.0		-1.2		1.5
Median:		-1.1		-0.2		-0.5		-0.3

Appendix C. Loss on Ignition – Organic Matter Percent by Sample.

Sample	OM LOI	Sample	OM LOI	Sample	OM LOI	Sample	OM LOI
1	3.7	90	7.0	180	4.7	275	5.4
2	2.5	91	8.0	181	4.4	276	8.8
3	1.8	92	5.7	181	4.4	277	8.1
4	2.6	92	5.8	182	6.0	278	8.3
5	3.3	93	6.0	183	4.8	279	5.2
6	2.9	94	6.2	184	3.9	280	5.8
7	4.1	95	3.7	185	3.5	281	4.2
8	3.3	96	5.8	186	3.2	282	4.7
9	5.7	97	5.4	186	3.3	283	4.1
10	5.9	98	7.3	187	3.1	283	4.1
10	6.1	99	6.6	188	3.2	284	3.6
11	5.0	100	4.9	189	3.1	500	8.1
12	6.7	101	5.8	190	2.6	501	5.7
12	5.9	102	6.0	191	2.7	502	5.5
13	5.8	102	6.1	191	2.7	503	5.6
14	5.4	103	5.7	192	2.7	503	5.5
15	4.4	104	5.5	193	2.7	504	4.8
16	6.1	105	6.2	194	2.4	505	5.4
16	6.2	106	5.1	195	2.5	506	4.5
17	5.6	107	5.3	196	2.4	507	4.1
18	1.5	108	6.8	197	2.4	508	3.3
19	3.7	109	5.1	198	5.9	509	3.1
19	3.7	109	5.1	205	7.4	510	3.5
20	5.1	110	7.0	206	6.8	511	3.0
21	4.2	111	6.8	206	6.5	512	4.8
22	4.2	111	7.0	207	6.0	513	6.1
23	3.8	112	6.1	208	8.3	513	6.2
24	3.9	113	6.3	209	4.4	514	4.7
25	4.1	114	4.7	210	5.0	515	5.1

Appendix C Continued.

Sample	OM LOI	Sample	OM LOI	Sample	OM LOI	Sample	OM LOI
25	3.9	115	5.6	211	3.5	516	4.4
26	4.3	116	4.6	211	3.5	517	6.2
27	4.1	117	3.9	212	3.7	518	4.4
28	5.1	118	4.6	213	4.0	519	5.1
28	5.3	119	4.6	214	5.0	520	4.6
29	4.0	120	4.6	215	5.3	520	4.6
30	4.4	121	5.1	216	5.3	521	4.7
31	3.9	121	5.0	216	5.3	522	5.7
32	5.8	122	4.5	217	5.3	523	3.2
33	5.0	123	4.6	217	5.5	524	2.0
34	4.9	124	4.2	218	5.9	525	2.6
35	5.0	125	4.8	219	5.8	525	2.5
35	5.1	126	4.4	220	5.5	600	6.4
36	4.9	126	4.5	220	5.6	601	6.2
37	5.9	127	3.7	221	5.3	602	2.4
38	5.1	128	12.0	222	4.4	603	2.6
39	5.4	129	5.5	223	7.9	604	2.7
40	5.6	130	4.6	224	6.0	605	2.6
41	7.6	131	3.3	225	5.0	606	2.8
42	5.6	132	3.2	226	6.0	607	2.7
43	4.2	133	4.1	227	5.4	608	2.5
43	4.3	134	6.0	228	4.3	609	6.2
44	3.6	135	4.9	229	4.6	609	6.4
45	3.5	136	4.0	230	5.1	610	8.3
46	3.5	136	4.2	231	5.3	611	4.7
47	3.9	137	3.8	231	5.3	612	3.3
48	4.0	138	4.5	232	3.8	613	3.7
49	3.9	139	4.3	233	3.8	614	4.1
50	3.6	140	4.1	234	4.2	615	4.2

Appendix C Continued.

Sample	OM LOI	Sample	OM LOI	Sample	OM LOI	Sample	OM LOI
51	3.6	141	4.1	235	4.0	616	4.1
52	3.5	142	4.0	236	4.2	617	4.4
53	3.2	143	3.8	237	4.2	618	5.6
53	3.1	144	6.2	238	4.5	618	5.6
54	3.0	145	6.6	239	4.2	619	2.3
55	2.8	145	6.6	240	3.6	620	8.3
56	9.2	146	5.3	241	3.2	620	8.4
57	5.6	147	4.1	242	2.7	1000	3.6
58	3.4	148	4.1	242	3.2	1001	4.4
59	2.5	149	4.8	243	3.3	1002	6.1
60	2.6	150	4.9	244	3.3	1003	4.6
61	2.5	151	2.6	245	5.0	1003	4.8
62	2.5	152	4.7	246	5.5	1004	5.2
63	2.5	153	4.5	247	5.1	1005	4.6
64	2.6	154	4.3	248	4.9	1006	3.9
64	2.6	155	5.9	248	5.0	1007	2.2
65	2.6	156	5.3	249	4.6	1008	2.2
66	2.6	156	5.3	250	4.3	1009	1.9
67	2.7	157	7.3	251	3.9	1010	2.4
68	2.9	157	7.4	252	3.4	1011	3.8
69	14.5	158	5.3	253	3.2	1012	3.7
70	9.9	159	5.8	254	3.3		
70	10.4	160	4.4	255	3.8		
71	7.5	161	5.0	256	3.9		
72	6.5	162	3.9	257	3.9		
73	6.6	163	3.5	258	3.7		
74	6.6	164	3.2	258	3.7		
75	7.1	165	4.0	259	3.3		
76	6.6	166	12.2	260	3.0		

Appendix C Continued.

Sample	OM LOI	Sample	OM LOI	Sample	OM LOI	Sample	OM LOI
77	6.1	167	8.4	261	3.4		
78	6.3	168	2.2	262	5.0		
79	7.4	169	2.4	263	7.2		
80	7.4	170	2.1	264	7.6		
81	10.6	171	3.1	265	6.3		
81	10.4	172	4.0	266	6.4		
82	10.0	173	5.1	267	5.7		
83	6.8	174	4.1	268	3.9		
84	6.5	175	4.0	269	5.4		
85	7.7	175	4.0	270	5.8		
86	7.6	176	3.9	271	6.1		
87	6.6	177	1.7	272	8.8		
88	6.8	178	4.0	273	9.5		
89	6.7	179	3.8	274	9.4		

Appendix D. Loss on Ignition Duplicate Errors.

Sample	Duplicate Error%	Sample	Duplicate Error%
10	-3.83	175	-0.34
13	-2.00	181	-0.10
16	-0.88	186	-3.16
19	0.57	191	-0.51
25	6.16	206	4.35
28	-3.31	211	-0.97
35	-2.14	216	0.26
43	-0.52	217	-5.22
53	3.11	220	-0.63
64	-2.37	231	-0.89
70	-4.37	248	-2.25
81	1.92	258	-1.32
92	-0.88	274	1.58
102	-1.03	283	-0.20
109	0.51	503	1.57
111	-2.49	513	-1.00
121	0.99	520	1.82
126	-1.66	525	2.93
136	-6.23	609	-4.43
145	-0.16	618	1.50
156	0.60	620	-1.00
157	-0.35	1003	-2.62

Appendix E. Floodplain Core Vertical Trends of Zn, Pb, Ca, Fe, and Organic Matter with Cut Bank Images .

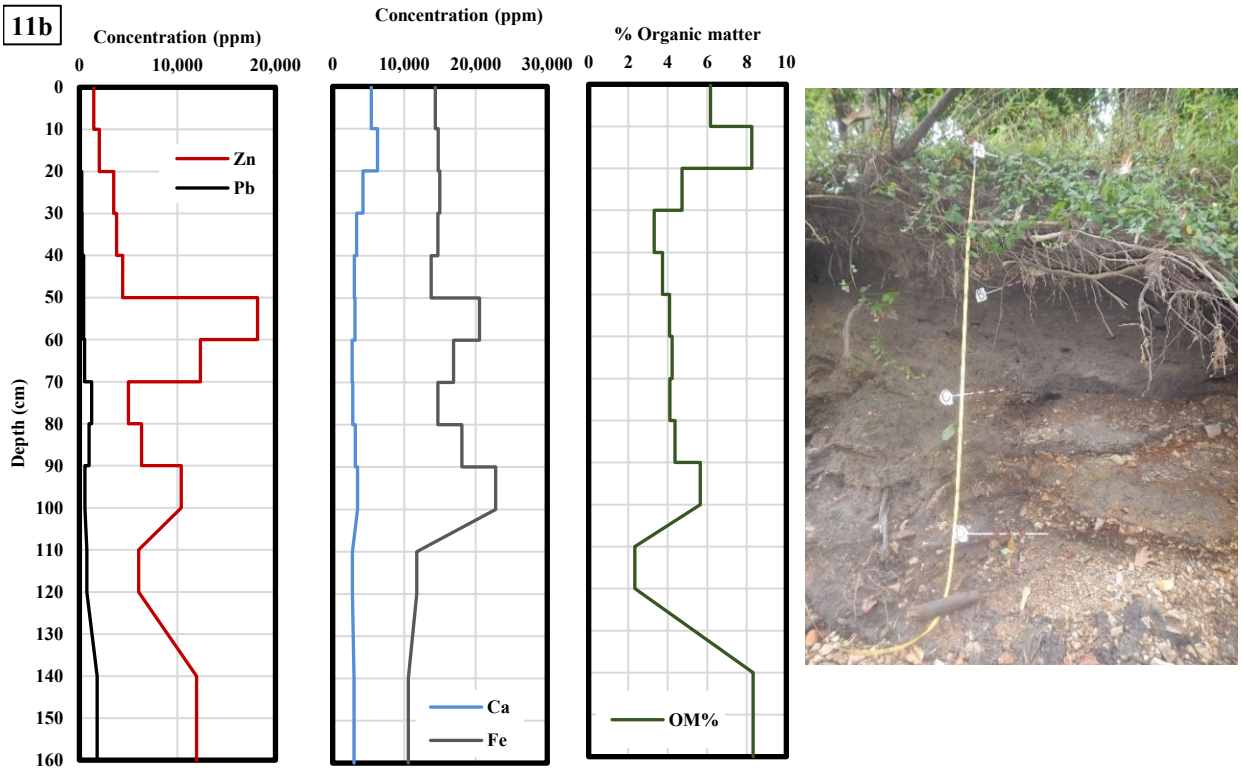

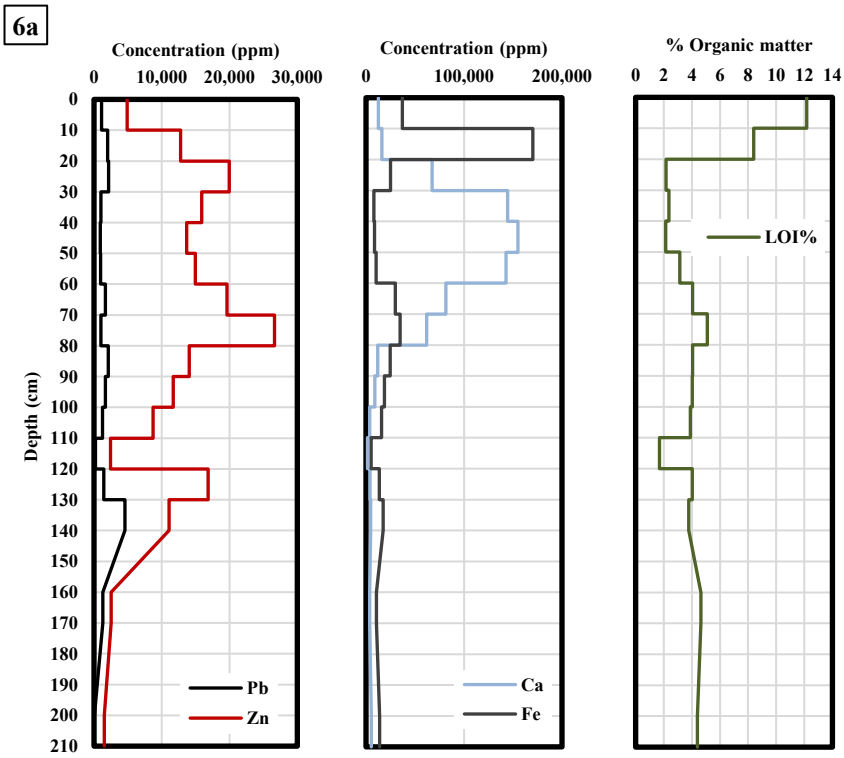

Appendix E Continued.

12a

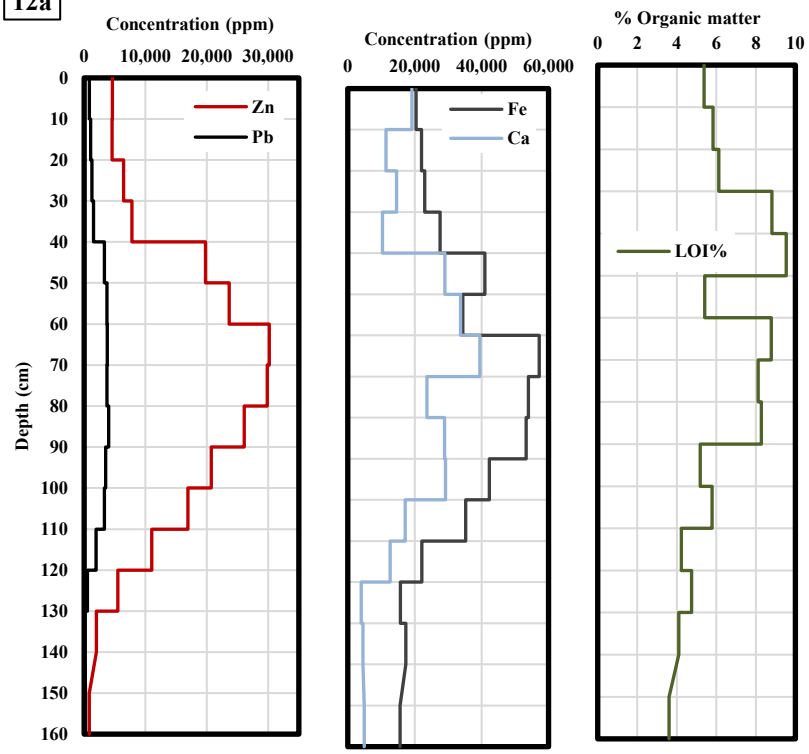

1a

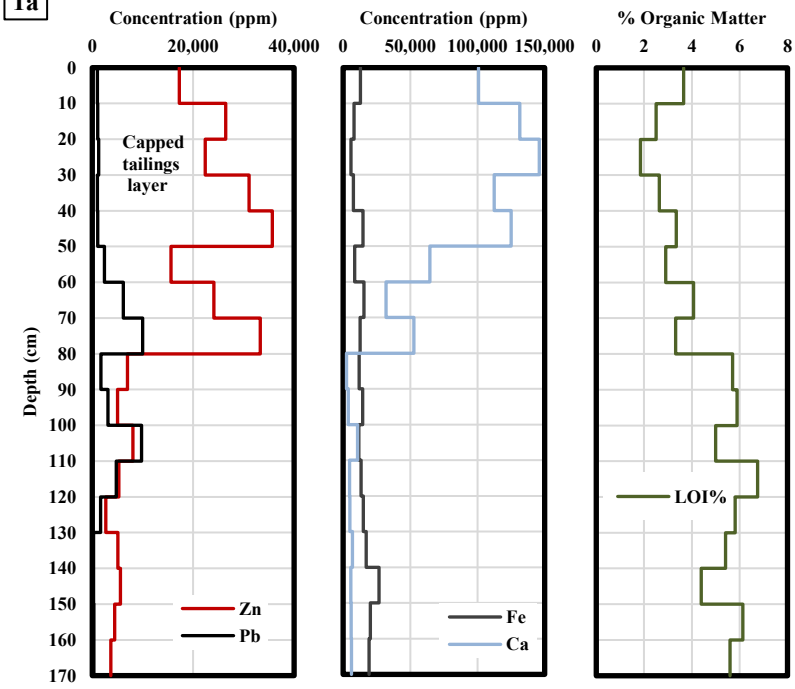

Appendix E Continued.

8a

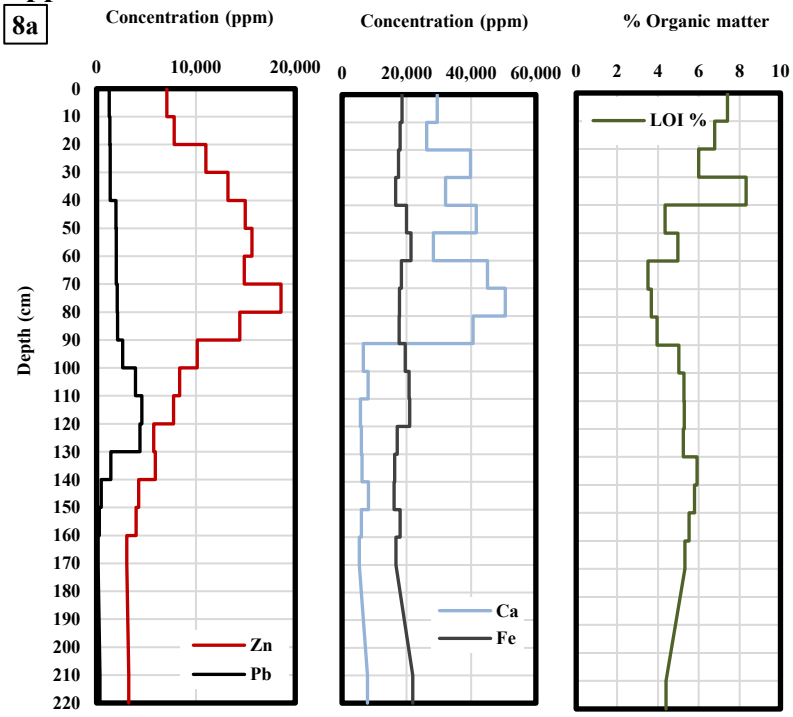

8b

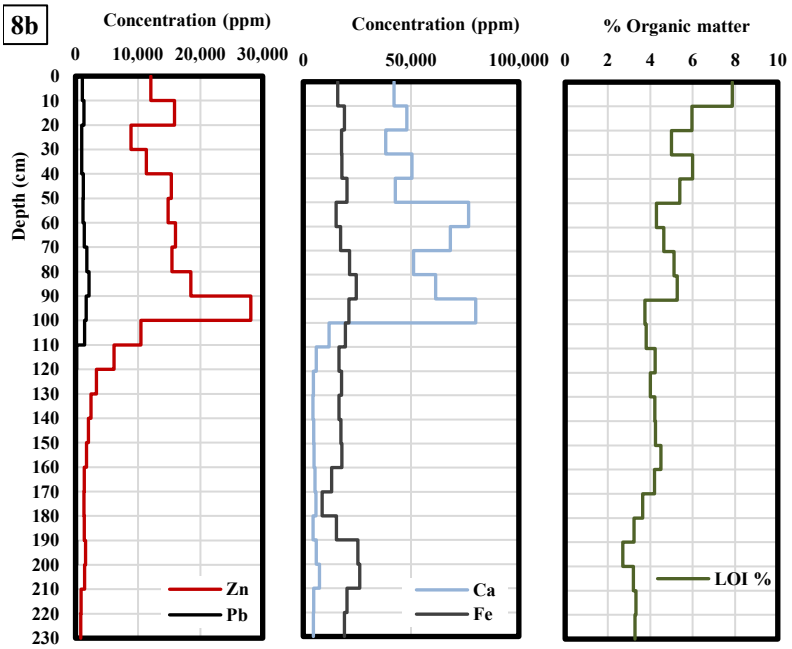

Appendix E Continued.

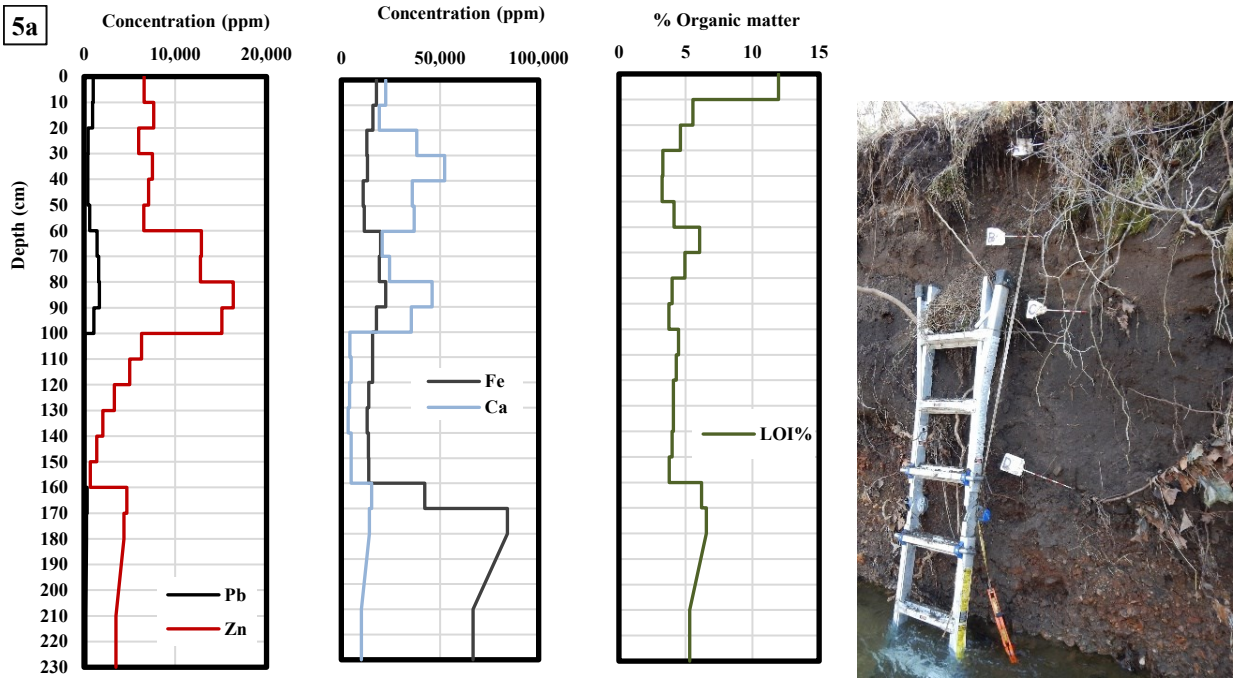

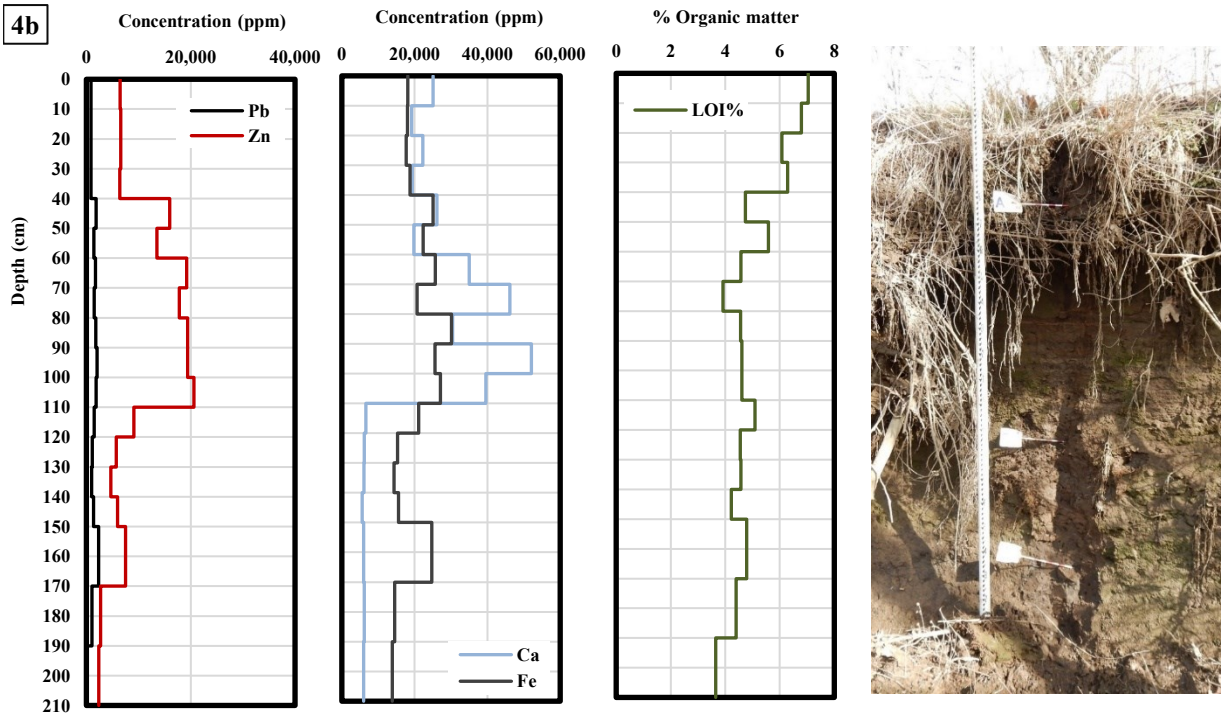

Appendix E Continued.

4a

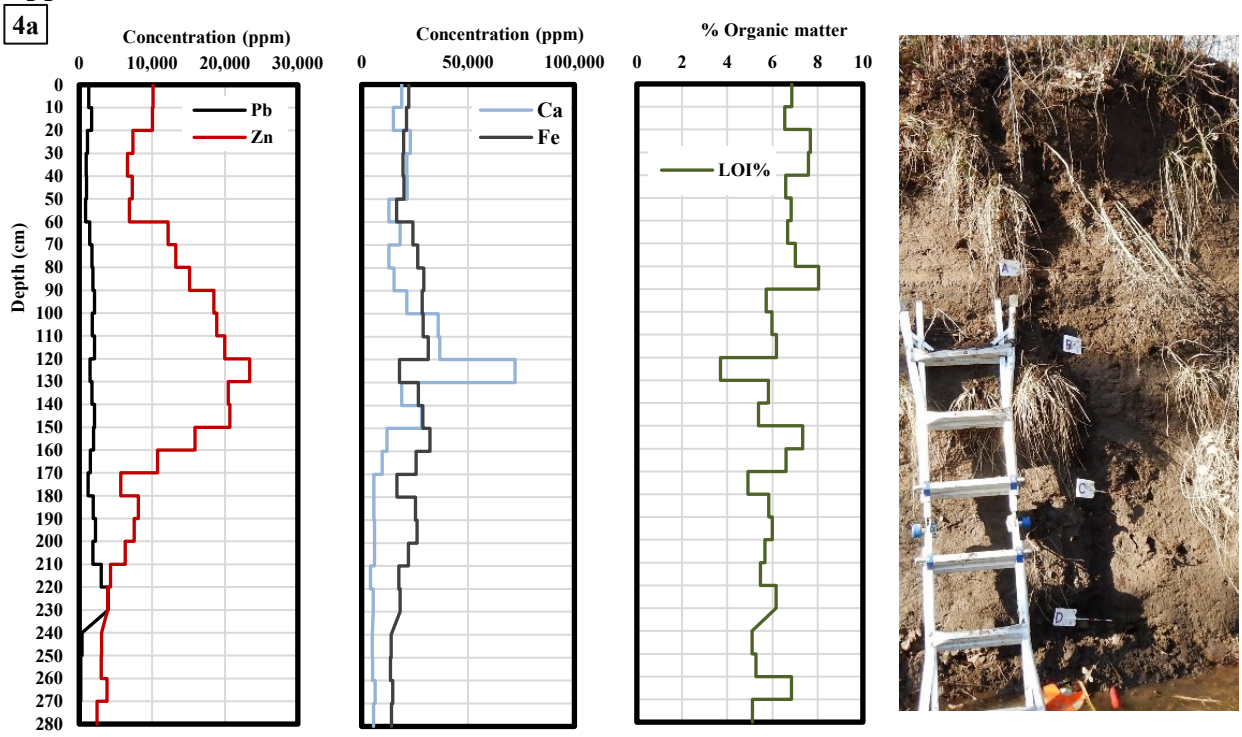

Appendix F. Dated Floodplain Cores with Sedimentation Rates and Storage Results.

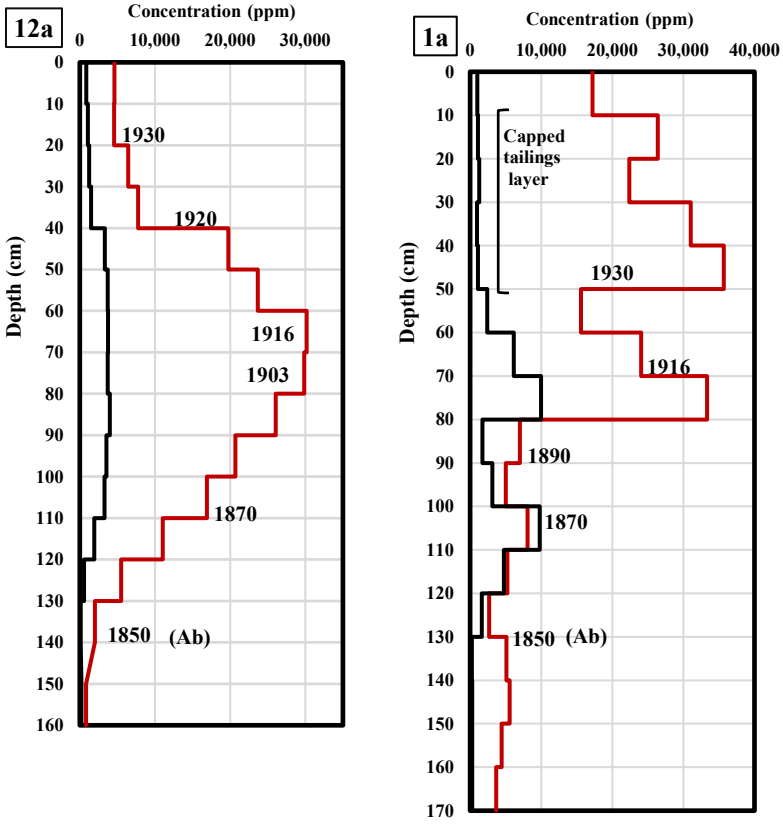

Time period	Rate cm/yr	Storage %	Time period	Rates cm/yr	Storage %
1850-1870	1.5	21.4	1850-1870	1.5	23.1
1870-1890	1.0	14.3	1870-1890	0.5	7.7
1890-1920	1.7	35.7	1890-1920	1	30.8
1870-1930	1.5	64.3	1870-1930	0.8	38.5
1930-2021	0.2	14.3	1930-2021	NA	38.5

Appendix F Continued.

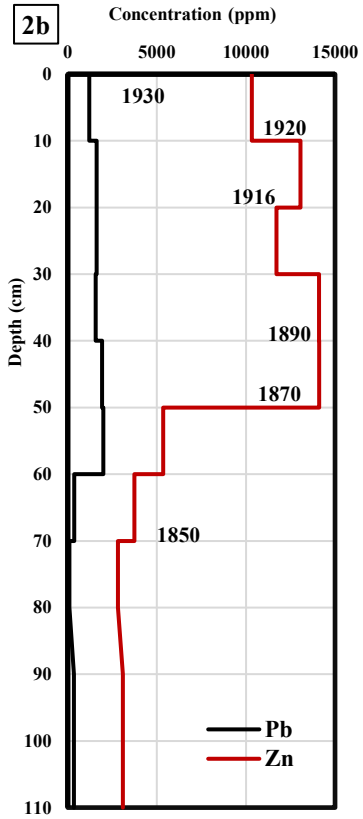

Time period	Rates cm/yr	Storage %
1850-1870	1	28.6
1870-1890	0.5	14.3
1890-1920	1.25	42.9
1870-1930	0.8	71.4
1930-2021	0	0.0

Appendix F Continued.

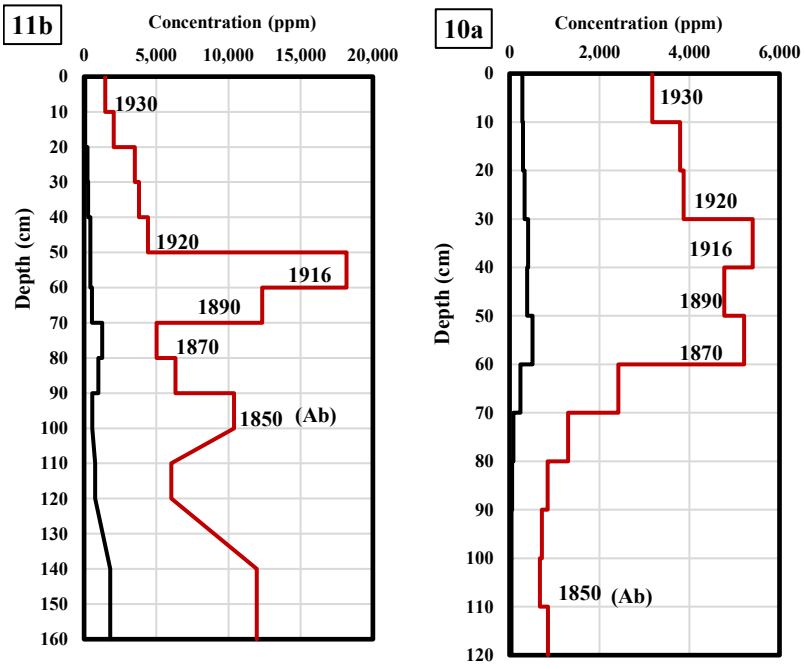

Time period	Rates cm/yr	Storage %	Time period	Rates cm/yr	Storage %
1850-1870	1.0	20.0	1850-1870	2.0	36.4
1870-1890	0.5	10.0	1870-1890	0.5	9.1
1890-1930	1.0	60.0	1890-1930	1.0	45.5
1870-1930	1.2	70.0	1870-1930	1.0	54.5
1930-2021	0.1	10.0	1930-2021	0.1	9.1

Appendix F Continued.

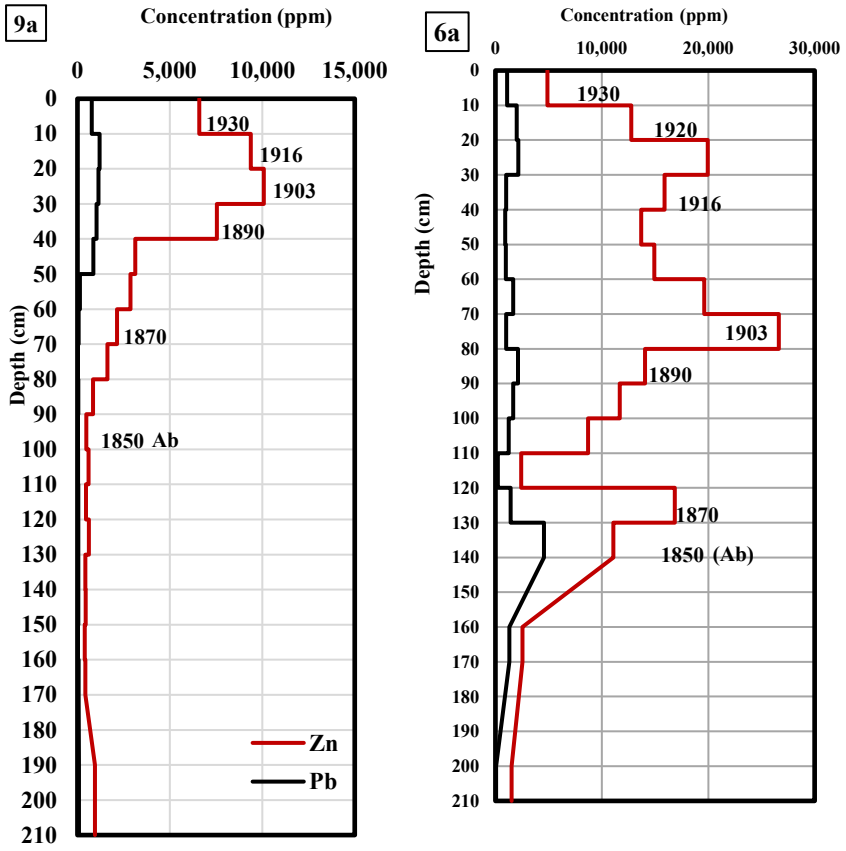

Time period	Rates cm/yr	Storage %	Time period	Rates cm/yr	Storage %
1850-1870	1.5	30.0	1850-1870	0.5	7.1
1870-1890	1.5	30.0	1870-1890	2.0	28.6
1890-1920	0.8	30.0	1890-1920	2.3	50.0
1870-1930	1.0	60.0	1870-1930	2.0	85.7
1930-2021	0.1	10.0	1930-2021	0.1	7.1

Appendix F Continued.

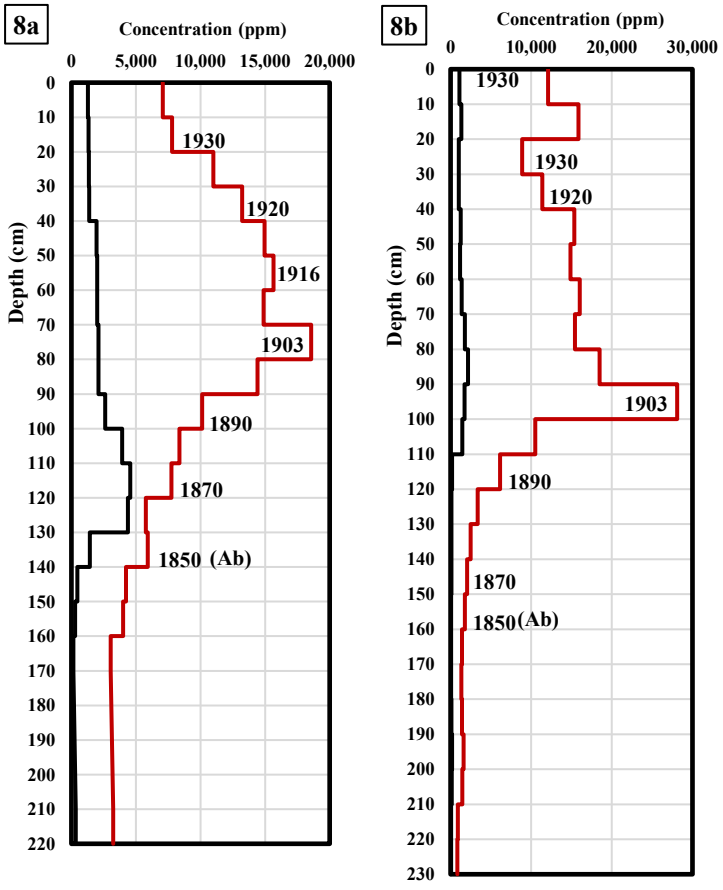

Time period	Rates cm/yr	Storage %	Time period	Rates cm/yr	Storage %
1850-1870	1.0	14.3	1850-1870	0.5	6.3
1870-1890	1.0	14.3	1870-1890	1.5	18.8
1890-1920	2.0	50.0	1890-1920	3.0	50.0
1870-1930	1.7	71.4	1870-1930	2.5	75.0
1930-2021	0.2	13.3	1930-2021	0.0	0.0

Appendix F Continued.

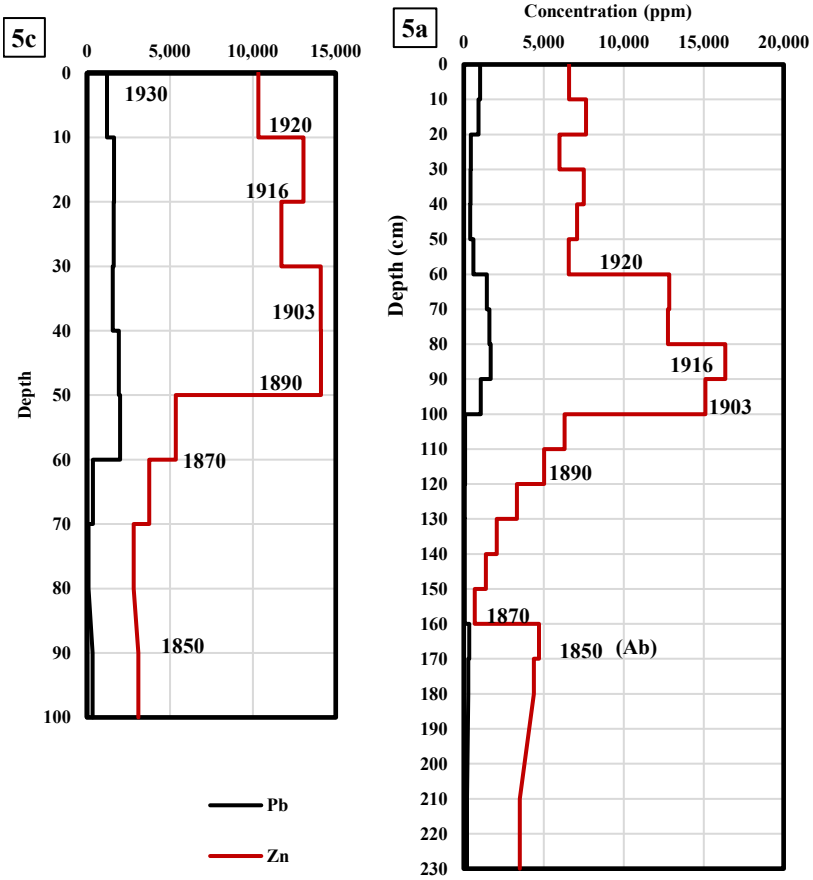

Time period	Rates cm/yr	Storage %	Time period	Rates cm/yr	Storage %
1850-1870	0.5	14.3	1850-1870	1.0	5.9
1870-1890	1.0	85.7	1870-1890	2.0	23.5
1890-1920	0.0	0.0	1890-1920	2.0	35.3
1870-1930	0.5	14.3	1870-1930	2.2	76.5
1930-2021	1.3	23.5	1930-2021	0.3	17.6

Appendix F Continued.

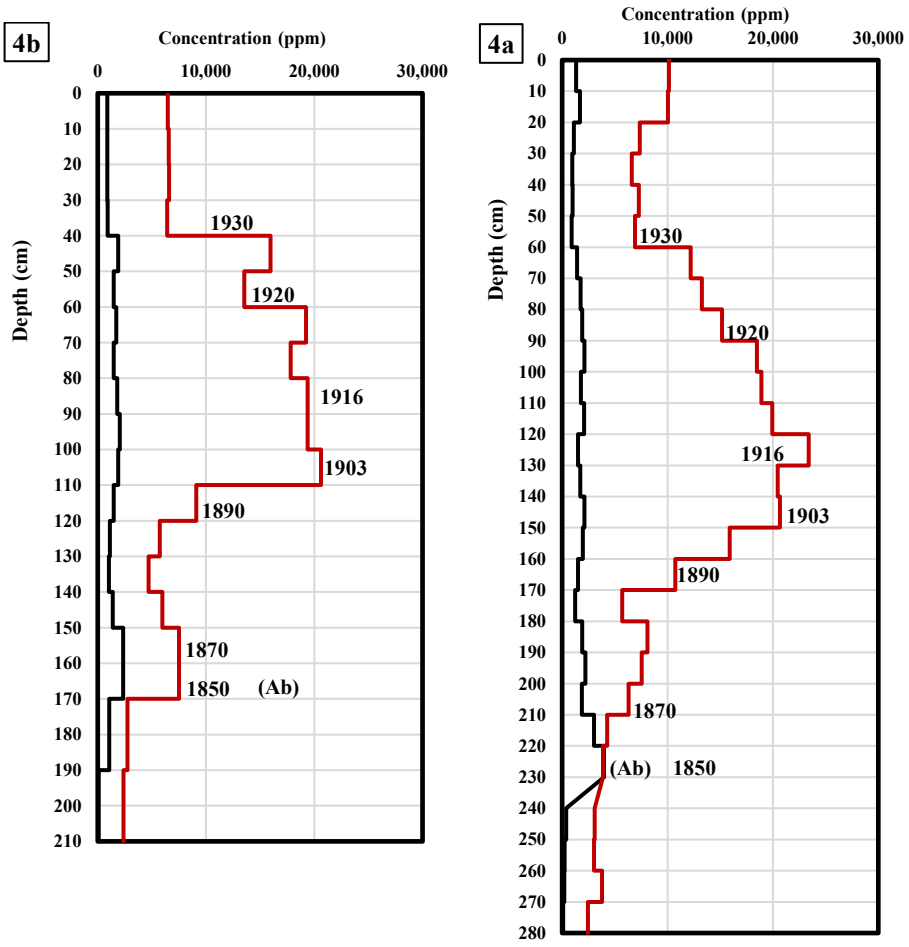

Time period	Rate cm/yr	Storage	Time period	Rate cm/yr	Storage
1850-1870	0.5	5.9	1850-1870	1.0	8.7
1870-1890	2.0	23.5	1870-1890	2.0	17.4
1890-1920	2.0	35.3	1890-1920	2.7	34.8
1870-1930	2.0	70.6	1870-1930	2.5	65.2
1930-2021	0.4	23.5	1930-2021	0.7	26.1